ORGANIZED SURFACTANT ASSEMBLIES : INTERFACIAL PHENOMENA AND APPLICATIONS

A THESIS

SUBMITTED TO THE

UNIVERSITY OF POONA

FOR THE DEGREE OF

DOCTOR OF PHILOSOPHY

IN CHEMISTRY

BY

BRAJESH KUMAR JHA

M.Sc. (Chemistry)

CHEMICAL ENGINEERING DIVISION

NATIONAL CHEMICAL LABORATORY

PUNE - 411 008

AUGUST 1995

TO MY PARENTS
AND
BROTHER

FORM - A

Certified that the work incorporated in the thesis **"Organized Surfactant Assemblies: Interfacial Phenomena and Applications"** submitted by Brajesh Kumar Jha was carried out by the candidate under my supervision. Such material as has been obtained from other sources has been duly acknowledged in the thesis.

BDKulkarni

Dr. B.D. Kulkarni

Research Guide

उपनिदेशक एवं अध्यक्ष
DY. DIRECTOR & HEAD
रासायनिक अभियांत्रिकी प्रभाग
Chemical Engineering Division
राष्ट्रीय रासायनिक प्रयोगशाला
National Chemical Laboratory
पुणे/PUNE-411 008.

Acknowledgement

I remain deeply indebted to my research advisor Dr. B.D. Kulkarni for introducing me to a fascinating and challenging frontier area of colloid science. This dissertation is an outcome of his exemplary interest, continuous inspiration and dynamic guidance. I record my deep sense of gratitude for his cogent advice, personal care, encouragemnt and enthusiastic support throughout the work.

My heartful thanks are due to Dr. A.S. Chhatre for his helpful suggestions during the initial stage of this research work. I would also like to express my deep sense of appreciation to Dr. S.S. Tambe who kindly responded to my request whenever I needed. It is my pleasure to thank Dr. V. Ravi Kumar, Dr. V.K. Jayaraman and Dr. N.K. Yadav for having inspired me throughout this research work. I highly appreciate the help rendered by my friends and lab colleagues during the course of this investigation.

A special mention goes to Dr. R.A. Joshi, Dr. (Mrs.) R.R. Joshi, Dr. U.R. Kalkote, Dr. S. Sivasanker, Dr. K. Vijayamohanan, Dr. Ashish Lele and Dr. S.N. Shintre for their co-operation, active interest and helpful suggestions while carrying the research work. It is indeed a pleasure to acknowledge the support received from them and their group members.

I am greatly indebted to the Director of National Chemical Laboratory, for providing me all the facilities for doing the presented research. Most importantly I thank the council of scientific and industrial research (CSIR) New Delhi for awarding me the research fellowship.

Finally, I record my profound sense of gratitude to my parents, brother and other family members for their exemplary patience, understanding and co-operation. Their sacrifice in various ways is gratefully acknowledged.

Brajesh

(Brajesh K. Jha)

ABSTRACT

In recent years there has been a growing interest in research on supramolecular surfactant assemblies that include micelles, reverse micelles, microemulsions, vesicles, monolayers and black lipid membrane (BLM). These aggregates of colloidal dimensions originate from the properties of surfactant or amphiphilic molecules [species consist of both apolar hydrophobic (lipophilic) and polar (hydrophilic) groups)] which can self assemble in aqueous solution to a variety of phase structures leading to macroscopically homogeneous but sub-microscopically heterogeneous systems. They exhibit a wide diversity of properties that can not be adequately described by random mixing models. A common feature among aggregates is interfacial regions separating the polar bulk aqueous phase from an apolar hydrocarbon-like region. In micelles, monolayers, BLM and vesicles, this region is formed by hydrophobic tails, and in microemulsions and reverse micelles, it also contains added oil. The interfacial region or Stern layer, is an extremely anisotropic region having a width about the size of the surfactant head group, and contains the ionic head groups of the amphiphile, a fraction of counterions and water.

The capability of micelles and microemulsions to solubilize a broad spectrum of substances in one-phase formulation has been found useful for many technical applications because of their potential ability to compartmentalize and concentrate reagents at the molecular level and thereby promoting catalysis, and also achieving better regioselectivity of organic reactions due to orientation of reactants at interface. Normally if the substrate is poorly soluble in the solvent, it will be solubilized at the interface where the reactive polar moities occupy the quasi-two dimensional (2D) surface of finite thickness rather than having them occupy a three dimensional (3D) volume as occurs in homogeneous solution environment. It is well documented that reactions associated with the participation of H^+-ions either as reactants or as catalytic species can substantially benefit in such media due to an increase in the local concentration of H^+-ions at the microscopic interface. The microscopic interface of these assemblies is sensitive to various parameters like temperature, salinity, surfactant and cosurfactant concentration, and shear. There have been a number of experimental and theoretical studies on micelles and microemulsions which reveal their complex behavior.

The thesis consists of six chapters, each centering around the study of a particular aspect of the micelles/microemulsions. Chapter 1 presents the brief introduction and background to surfactant organized assemblies with pertinent literature in the area of micelles and microemulsions, and their technological applications.

D(-) phenylglycine, an optically active amino acid, is a useful starting material in the preparation of semi-synthetic penicillins and cephalosporins such as amoxicillin, cephadroxil, cefatrizine, cefaparole and cefaperazon. The conventional preparation for D(-) phenylglycine is customarily a heterogeneous reaction, wherein D(-)-N-carbamoyl phenylglycine forms a separate solid phase due to its poor solubility with nitrous acid as the second phase. The amount of mineral acid required for the reaction is very high. The product formed is isolated from the reaction mixture by concentrating the solution and neutralizing the excess acid with an alkali. This results in formation of mineral salts with which the product gets contaminated. Also, as a consequence of other parallel reactions between the product D(-) phenylglycine and the excess nitrous acid, unwanted by-products such as mandelic acid and benzaldehyde are formed. Due to these consecutive parallel reactions, the overall rate and hence the percent yield of the reaction is low.

Chapter 2 reports the effect of dilute aqueous micellar and microemulsion solutions of sulfuric acid on the interfacial solubility of D(-)-N-carbamoyl phenylglycine. Results of the decarbamoylation reaction of the D(-)-N-carbamoyl phenylglycine carried out under micellar conditions by using a concentrated aqueous solution of sodium nitrite as a limiting component has also been elucidated. Experimental observations reveal that enhancement in interfacial solubility has enhanced the overall rate of reaction, the selectivity and hence the percentage yield. This study points to possible exploitation of the important regions in the phase diagram for conducting chemical reactions.

Reports on use of micelles and microemulsions for carrying out nonphotochemical cyclization/rearrangement reactions have been sparse despite the importance. Chapter 3 presents investigations on the organized assemblies exhibiting a particular function. Enhancecd H^+ - ion concentration in some of the assemblies have been exploited to perform cyclization of D(-)-N-carbamoyl phenylglycin to phenylhydantoin. As another example, Beckmann rearrangement reaction of cyclohexanone oxime to caprolactam under mild acidic conditions has also been

studied. The phase behavior of ternary system (sodium dodecyl sulfate (SDS), cyclohexanone oxime and aq. H_2SO_4) and reaction product distribution have been analysed with a view to optimize the system performance. The reactions reported here are generic in character and demonstrate that other similar reactions can substantially benefit from this mode of operation.

The advent of ultramicroelectrode (UMEs) makes it possible to explore electrochemistry in surfactant assemblies with high sensitivity. Chapter 4 focuses on the effect of SDS, an anionic surfactant on the electrochemical behavior of a water soluble redox-species, potassium ferricyanide with a view to obtain information pertaining to micellization. The electrochemical behavior of redox species, ferrocene, solubilized in aqueous microemulsion has also been studied. The cyclic voltammetric results show the effect of acid concentration on the redox behavior of ferrocene. Contrary to the generally expected reversible peak, experiments show an unusual second oxidation peak during the reverse scan at low scan rates. These observations have been rationalized using the concept of coupling between electrochemical and chemical reactions and would be significant in designing the electrochemical reactors for inorganic and organic materials as also in biologically important mediated electron transfer process.

Shear induced phenomenon plays an important role in surfactant chemistry. Shear is directional in nature and can change the structure of amphiphilic assemblies. Therefore coupling flow to phase transitions in these assemblies can give rise to exotic behavior. This is an emerging area offering considerable scope.

On studying the SDS/alkanol/water phase diagrams the presence of various regions was noticed. In view of the different microstructures of these regions they were expected to exhibit interesting rheological behavior. Chapter 5 presents the flow behavior of L_2 and L_2+D phases and its dependence on composition and temperature.

The physico-chemical characterization of micelles and microemulsions is carried out mainly by measuring diffusion coefficient which provides vital informations about micelle size, shape and the associated transport phenomena. Several measurements of the diffusion coefficient of micelles have been performed using quasi elastic light scattering (QELS), Taylor dispersion (TD), boundary spreading, nuclear magnetic resonance (NMR) and electrochemical techniques. Statistical and

thermodynamics approaches have also been used for molecular description or theoretical prediction of micellar shape and polydispersity based on diffusion coefficient and intensity data. However, the nonlinear dependence of micellar diffusion coefficient on temperature and concentration of surfactant and electrolyte, together with the complex nature of the interactions between them makes it difficult to describe the diffusion phenomena using simple phenomenological or empirical models. The *Artificial Neural Network* (ANN), possesses the ability to learn and generalize nonlinear functional relationship and can be employed for developing accurate models for estimating diffusion coefficient of micelles.

Chapter 6 illustrates the application of ANN for estimating the diffusion coefficients of SDS micellar system over a wide range of operating parameters such as temperature and concentrations of SDS and NaCl. The network model validates the experimentally observed qualitative and quantitative trends. The optimal model parameters in terms of network weights have also been estimated and can be used for computing diffusion coefficients over wide ranging experimental conditions.

C O N T E N T S

CHAPTER 1

INTRODUCTION

TH-1000

and temperature on the phase stability. Three component systems are generally studied under isothermal conditions and include third component such as hydrocarbon, alcohols of different lengths, fatty acids and electrolytes. The phase behavior of ternary surfactant-oil-water system was first elucidated by Winsor [38] 40 years ago. A lot of research has been carried out to understand more and more complex situations. Infact one of the very first phase diagrams illustrating solubilization phenomena was reported by McBain et. al [39]. The phase diagrams are visualized in a triangular representation such that there is 100 % of one component at the apex; the composition is obtained as the distance from the opposite base of the triangle. In general, compositions are given as weight percentage for reasons of convenience and clarity of representations. The study of four components systems of surfactant, hydrocarbon, alcohol (often termed cosurfactant) and water has become important especially in the case of microemulsions [40, 41]. Isothermal phase diagrams of four component systems are normally illustrated in a tetrahedron where each apex represents one pure component and the distance from the opposite triangle gives the amount of the component. A pseudo-ternary phase diagram is often used by grouping two components together at the same vertex to simplify the three dimensional presentation of the quaternary diagram. An idealized phase diagram illustrating various classes of microemulsion types in oil-water-surfactant system is shown in Figure 1.4. The stability ranges and the appearance of different phases are strongly dependent on formulation variables which can alter the interactions of the surfactant with the water and oil phase and hence can change the Winsor R ratio (ACO/ACW, where ACO indicates the interaction between the surfactant and the oil phase, and ACW, the interaction between the aqueous phase) [42]. When $R < 1$ (respectively $R > 1$) the interaction of the surfactant with the water (respectively oil) phase dominates and the phase behavior in the polyphasic region corresponds to the so-called Winsor type I or WI (respectively type II or WII) phase behavior in which an equilibrium with an excess phase which contains essentially oil (respectively water). Whenever the R ratio is unity, a three-phase behavior is exhibited, and is referred to as Winsor type III or WIII.

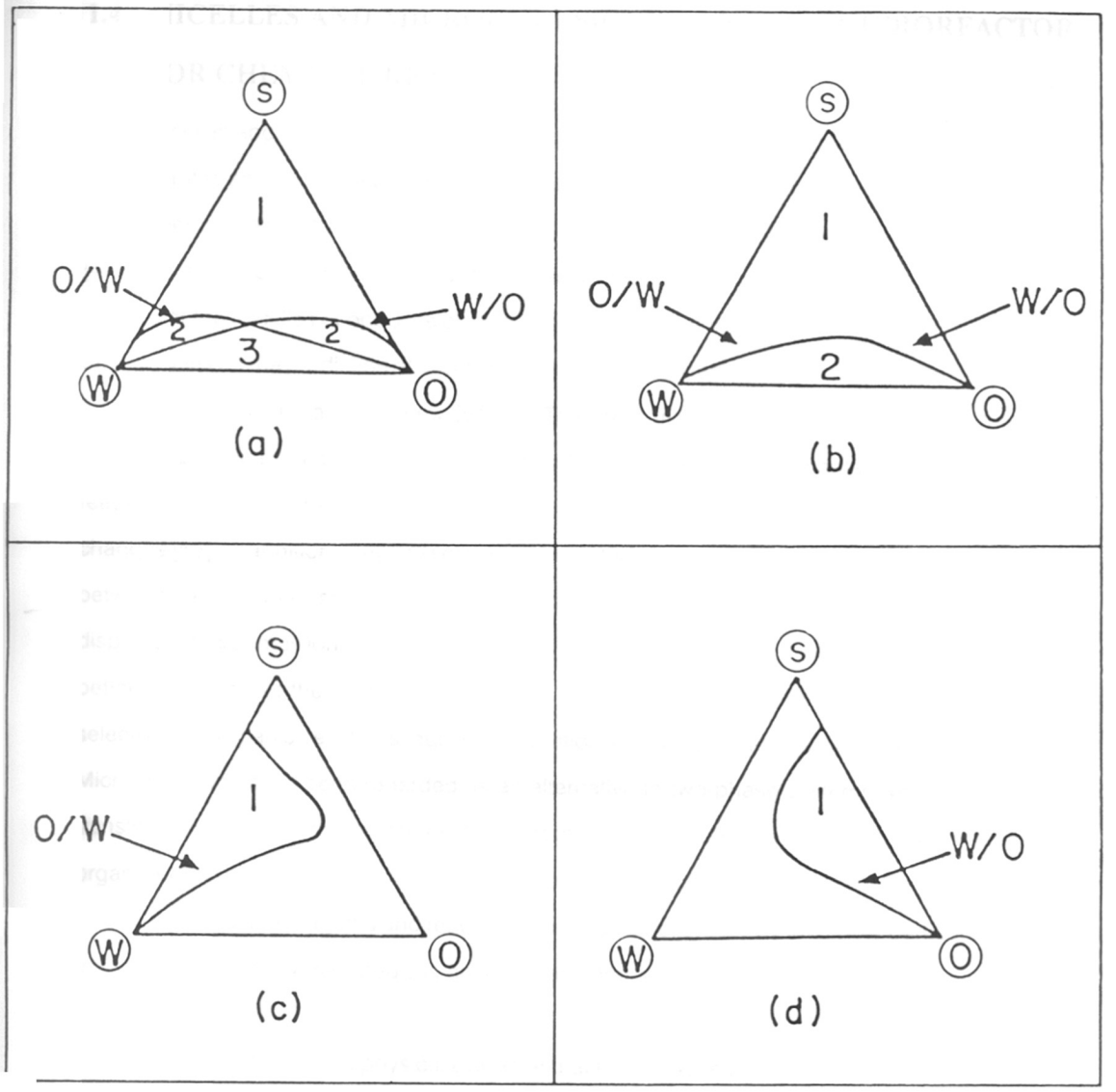

Figures 1.3(a-d) : Various types of phase behavior in water (W), oil (O), surfactant (S) systems. The numbers 1, 2, and 3 refer to the number of phases; O/W and W/O refer to oil in water (Winsor I), and water in oil (Winsor II) microemulsions respectively.

1.4 MICELLES AND MICROEMULSIONS AS NOVEL MICROREACTOR FOR CHEMICAL REACTIONS

Micelles and microemulsions can be regarded as a set of microreactors and influence the reaction rates and equilibria by providing a medium different from that of the bulk solvent [43-46]. It has been well known that micellar systems have a considerable effect on indicator equilibria [47]. A "sign" rule to account for the shift in equilibria was proposed by Hartley [48, 49] which states that the micelles of opposite charge affect the equilibrium. Substantial use has been made of these rules for the prediction of micellar effects on reaction rates [50]. The use of microemulsions as reaction media is relatively new [51-54]. The great utility of microemulsion is that they can dissolve large quantities of both oil and water soluble solutes, compartmentalize and concentrate reagents, and are generally stable at fairly wide range of temperature, compositional and pH changes [55]. In addition, they possess a large interfacial area of the order of 100 m^2/g. Reactions between oil and water soluble reagents can take place across the interface. Moreover, mono-dispersed microemulsion droplets with radii as small as 100 to 1000 Å offer promising means for better controlling of the product morphology. Microemulsions also affect the regio and stereo selectivity of organic reactions due to orientation of reactants at the oil-water interface [56]. Microemulsions have been regarded as an alternative to two-phase systems with added phase transfer reagents and are of interest to overcome incompatibility problems between nonpolar organic compounds and inorganic salts in preparative organic synthesis [57]. Thus manipulation of the location of the reagents and reactive substrates functionality by favorable partitioning in the microscopically structured media is an important strategy for fine-tuning chemical reactivity and selectivity.

There is considerable physical evidence that the interface provides the most likely reaction site in the micelles and microemulsions [58, 59]. The "Stern layer" is the interface between the hydrocarbon like interior and solvent, with small thickness, having a size of the surfactant head group, and a fraction of the counter-ions (0.6-0.9/ionic head group) [60, 61]. Ionic micelles have appreciable surface potentials and charge densities (Figure 1.5). Ionic micelles attract counter-ions that partially neutralize the charge of the surfactant head groups. Charge distribution at the

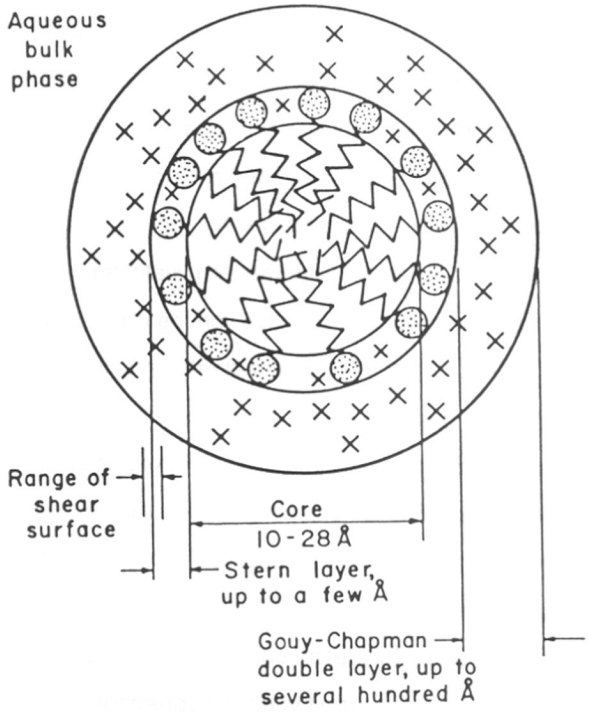

Figure 1.5 : Schematic representation of the regions of a spherical micelle. The counterions (X), the head group (⊙), and the hydrocarbon chains are (∿) schematically indicated to denote their relative locations.

microscopic surface has been treated by the various electric double-layer theories [60]. The important result is that negatively charged micelles attract positive counter-ions while positively charged ones are surrounded by the negative counter-ions (Figure 1.6). Ion selective electrodes and NMR spectroscopy have been used to estimate concentration of micellar-bound counter ions [62, 63]. These methods show that concentrations of counter-ions at the micellar/microemulsion surfaces are much higher than in the aqueous pseudophase. Estimated local concentrations are in the range of 3-5 M [64, 65]. Theoretical models such as pseudophase ion exchange (PIE) and Poisson-Boltzmann equation (PBE), as a first order approximation have also been developed to explain and to provide a quantitative treatment of micellar rate enhancement of bimolecular reactions [66, 67]. It should be noted, however, that an effective concentration effect applies only to reactions whose total order is greater than one.

Catalysis and enhancement of chemical reaction rates involving hydronium ion (H_3O^+) by several orders of magnitude and excellent product selectivity control have been demonstrated for several cases [68]. The increase in the concentration of semi-polar reactants at the interface and high concentration of hydrogen ions associated with the Stern layer may promote the acid catalyzed reactions more efficiently even under mild acidic conditions. This concept has been illustrated in chapter 2 and 3 to emphasize the novelty of microheterogeneous structured media in cyclization and molecular rearrangement reactions.

1.5 VOLTAMMETRY WITH ULTRAMICROELECTRODE IN MICELLES AND MICROEMULSIONS

Recent years have seen an upsurge of interest in the application of electroanalytical techniques to study redox processes in micelles and microemulsions [69-75]. These methods have been used to obtain self-diffusion coefficients of micelles and microemulsion droplets, and to characterize the diffusion in continuous phases [76-78]. Numerous electrochemical techniques have been developed for measuring the CMC values, and to characterize the aggregates in micelles

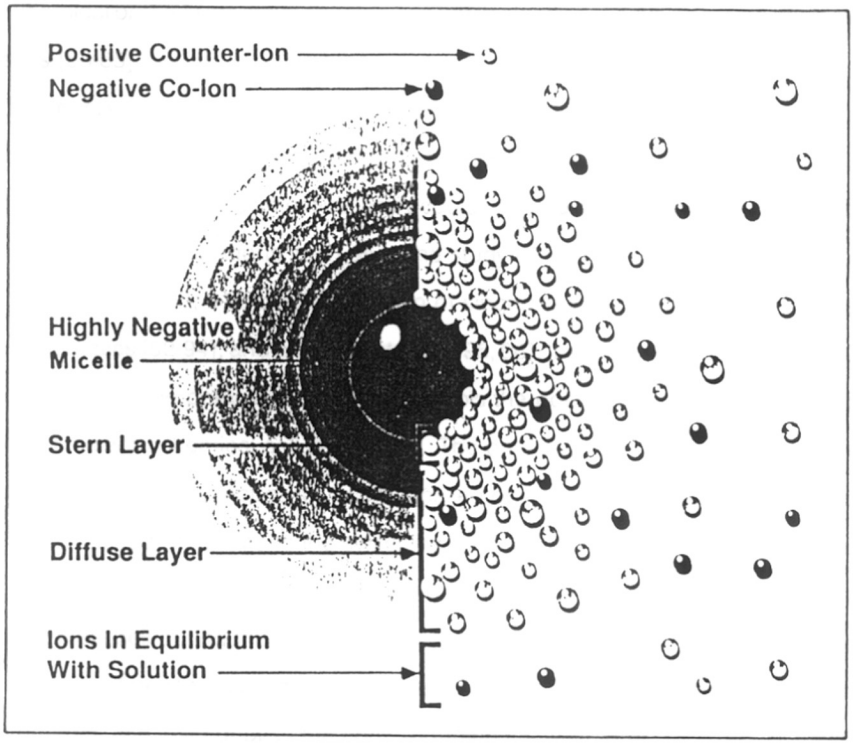

Figure 1.6 : Simplified illustrations of the electrical double layer around a negatively charged micelle. The left view shows the change in charge density around the droplet. The right view shows the distribution of ions around the charged droplet.

and microemulsions [79-82]. The use of micelles and microemulsions as a means of solubilizing electrochemical probe in aqueous solution has led to significant developments of electrochemical processes [83-85].

The most widely used dynamic electrochemical technique is cyclic voltammetry (CV) which provides qualitative information regarding mechanistic steps in a redox reaction [86, 87]. Moreover, the technique is time and cost effective, and acquisition and interpretation of data is easy [88, 89]. It has wide ranging applications such as in the study of simple redox processes in organic and inorganic chemistry [90, 91], characterization of single/multi electron transfer processes in surfactant assemblies [92-94], and biochemistry etc [95, 96]. Instrumentation for modern CV is based on the three electrode potentiostat, which controls the potential wave form. In CV the potential applied to an electrochemical cell is scanned. The potential scan is programmed to begin at an initial potential where no electrolysis occurs (called open circuit potential (OCV)). The scan continues at the desired linear rate to the switching potential, reverses its direction and returns back to the initial potential. The output of cyclic voltammetry is a plot of the current flowing in the electrochemical cell during the cyclic potential scan. Figure 1.7 shows a typical three electrode cell (showing a reference electrode, a counter electrode, and a working electrode) for voltammetric measurements, and inset depicts the corresponding CV waveform.

In the voltammetric experiment the electrode performs two tasks: controlling the current or the electrode potential and, monitoring the solvent reactions [87, 97, 98]. The voltammetric behavior is changed when the size of electrode changes from the millimeter to micrometer scale and offers dramatic improvements in the electrochemical data acquisition and also facilitates several types of measurements that were previously impossible. Recent developments in voltammetry using ultramicroelectrodes (UMEs) offer a promising route to overcome some of the limitations of CV that uses macroelectrode [99]. Indeed, UMEs possess a number of attractive characteristics [100, 101]. They are capable of producing signals that are less subject to interference and capacitance problems. Voltammetry with UME is time independent process and therefore rapid changes of potentials are possible without any distortions from nonfaradaic currents. Other features like reduced double layer capacity and small current (generally in the range of nano-pico amperes) often completely eliminate the effect of uncompensated iR drop

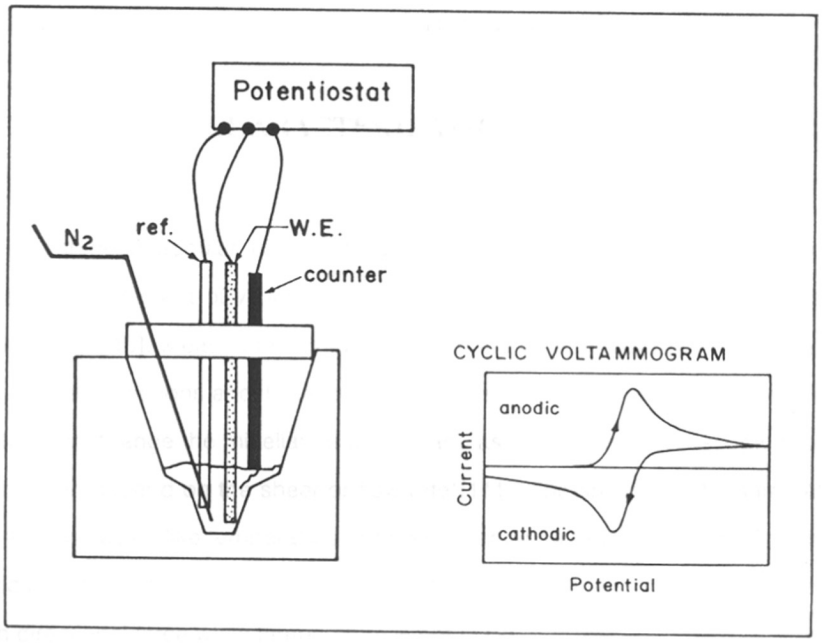

Figure 1.7 : Schematic set up of three-electrode potentiostat. W.E.: working electrode; ref.: reference electrode. Inset depicts an ideal shape of cyclic voltammogram.

(ohmic effects) problems and facilitate their use in resistive solvent or solution with low supporting electrolyte concentration [102]. Besides, microsized electrode makes it possible to conduct electrochemical measurements in minute volumes and observe discrete spatial events in microscopically small areas with high sensitivity [103].

Chapter 4 of this thesis reports the utility of CV with ultramicroelectrode (in the $10\mu m$ diameter range) for the detection of micelles in aqueous anionic surfactant. The chapter also demonstrates UME's ability to explore coupled chemical reactions in aqueous microemulsions.

1.6 RHEOLOGICAL CHARACTERIZATIONS: PHENOMENA UNDER SHEAR

Micelles can be of globular, rodlike or disklike shape [104-106]. The shape of micelles can be controlled by adjustment of various parameters like temperature, salinity and cosurfactant concentration [107-110]. Measurements focussing on the structure of micelles are usually performed in quiescent solutions and it is assumed that the shape of micelles is not varied by flow. However, flow can change the micellar structures and as a result the microscopic properties of such systems can depend on the shear or flow rate [111]. The shear has the same effect as a thermodynamic variables like temperature or pressure and contribute to a shift of phase boundaries. In addition, the shear may affect systems differently than the temperature; since it is connected with directional force while temperature is not [112].

The rheology of surfactant solutions under shear flow has been studied extensively [113-117]. There are scattered reports in which rheology has been used to probe the dynamics and structure of ternary microemulsions [118, 119]. Disruption of the equilibrium liquid structure by the flow field and alignment of crystallites with shear have been proposed as a mechanism for shear thinning behavior in microemulsions and liquid crystals [120-122]. Some studies report the mechanisms for rheological phenomena such as rheopectic and shear thickenning [111, 112, 123, 124]. It is generally accepted that the shear induced structure (SIS) formation is responsible for the unusual flow behavior of micelles, and other assemblies [112, 125-127]. Figure 1.8 depicts the shear-induced aligning of the rod like micelles. The small rod like micelles undergo collisions

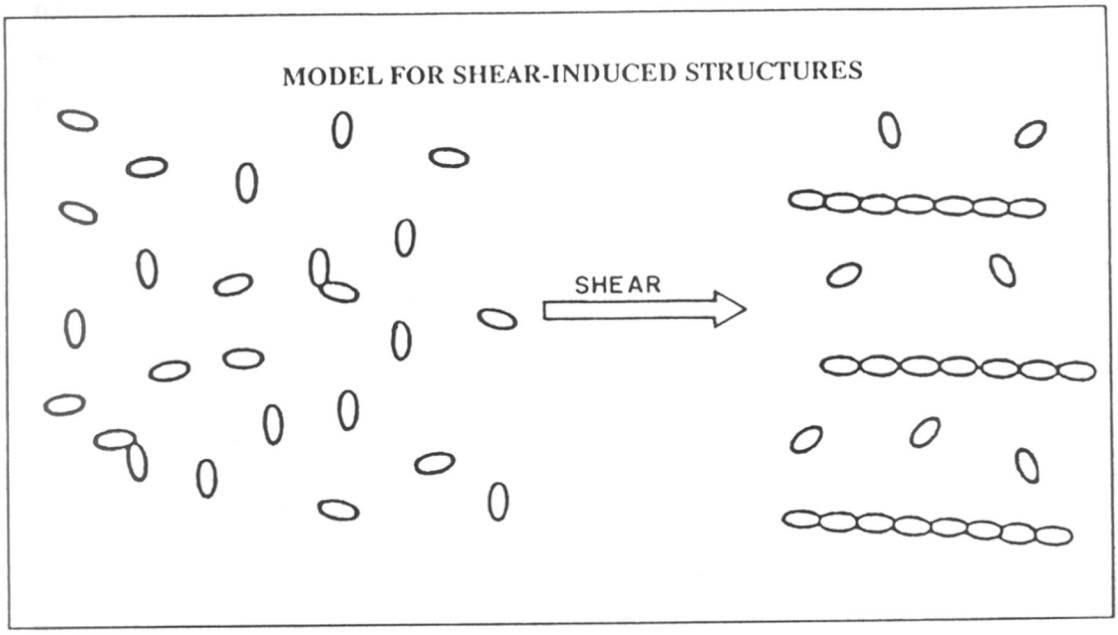

Figure 1.8 : Schematic drawing of the build up of shear-induced micellar structures. The small rodlike micelles can form long band or necklace-type structures under shear.

1.1 PREFACE

It has been known since the work of Emil Fisher (1894) that supramolecular interactions can be a source of molecular function [1]. The idea has formed the basis of one of the most stimulating fields - that of 'supramolecular science', which simultaneously involves the principles of self-organization, regulation, replication, communication and cooperativity. Interestingly, it offers a new route for the design of materials where the organization precedes the function [2, 3]. Mother nature demonstrates the interplay of molecular self-organization and molecular regulation to assemble systems, the function of which is based on their organization. To mimic nature's structures has led to the development of a large number of organized assemblies such as micelles, liquid crystals, monolayers, bilayers and vesicles (which are typically formed from surfactants); and supramolecular hosts such as crown ethers, silica clays and zeolites etc [4, 5]. These are broadly known as microheterogeneous systems. The prime motivation of supramolecular assemblies of surfactants is their potential applications in reactivity control, photochemical solar energy conversion and storage, molecular recognition and transport, drug encapsulation, and in providing unique enviornments for substrates and enzymes.

1.2 GENERAL BEHAVIOR OF SURFACTANTS

Molecules that possess both hydrophilic and hydrophobic (lipophilic) parts are termed amphiphiles or amphiphathics [6]. They are also referred to as surfactants since they adsorb to surfaces and interfaces of dispersed and continuous phases and bring about a change in the interfacial free energy [7, 8]. Figure 1.1 illustrates a schematic diagram of surfactant or amphiphilic molecule. The hydrophilic part (sometimes called the head of the amphiphile) can have a charge (anionic, cationic, zwitterionic) or can be polar (poly oxyethylene chain, amine oxide, etc). The hydrophobic part is usually some hydrocarbon of different length (typically 8-20 carbon atoms). Table 1.1 lists a representative class of surfactants.

Surfactant molecules dynamically and spontaneously self-assemble into aggregates in aqueous solution above the so-called *critical micelle concentration* (CMC) [9, 10]. Usually the

in the shear flow and their interfacial properties are such that they stick together for some time. In this way long band or necklace type structures are formed under shear which aligned themselves in the shear flow. Interestingly, micellar structures are self-healing [128] and suppress flow resistance in the region of turbulent flow. This effect can therefore be used to save energy in the transport of large quantities of fluid [129-131]. Eventually, coupling flow to structural changes in micelles and microemulsions has considerable potential for technical applications where it is necessary to control the flow behavior of aqueous solutions [132, 133].

In the framework of these features, chapter 5 describes the influence of various parameters on the rheological properties of the ternary systems comprising anionic surfactant, water and the alkanol, which undergo dramatic changes with shear.

1.7 ARTIFICIAL NEURAL NETWORKS (ANNs) AND MICELLAR DIFFUSION COEFFICIENTS

In the last decade *Artificial Neural Networks* (ANNs) have emerged as an important tool to implement artificial intelligence [134]. ANNs have been employed in wide ranging applications covering every scientific, engineering and technological discipline due to the ease with which they can handle complex non-linear problems [135-141]. Essentially, they are oversimplified mathematical models of biological neural system of human brain [142]. Figure 1.9(a) describes a simplified picture of biological neuron. A typical biological neuron consists of a cell-body (soma) with a nucleus. The cell body has two types of extensions: the dendrites and the axon. The dendrites receive electrochemical signals from other cells and send them to the soma where they are processed nonlinearly. The axon transmits signals to other neurons. Communication between neurons takes place at a junction called, synapse.

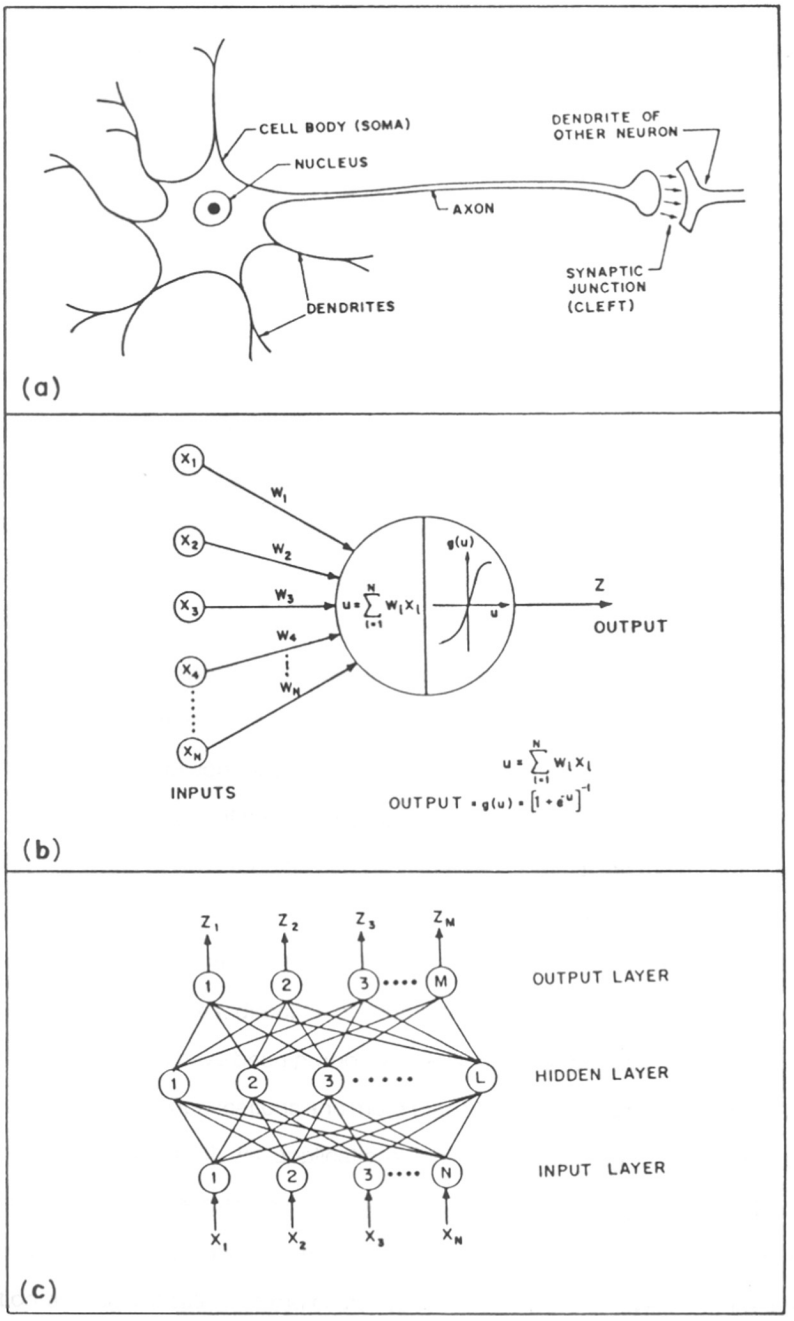

Figure 1.9 : Schematic representation of - (a) a biological neuron; (b) an artificial neuron; (c) back-propagation neural network architecture.

The mathematical model of a biological neuron - the artificial neuron is depicted in Figure 1.9(b). It possesses several inputs (X_i), each of which is connected to neurons in the next layer through synaptic strengths W_i. The artificial neuron computes its activation (u) according to the weighted sum formula ($u = \sum_{i=1}^{N} W_i X_i$) which is then transformed employing a non-linear transfer function (usually sigmoid) to generate neural output ($Z = \frac{1}{1+\exp(-u)}$).

Linking layers of artificial neurons in a particular fashion gives rise to Artificial Neural Networks. Formally ANN is defined as *the massively parallel interconnected networks of simple (usually adaptive) elements and their hierarchical organizations which are intended to interact with the objects of the real world in the same way as biological nervous systems do* [143]. ANNs are found extremely useful for tasks such as pattern recognition, classification, memory and nonlinear function approximation (mapping). In order that a network performs any of these tasks it must be first trained using examples (the training set). The net not only learns the hidden information (rule) in the data but also possesses ability of generalizing the learned information. It means that a trained network based on its learning responds appropriately to new data set (the test set) which is not a part of the training set.

Different types of ANN models can be visualised. Typical examples are Back-propagation (BP) [144], Counter-propagation (CP) [145], Adaptive resonance theory (ART) [146, 147], Adaptive bidirectional associative memory (ABAM) [148], Hopfield [149, 150] etc. These models differ in their structure, learning rules, direction of information flow and applications. Despite the fact that numerous ANN models have been proposed, BP is the most popular ANN algorithms [144, 151]. Eighty five percent of all applications and more than 97% of chemistry applications have employed the BP network [152, 153]. Its applications include developing quantitative structure-activity relationships (QSAR) or structure-property relationships (QSPR), predicting chemical reactivity, protein structure determinations, process control, process modelling, fault detection, pattern recognition and classification of molecular spectra, and data analysis. Figure 1.9(c) shows the

standard architecture of the BP network with three layers - input, hidden and output. We have made use of BP network for estimation of diffusion coefficients of micelles. The ensuing paragraph outlines in brief the importance of the conducted study.

Diffusion coefficient is one of the parameters used to characterize micellar systems and provides vital information regarding micelle size, shape and associated phenomena [60, 154-156]. Diffusion coefficient in combination with a sedimentation coefficient can be used under ideal conditions to calculate a particle weight. Several experimental measurements for diffusion coefficient of micellar systems have been described in the literature [72, 157-163]. The nonlinear dependence of micellar diffusion coefficient on temperature and concentrations of surfactant and electrolyte, together with the complex nature of interactions between them makes it difficult to describe the diffusion phenomena by computationally simple and unique phenomenological or empirical models. Although correlations that predict diffusion coefficients of micelles are available [164, 165], they require knowledge of several experimentally determined parameters. ANNs, that possess the ability to learn and generalize nonlinear functional relationships can be very effectively employed to arrive at correlation for estimating diffusion coefficients.

Chapter 6 illustrates the BP neural network's ability to estimate the diffusion coefficient of micelles. The approach requires limited data and measurable experimental conditions.

1.8 POTENTIAL APPLICATIONS AND TECHNOLOGICAL RELEVANCES

The important research in the field of micellar systems and microemulsions have led to parallel development of technological applications [166, 167]. Compartmentalized liquid structures of high surface area provided by the oil-water dispersions suggest their use as a novel and versatile medium for chemical and biochemical transformations [168-170]. The possibility of precisely controlling the size and stability of the microstructure domain offer interesting applications in the preparation of microscopic particles of desired size or shape [171]. Moreover, a rich diversity of structures in the surfactant-water system with potentially interesting rheological and electrical properties can have a wide utilization in oil industry, to explore the gasoline substitutes based on

a liquid blends with alcohols, and as novel elements of molecular devices for information processing and signal generation in material sciences [172]. Table 1.3 summarizes the application of surfactant assemblies.

Table 1.3 : Applications of Organized Surfactant Assemblies

Serial No.	Application domain	Feature used	Reference
i	Chemical reactions	Solubilization, large interfacial area, local concentration and orientation effect,	[43, 46, 52, 173, 174]
ii	Tertiary oil recovery	Ultralow interfacial tension (10^{-2} - 10^{-3} dyne/cm and low viscosity	[175]
iii	Polymerization	Small droplet size (in the ranges of 5 - 40 nm), stability, continuous nucleation and large number of polymeric loci.	[176-178]
iv	Precipitation & controlled crystallization	Controlled environment nano-size reactor, limited nucleation and growth	[179-181]
v	Semi/super conductors & magnetic particles	Controlled environment nano-size reactor, limited nucleation and growth	[182-187]
vi	Development of small & uniform catalytic particles	Droplet diameter (< 10 nm), stability and ease of transfer to solid support.	[188, 189]
vii	Separation	Faster mass transfer rates, thermodynamic stability, high loading capacity, low leakage, Micellar enhanced ultrafiltration (MEUF), ease of de-emulsifications, high charge density and a high absolute electric potential of surface.	[190-195]
viii	Detoxifications of organic pollutants/environmental cleanup	Solubilization, capability, cloud-points, lower interfacial tension	[54, 196-201]
ix	Lubrication, metal cutting and corrosion inhibition	Solubilization, stability	[55, 202]
x	Food processing	Density, viscosity, solubilization and stability	[203, 204]
xi	Drug-delivery	Solubilization, vehicles/carriers or as a targeting system.	[205-209]
xii	Biotechnology	Solubilization of enzyme with retention of activity and stability, absence of rate-limiting mass transfer effects.	[170, 210-212]

REFERENCES

[1] E. Fisher, *Ber. Dtsch. Chem. Ges.*, **27** (1894) 2985.

[2] J. M. Lehn, *Science*, **227** (1985) 849.

[3] J. M. Lehn, *Angew. Che. Int. Ed. Engl.*, **27** (1988) 89.

[4] J. H. Fendler, *Membrane Mimetic Chemistry*; Wiley: New York, 1982.

[5] D. F. Evans and H. Wennerstrom, *The Colloidal Domain: Where Physics, Chemistry, Biology and Technology Meet*; VCH: New York, 1994.

[6] G. S. Hartley, *Aqueous Solutions of Paraffin Chain salts*; Hermann et Cie, Paris, 1936.

[7] R. Nagarajan, *Adv. Colloid Interface Sci.*, **26** (1986) 205.

[8] R. Nagarajan and E. Ruckenstein, *Langmuir*, **7** (1991) 2934

[9] M. J. Rosen, Micelle Formation by Surfactants. In *Surfactants and Interfacial Phenomena*; Wiley: New York, 1978; chapter 3, pp 83-121.

[10] B. Lindman and H. Wennerstrom, Micelles: Amphiphile Aggregation in Aqueous Solution. In *Topics in Current Chemistry*; M. J. S. Dewar, H. Hafner, E. Heilbronner, S. Ito, J. M. Lehn, K. Niedenzu, C. W. Rees, K. Schafer and G. Witting, Spring-Verlag: Berlin, 1980; Vol. **87**, pp 1-83.

[11] J. W. McBain, *Trans. Faraday Soc.*, **9** (1913) 99.

[12] C. Tanford, *The Hydrophobic Effect: Formation of Micelles and Biological Membranes*; Wiley: New York, 1980.

[13] P. Mukerjee and K. J. Mysels, *Critical Micelle Concentrations of Aqueous Surfactant Systems;* NSRDS-NBS 36, Washington, 1971.

[14] N. J. Turro, A. L. Buchachenko and V. F. Tarasov, *Acc. Chem. Res.*, **28** (1995) 69.

[15] A. Firouzi, D. Kumar, L. M. Bull, T. Basier, P. Sieger, Q. Huo, S. A. Walker, J. A. Zasadzinski, C. Glinka, J. Nicol, D. Margolese, G. D. Stucky and B. F. Chmelka, *Science*, **267** (1995) 1138.

[16] K. Shinoda, *J. Phys. Chem.*, **89** (1985) 2429.

[17] K. Shinoda, *Colloidal Surfactants*; Academic: New York, 1963; Chapter 1, pp 6-8.

[18] K. Shinoda, *Langmuir*, **7** (1991) 2877.

[19] D. Attwood and A. T. Florence, *Surfactant systems: Their Chemistry, Pharmacy and Biology*; Chapmann: London, 1983.

[20] A. T. I. Bard, *Langmuir*, **10** (1994) 1358.

[21] M. E. L. McBain and E. Hutchinson, *Solubilization and Related Phenomena*; Academic: New York, 1955.

[22] G. S. Hartley, *J. Chem. Soc.*, Part I, (1938) 1968.

[23] A. S. C. Lawrence, *Trans. Faraday Soc.*, **33** (1937) 325.

[24] A. S. C. Lawrence, *Trans. Faraday Soc.*, **33** (1937) 815.

[25] A. S. C. Lawrence, *Ann. Reports*, **37** (1940) 107.

[26] K. Shinoda, T. Nakagawa, B. Tamamushi and T. Asemura, *Colloidal Surfactants*; Academic: New York, 1963.

[27] P. H. Elworth, A. T. Florence and C. B. McFarane, *Solubilization by Surface Active Agents and its Applications in Chemistry and the Biological Science*; Chapmann: London, 1968.

[28] A. E. Alexander and P. Johnson, *Colloid Science*; Carendon: Oxford, 1949.

[29] H. Scott, *J. Phys. Chem.*, **71** (1967) 3611.

[30] K. Shinoda and B. Lindman, *Langmuir*, **3** (1987) 135.

[31] E. B. Leodis and T. A. Hatton, *J. Phys. Chem.*, **94** (1990) 6400.

[32] G. S. Hartley, *Nature*, **163** (1949) 787.

[33] P. G. de Gennes and C. Taupin, *J. Phys. Chem.*, **86** (1982) 2294.

[34] C. A. Miller, R. N. Hwan, W. J. Benton and T. J. Fort, *J. colloid Interface Sci.*, **61** (1977) 554.

[35] C. Huh, *J. Colloid Interface Sci.*, **97** (1984) 201.

[36] P. A. Winsor, *Trans. Farady Soc.*, **46** (1950) 762.

[37] M. L. Robbins, Theory for the Phase Behavior of Microemulsions. In *Micellization, Solubilization, and Microemulsions*; K. L. Mittal, Ed.; Plenum: New York, 1977, Vol. **2**, Chapter 4, pp 713-754.

[38] P. A. Winsor, *Solvent Properties of Amphiphilic Compounds*; Butterworth: London, 1954.

[39] S. S. Marsden and J. W. McBain, *J. Phys. Chem.*, **32** (1948) 110.

[40] P. Bothorel, Phase Diagram of Quaternary systems. In *Physics of Amphiphiles: Micelles, Vescicles, and Microemulsions*; V. Degiorgio and M. Corti, Eds.; 1985, pp 702-720.

[41] T. P. Hoar, J. H. Shulman, *Nature*, **152** (1943) 102.

[42] P. A. Winsor, *Trans. Farady Soc.*, **44** (1948) 376.

[43] J. H. Fendler and E. J. Fendler, *Catalysis in Micellar and Macromolecular Systems*; Academic: New York, 1975.

[44] V. Berezin, K. Martinek and A. K. Yatsimirski, *Russ. Chem. Rev.*, **42** (1973) 487.

[45] F. M. Menger, *Angew. Chem. Int. Ed. Engl.*, **30** (1991) 1086.

[46] B. Janakiraman and M. M. Sharma, *Chem. Eng. Sci.*, **37** (1982) 1497.

[47] O. A. Elseoud, *Adv. Colloid Interface Sci.*, **30** (1989) 1.

[48] G. S. Hartley, *Trans. Faraday Soc.*, **30** (1934) 444.

[49] G. S. Hartley and J. W. Roe, *Trans. Faraday Soc.*, **36** (1940) 101.

[50] C. A. Bunton, G. Savelli, Organic Reactivity in Aqueous Micelles and Similar Assemblies, In *Adv. Phys. Org. Chem.*, V. Gold and D. Bethell, Eds.; Academic: San Dieago, 1986; Vol. **22**, pp 213-309.

[51] J. H. Shulman, W. Stoeckenius and L. M. Prince, *J. Phys. Chem.*, **63** (1959) 1677.

[52] R. A. Mackay, *Adv. Colloid Interface Sci.*, **15** (1981) 131.

[53] R. E. Barden and S. L. Holt, Reactions in Microemulsions Media. In *Solution Chemistry of Surfactants*; K. L. Mittal, Ed.; Plenum: New York, 1979, Vol. **2**, Part V, pp 707-722.

[54] F. M. Menger and H. Park, *Recl. Trav. Chim. Pays-Bas*, **113** (1994) 176.

[55] L. M. Prince, *Microemulsions : Theory and Practice*; Academy: New York, 1974.

[56] M. Gratzel, *Tetrahedron*, **43** (1987) 2934.

[57] K. Holmberg, *Adv. Colloid Interface Sci.*, **51** (1994) 137.

[58] N. Muller, *Acc. Chem. Res.*, **23** (1990) 23.

[59] C. A. Bunton, F. Nome, F. H. Quina and L. S. Romsted, *Acc. Chem. Res.*, **24** (1991) 357.

[60] D. J. Stigter, *J. Chem. Phys.*, **68** (1964) 3603.

[61] D. W. R. Gruen, *Prog. Colloid Polym. Sci.*, **70** (1985) 6.

[62] E. Abuin, E. Lissi, P. S. Araujo, R. M. V. Alcixo, H. Chaimovich, N. Bianchi, L. Miola, and F. H. Quina, *J. Colloid Interface Sci.*, **96** (1983) 293.

[63] R. Bacaloglu, C. A. Bunton, G. Cerichelli and F. Ortega, *J. Phys. Chem.*, **47** (1973) 2531.

[64] C. A. Bunton, M. M. Mhala, J. R. Moffatt, *J. Phys. Chem.*, **93** (1989) 7851.

[65] L. S. Romsted, A General Kinetic Theory of Rate Enhancement for Reaction between Organic Substrates and Hydrophilic Ions in Micellar Systems. In *Micellization, Solubilization and Microemulsions*; K. L. Mittal, Ed.; Plenum: New York, 1977; Vol. **2**, pp 509-530.

[66] L. S. Romsted, *J. Phys. Chem.*, **89** (1985) 5107.

[67] D. Bratko and B. Lindman, *J. Phys. Chem.*, **89** (1985) 1437.

[68] C. A. Bunton, Micellar Reactions. In *Application of Biochemical Systems in Organic Chemistry*; J. B. Jones, C. J. Sih and D. Perlman, Eds.; Wiley: New York, 1976; Part 2, Chapter 4, pp 731-814.

[69] N. Shinozuka and S. Hayano, Electrochemical Investigations in Micellar Media. In *Solution Chemistry of Surfactants*; K. L. Mittal, Ed.; Plenum: New York, 1979; Vol. 2, pp 599-623.

[70] J. Texter, In Colloidal Electrochemistry - Genesis and Scope. In *Electrochemistry in Colloids and Dispersions*; R. A. Mackay and J. Texter, Eds.; VCH: New York, 1992; Chapter 1, pp 3-21.

[71] J. F. Rusling, Electrochemistry in Micelles, Microemulsions, and Related Microheterogeneous Fluids. In *Electroanalytical Chemistry*; A. J. Bard, Ed.; Dekker: New York, 1994; Vol. **18**, pp 1-88.

[72] J. R. Kirchhoff, J. D. Skelton, Jr., and K. T. Brooks, Electrochemical and Spectroelectrochemical Measurements in Sodium Dodecyl Sulfate Micellar Solutions as a Function of Electrolyte Concentration. In *Electrochemistry in Colloids and Dispersions*; R. A. Mackay and J. Texter, Eds.; VCH: New York, 1992; Chapter 4, pp 119-235.

[73] G. L. McIntire, *Crit. Rev. Anal. Chem.*, **21** (1990) 257.

[74] E. Dayalan and S. Qutubuddin and A. Hussam, *Langmuir*, **6** (1990) 715.

[75] M. Fujihira, M. Yanagisawa and T. Kondo, *Bull. Chem. Soc. Jpn.*, **66** (1993) 3600.

[76] R. Zana and R. Mackay, *Langmuir*, **2** (1986) 109.

[77] J. F. Rusling, C. N. Shi, T. F. Kumosinski, *Anal. Chem.*, **60** (1988) 1260.

[78] R. E. Verrall, S. Miloto, A. Giraudeau and R. Zana, *Langmuir*, **5** (1989) 1242.

[79] C. Treiner and A. Makayssi, *Langmuir*, **8** (1992) 794.

[80] E. Dayalan, S. Qutubddin and J. Texter, Micelle and Microemulsion Diffusion Coefficents. In *Electrochemistry in Colloids and Dispersions*; R. A. Mackay and J. Texter, Eds.; VCH: New York, 1992; Chapter 10, pp 119-135.

[81] J. Textor, F. R. Horch, S. Qutubuddin and E. Dayalan, *J. Colloid Interface Sci.*, **135** (1990) 263.

[82] S. A. Myers, R. A. Mackay and A. Brajter-Toth, *Anal. Chem.*, **65** (1993) 3447.

[83] S. Zhang and J. F. Rusling, *Environ. Sci. & Technol.*, **27** (1993) 1375.

[84] J. M. Rusling, Electrochemistry and Electroanalytical Catalysis in Microemulsions. In *Modern Aspects of Electrochemistry;* Plenum: New York, 1994; Number **26**, Chapter 2, pp 49-104.

[85] P. M. Bersier, L. Carlsson and J. Bersier, Electrochemistry for a Better Environment. In *Topics in Current Chemistry*; J. D. Dunitz, K. Hafner, S. Ito, J. -M. Lehn, K. N. Raymond, C. W. Rees, J. Thiem and F. Vogtle, Eds.; Springer: Berlin, 1994; Vol. **170**. pp 114-218.

[86] D. H. Evans, K. M. O'Connell, R. A. Peterson and M. J. Kelly, *J. Chem. Edu.*, **60** (1983) 290.

[87] A. J. Bard and L. R. Faulkner, In *Electrochemical Methods: Fundamental and Applications*; A. J. Bard, Ed.; Wiley: New York, 1980.

[88] D. J. Heinze, *Angew. Chem. Int. Ed. Engl.*, **23** (1984) 831.

[89] R. A. Mackay, S. A. Myers, L. Bodalbhai and A. Brajter-Toth, *Anal. Chem.*, **62** (1990) 1084.

[90] M. J. Hazelrigg and A. J. Bard, *J. Electrochem. Soc.*, **122** (1975) 211.

[91] D. Rong, Y. L. Kim and T. E. Mallouk, *Inorg. Chem.*, **32** (1993) 1454.

[92] A. E. Kaifer and A. J. Bard, *J. Phys. Chem.*, **89** (1985) 4876.

[93] A. B. Mandal and B. U Nair, *J. Phys. Chem.*, **95** (1991) 9008.

[94] J. Texter, Reaction, Convection, and Diffusion in Emulsion and Micellar Solution Voltammetry. In *Electrochemistry in Colloids and Dispersions;* R. A. Mackay and J. Texter, Eds.; VCH: New York, 1992; Chapter 15, pp 195-213.

[95] A. Owlia, Z. Wang and J. F. Rusling, *J. Am. Chem. Soc.*, **111** (1989) 5091.
[96] Y. Fujihira, T. Kuwana and C. R. Hartzell, *Biochem. Res. Commun.*, **61** (1974) 538.
[97] A. J. Bard, *J. Chem. Edu.*, **60** (1983) 302.
[98] C. P. Andrieux, P. Hapiot and J. M. Saveant, *J. Phys. Chem.*, **92** (1986) 5987.
[99] R. M. Wightman, *Science*, **240** (1988) 415.
[100] J. Heinz, *Angew. Chem. Int. Ed. Engl.*, **32** (1993) 1268.
[101] R. J. Forster, *Chem. Soc. Rev.*, **23** (1994) 289.
[102] J. W. Chen and J. Georges, *J. Electroanal. Chem.*, **210** (1986) 205.
[103] C. P. Andrieux, P. Hapiot and M. Saveant, *Chem. Rev.*, **90** (1990) 723.
[04] G. Porte, J. Appel and Y. Poggi, *J. Phys. Chem.*, **85** (1981) 2511.
[105] Z. Zin, J. J. Cai, L. E. Scriven and H. T. Davis, *J. Phys. Chem.*, **98** (1994) 5984.
[106] J. F. Goodman and T. Walker, Micellization in Aqueous Solution. In *Colloid Science*; D. H. Everett, Ed.; The Chemical Society: London, 1979; Vol. **3**, Chapter 5, pp 230-252.
[107] F. Husson and V. Luzzatti, *J. Phys. Chem.*, **68** (1964) 3504.
[108] P. Missel, N. Mazer, G. Benedek and M. C. Carey, *J. Phys. Chem.*, **87** (1983) 1264.
[109] S. Hayashi and S. Ikeda, *J. Phys. Chem.*, **84** (1980) 744.
[110] J. Ulmius, B. Lindman, G. Lindblom and T. Drakenberg, *J. Colloid Interface Sci.*, **65** (1978) 88.
[111] S. Hoffmann, A. Rauscher and H. Hoffmann, *Ber. Bunsenges. Phys. Chem.*, **95** (1991) 153.
[112] H. Hoffmann and G. Ebert, *Angew. Chem. Int. Ed. Engl.*, **27** (1988) 902.
[113] H. A. Bernes, *Colloids and surfaces* A, **91** (1994) 89.
[114] H. Hoffmann and H. Rehage, Rheology of surfactant solutions. In *Surfactant Solutions: New Method of Investigations: Surfactant Science Series*; R. Zana, Eds.; Dekker: New York, 1987; Vol. **22**, Chapter 4, pp 209-239.
[115] H. Rehage and H. Hoffmann, *J. Phys. Chem.*, **92** (1988) 4712.
[116] S. J. Candau, E. Hirsch and R. Zana, *J. Phys. (Paris)*, **45** (1984) 1263.
[117] C. Herb and R. Prud'homme, *ACS Symp. Ser.*, American Chemical Society: Washington DC, 1994; No. 578.
[118] C. -M. Chen and G. G. Warr, *J. Phys. Chem.*, **96** (1992) 9492.
[119] M. R. Anklam, R. K. Prud'homme and G. G. Warr, *AIChE J.*, **41** (1995) 677.
[120] P. Solyom and P. Ekwall, *Rheol. Acta*, **8** (1969) 316.
[121] J. L. Jones and T. C. B. McLeish, *Langmuir*, **11** (1995) 785.
[122] J. M. Franco, J. Munoz and C. Gallegos, *Langmuir*, **11** (1995) 669.
[123] I. Wunderlich, H. Hoffmann, H. Rehage, *Rheol. Acta*, **26** (1987) 532.
[124] Y. Hu, S. Q. Wang and A. M. Jamieson, *J. Phys. Chem.*, **98** (1994) 8555.
[125] A. White, *Nature*, **214** (1967) 585.
[126] T. A. Strivens, *Colloid Polym. Sci.*, **267** (1989) 269.
[127] I. Wunderlich, H. Hoffmann and H. Rehage, *Rheol. Acta.*, **26** (1987) 532.
[128] H. Hoffmann and W. Ulbricht, *Tenside Surfactants Deterg.*, **24** (1987) 1.
[129] P. S. Virk, *AIChE J.*, **21** (1975) 625.
[130] W. Interthal, G. Slebos and H. Wilski, *Proc. VIII. Int. Conf. on Slurry Transp.*, San Francisco, USA, 1983, pp 125.
[131] Th. F. Tadros, *Colloids and Surfaces* A, **91** (1994) 39.
[132] C. Manohar, *Current Science*, **67** (1994) 834.

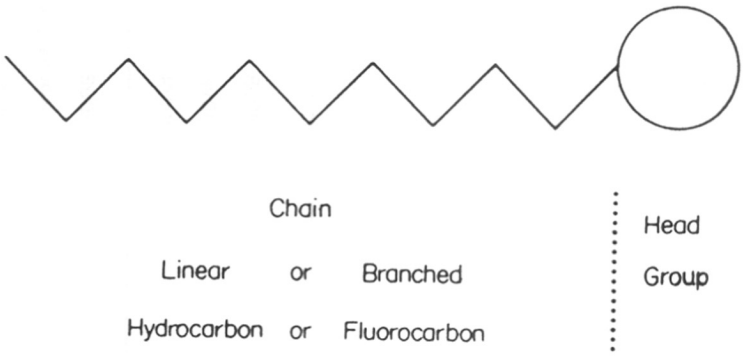

Figure 1.1 : Schematic diagram of surface active molecule.

[133] H. Hoffmann, *Adv. Mater.*, **6** (1994) 116.

[134] A. Moren, C. Harsten and R. Pap, *Handbook of Neural Computing Applications*; Academic: New York, 1990.

[135] J. Gasteiger and J. Zupan, *Angew. Chem. Int. Ed. Engl.*, **32** (1993) 503.

[136] J. A. Burns and G. M. Whitesides, *Chem. Rev.*, **93** (1993) 2583.

[137] M. T. Spining, J. A. Darsey, B. G. Sumpter and D. W. Noid, *J. Chem. Edu.*, **71** (1994) 406.

[138] N. V. Bhat and T. J. McAvoy, *Comp. Chem. Eng.*, **14** (1990) 573.

[139] P. D. Wasserman, *Neural Computing: Theory and Practice*; Van Nostrand Reinhold: New York, 1989.

[140] R. Hecht-Nielsen, *Neuro Computing*; Addision-Wesley: Reading, MA, 1990.

[141] I. Aleksander and H. Marton, *An Introduction to Neural Computing*; Chapmann & Hall: London, 1990.

[142] W. S. McCulloch and W. A. Pitts, *Bull. Math. Biol.*, **5** (1943) 115.

[143] T. Kohonen, *Neural Networks*, **1** (1988) 3.

[144] D. E. Rumelhart, G. E. Hinton and R. J. Williams, Learning Internal Representation by Error Propagation. In *Parallel Distributed Processing: Explorations in the Microstructures of Cognition*; D. E. Rumelhart and J. L. McClelland, Eds.; MIT: Cambridge, MA, 1988, Vol. **1**, pp 318-362.

[145] R. Hecht-Nielsen, *Appl. Optics*, **26** (1987) 4979.

[146] G. A. Carpenter and S. Grossberg, *IEEE Computer*, **21** (1988) 77.

[147] G. A. Carpenter and S. Grossberg, *Appl. Optics*, **12** (1987) 4919.

[148] B. Kosko, *Appl. Optics*, **26** (1987) 4947.

[149] J. J. Hopfield, *Proc. Natl. Acad. Sci.* USA, **79** (1982) 2554.

[150] J. J. Hopfield and D. W. Tank, *Science*, **233** (1986) 625.

[151] D. E. Rumelhart, G. E. Hinton and R. J. Williams, *Nature*, **323** (1986) 532.

[152] J. Zupan and J. Gastiger, *Neural Networks for Chemists*, VCH: Weinheim, 1993.

[153] B. G. Sumpter, C. Getino and D. W. Noid, *Ann. Rev. Phys. Chem.*, **45** (1994) 439.

[154] G. S. Hartley and D. F. Runnicles, *Proc. Roy. Soc. (London)*, **168 A** (1938) 420.

[155] M. E. L. McBain, *J. Am. Chem. Soc.*, **55** (1933) 545.

[156] D. Stigter, R. J. Williams and K. J. Mysels, *J. Phys. Chem.*, **59** (1955) 330.

[157] P. N. Pusey, Diffusion of Spherical Particles in Concentrated Dispersions. In *Physics of Amphiphiles: Micelles, Vesicles and Microemulsions*; V. Degiordio, Ed.; N-H: Netherland, 1985, pp 152-156.

[158] R. M. Weinheimer, D. F. Evans and E. L. Cussler, *J. Colloid Inteface Sci.*, **86** (1982) 1264.

[159] D. F. Evans, S. Mukherjee, D. J. Mitchell and A. B. Ninham, *J. Colloid Interface Sci.*, **93** (1983) 184.

[160] A. M. Cazabat, D. Chatency, D. Langevin, J. Meuiner and L. Leger, Mutual and Self Diffusion Coefficients of microemulsions from Spontaneous and Forced Light Scattering Techniques. In *Surfactants in Solution*; K. L. Mittal and B. Lindman, Eds.; Plenum: New York, 1984; Vol. **3**, pp 1729-1736.

[161] J. M. Brown and R. L. Elliot, Micellar Structure and Catalysis. In *Colloid Science*; D. H. Everett, Ed.; The Chemical Society: London, 1982; Vol. **4**, pp 180-190.

[162] R. E. Verrall, S. Miliot, A. Giraudeau and R. Zana, *Langmuir*, **5** (1989) 1242.

[163] M. T. Clarkson, D. Beaglehole, P. T. Callagham, *Phys. Rev. Lett.*, **54** (1985) 1722.

[164] R. M. Mazo, *J. Chem. Phys.*, **43** (1965) 2873.

[165] R. M. Weinheimer, D. F. Evans and E. L. Cussler, *J. Colloid Inteface Sci.*, **80** (1981) 357.

[166] G. D. Rees and B. H. Robinson, *Adv. Mater.*, **5** (1993) 608.

[167] L. -S. F. Rathman, A. G. Dastidar, A. W. Weimer and S. Kimura, *Chem. Engng. Prog.*, **April** 1994; pp 55-64.

[168] J. H. Fendler, *Chem. Rev.*, **87** (1987) 877.

[169] S. E. Friberg, *Adv. Colloid Interface Sci.*, **32** (1990) 167.
[170] M. E. Leser, K. Mrkoci, P. L. Luisi, *Biotechnol. Bioeng.*, **41** (1993) 489.
[171] G. M. Whitesides, J. P. Mathias and C. T. Seto, *Science*, **254** (1991) 1312.
[172] B. H. Robinson, *Nature*, **327** (1986) 309.
[173] A. S. Chhatre, R. A. Joshi and B. D. Kulkarni, *J. Colloid Interface Sci.*, **158** (1993) 183.
[174] B. K. Jha, A. S. Chhatre and B. D. Kulkani, *J. Chem. Soc. Perkin Trans.* 2, **6** (1994) 1383.
[175] D. O. Shah, *Surface Phenomena in Enhanced Oil Recovery*; Plenum: New York, 1981.
[176] J. S. Guo, M. S. El-Asser and J. W. Vanderhoff, *J. Polym. Sci.*, **27** (1989) 710.
[177] R. Laversanne, *Macromolecules*, **25** (1992) 489.
[178] L. M. Gan, K. C. Lee, C. H. Chew and S. C. Ng, *Langmuir*, **11** (1995) 449.
[179] P. Ayyub, A. N. Maitra and D. O. Shah, *Physica C*, **168** (1990) 571.
[180] R. L. Whetten and W. M. Gelbart, *J. Phys. Chem.*, **98** (1994) 3544.
[181] M. Goffredi and V. T. Liven, *Thermodynamic Acta*, **233** (1994) 187.
[182] P. Kumar, V. Pillai and D. O. Shah, *Appl. Phys. Lett.*, **62** (1993) 765.
[183] Y. -M. Tricot and J. H. Fendler, *J. Am. Chem. Soc.*, **106** (1984) 7359.
[184] H. Hirai, Sato and I. Komasawa, *Ind. Eng. Chem. Res.*, **32** (1993) 3015.
[185] D. O. Shah, *Materials Lett.*, **16** (1993) 68.
[186] L. Liz, M. A. L. Quintela, J. Mira and J. Rivas, *J. Mater. Sci.*, **29** (1994) 3797.
[187] M. A. L. Quitela, J. Rivas and J. Quiben, U.S. Patent No., **4,983,217** (1991).
[188] P. K. Dutta and D. Robins, *Langmuir*, **7** (1991) 1048.
[189] J. P. Chen, K. M. Lee, C. M. Sorensen, K. J. Klabumde and G. C. Hadjpanyis, *Nanophase Materials*, G. C. Hadjpanyis and R. V. Siegel, Eds.; Kluwer: Netherlands, 1994, pp 613-616.
[190] J. F. Scamehorn, R. T. Ellington, S. D. Christian, B. W. Penney, R. O. Runn and S. N. Bhat, *AICHE Sym. Ser.*, **82** (1982) 48.
[191] J. M. Winecek and S. Qutubuddin, *Sep. Sci. Technol.*, **27** (1992) 1407.
[192] A. S. Chhatre and N. K. Yadav and B. D. Kulkarni, *Sep. Sci. Technol.*, **28** (1993) 1465.
[193] J. F. Scamehorn and J. H. Harwell, An Overview of Surfactant-Based Separation Process. In *Surfactants in Emerging Technologies: Surfactant Science Series;* M. J. Rosen, Ed.; Dekker: New York, 1987; Vol. **26**, pp 169-185.
[194] W. L. Hinze and D. F. Armstrong, Ordered Media in Chemical Separation. In *ACS Symp. Ser.*; Americal chemical Society: washington, 1987, Vol. **342**.
[195] V. G. Gaikar and M. M. Sharma, *Sep. Purif. Methods*, **18** (1989) 111.
[196] R. S. Chawla, C. Porzucek, J. N. Cannon and J. H. Johnson, *Emerging Technologies in Hazardous Waste Management*. In *ACS Sympo. Ser.*; American Chemical Scociety: Washington, 1991, Vol. **468**.
[197] A. S. Abdul and T. L. Gibson, *Environ. Sci. Technol.*, **25** (1991) 665.
[198] S. Laha and R. G. Luthy, *Environ. Sci. Technol.*, **25** (1991) 1920.
[199] B. N. Aronstein, Y. M. Calvillo and M. Alexander, *Environ. Sci. Technol.*, **25** (1991) 1728.
[200] E. Pramauro, A. B. Prevot, P. Savarino, G. Viscardi, M. D. Guardia and E. P. Cardells, *Analyst*, **118** (1993) 23.
[201] J. F. Scamehorn and J. H. Harwell, Surfactant-Based Treatments of Aqueous Process streams. In *Surfactants in Chemical/Process Engineering: Surfactant Science Series*; D. T. Wasan, M. E. Ginn and D. O. Shah, Eds.; Dekker: New York; 1988, Vol. **28**, pp 78-122.
[202] K. Kandori, K. Kon-no, A. Kitahara, *J. Disp. Sci. Technol.*, **9** (1988) 61.

[203] S. S. H. Rizvi, A. L. Benado, J. A. Daniels, *Food Technol.*, **June** 1989, pp 55.

[204] K. Larsen, Emulsions in the Food Industry. In *Emulsions - A Fundamental and Practical Approach*; J. Sjoblom, Ed., Kluwer Academic: Dordrecht, 1992.

[205] R. Leung and D. O. Shah, Microemulsion: An Evolving Technology for Pharmaceutical Applications. In *Controlled Release of Drugs: Polymers and Aggregate Systems*; M. Rosoff, Ed.; VCH: New York, 1989; Chapter 6, pp 185-215.

[206] M. J. Lawrence, *Chem. Soc. Revs.*, **23** (1994) 417.

[207] D. W. Osborne, A. J. I. Ward and K. J. O.' Neill, *J. Pharm. Pharmacol.*, **43** (1991) 451.

[208] T. Skodrin and J. Sjoblom, *J. Colloid Interface Sci.*, **155** (1993) 392.

[209] A. Luzar and D. Bratko, *J. Chem. Phys.*, **92** (1990) 642.

[210] K. Martinek, A. V. Levashov, N. Klyachko, Y. L. Khelnitski and I. V. Berezin, *Eur. J. Bio. Chem.*, **155** (1986) 453.

[211] P. D. I. Fletcher, G. D. Rees, B. H. Robinson, R. B. Freedom, *Biochim. Biophys. Acta*, **832** (1985) 204.

[212] H. Stamatis, A. Xenakis, M. Provelegiou and K. N. Kolisis, *Biotechnol. Bioeng.*, **42** (1993) 103.

CHAPTER 2

INTERFACIAL SOLUBILIZATION AND DECARBAMOYLATION OF AMINO ACID DERIVATIVE

2.1 INTRODUCTION

Interfacial solubilization by micellar solutions and microemulsions is an established phenomena. The interfacial properties of the micellar globule such as surface pressure and bending moment affects the solubilization [1, 2] of the reactant as does the type of organic solvent used, the nature of free ions, the electric charge state and hydrophobicities of the solute [3]. These properties and their effect on the structure, dynamics and interactions of the pseudo-phases have been elucidated by studying and analyzing the relevant phase behavior. The most important properties of micellar solutions have been exploited in variety of instances like facilitation and regulation of the growth process for particles of polymers [4, 5], separation and purification [6] and in enhancing the rates of chemical reactions [7-9]. Enhancement in the reaction performance has been attributed, in many cases, to the interfacial solubility of the substrate. It can be noted here that besides solubilization studies, the phase behavior studies of systems involved in such reactions are also important from process optimization point of view.

Micellar solutions are considered to be models of biological membranes and have been used to gain insights into protein solubilization, structure and activity within the membrane [10]. In some of the recent papers, studies in the solubilization of amino acids and their derivatives into microemulsions and super critical fluids have been reported [3, 11]. It is therefore conceivable that micellar solutions can be used as media for carrying out reactions involving amino acids. Amino acids play important role as physiologically active components and are extensively used in pharmaceutical industry as intermediates and as starting compounds in production of β-lactam antibiotics, peptide hormones, pyrethroids, and others. Optically active amino acids like D(-) phenylglycine, D(-)-p-hydroxyphenylglycine, etc are useful starting materials in the preparation of semi-synthetic penicillins and cephalosporins such as amoxicillin, cephadroxil, cefatrizine, cefaparole and cefaperazon.

The conventional method of preparation of an optically active amino acid, for example D(-) phenylglycine, involves preparation of DL-5-phenylglycine hydantoin from benzaldehyde, potassium cyanide and ammonium carbonate by Strecker's method [12]. Hydrolysis of the

DL-5-phenylglycine hydantoin [13] gives a racemic mixture of phenylglycine which is later resolved using resolving agents, or by converting into esters of phenylglycine. The chemical resolution process involves a large number of operational steps which include recovery and recycle of the resolving agents. Recently, an enzymatic process for hydrolysis of a mixture of racemic hydantoins has been reported [14]. This process has been found to yield optically active D(-)-N-carbamoyl derivative of the amino acid having high optical purity. Decarbamoylation of the D(-)-N-carbamoyl derivative of the amino acid is then carried out by treating the derivative with nitrous acid under acidic conditions to yield the corresponding D(-) amino acid [15, 16]. The scheme for decarbamoylation of D(-)-N-carbamoyl phenylglycine to D(-) phenylglycine is given as follows (Scheme 2.1).

Scheme 2.1

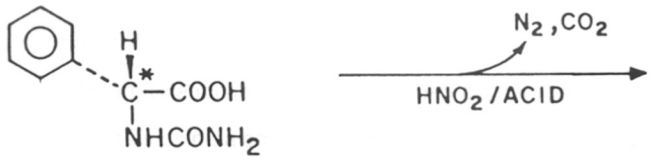

D(-)-N-Carbamoyl phenylglycine

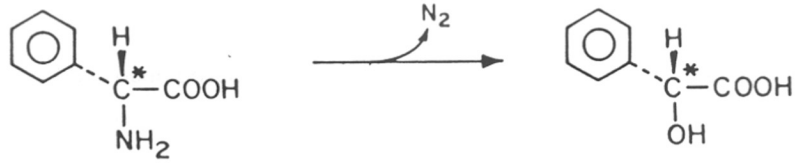

D(-) Phenylglycine D(-) Mandelic acid

The last reaction is customarily a heterogeneous reaction, wherein D(-)-N-carbamoyl phenylglycine forms a separate solid phase with nitrous acid due to its poor solubility. The

conventional process of decarbamoylation of D(-)-N-carbamoyl phenylglycine reaction is very slow due to poor solubilities of the reagents and mass transport limitations. The amount of mineral acid such as sulfuric acid or hydrochloric acid required for the reaction is very high; a typical batch of one mole of D(-)-N-carbamoyl phenylglycine may require about 4 mol/liter of mineral acid for the reaction. The product formed is isolated from the reaction mixture by concentrating the solution and neutralizing the excess acid with an alkali. This results in formation of mineral salts with which the product gets contaminated. The reaction is usually carried out in a batch mode. Also, as a consequence of other parallel reactions between the product D(-) phenylglycine and the excess nitrous acid, unwanted by-products such as mandelic acid and benzaldehyde are formed. Benzaldehyde consequently gets oxidized in the reaction mixture to form benzoic acid, which adds to the by-products of the reaction. Due to these consecutive parallel reactions, the overall rate and hence the percent yield of the reaction is low.

In this chapter we analyze the effect of dilute aqueous micellar or microemulsion solutions of sulfuric acid on the interfacial solubility of D(-)-N-carbamoyl phenylglycine. We also report the results of the decarbamoylation reaction of the D(-)-N-carbamoyl phenylglycine carried out under micellar conditions by using a concentrated aqueous solution of sodium nitrite. This has circumvented the step of concentrating the reaction mixture for product isolation which is generally followed in the conventional route. Since the decarbamoylation reaction is an exothermic reaction and generates large quantities of gas (N_2 and CO_2), so by choosing sodium nitrite as a limiting component and by introducing the sodium nitrite solution into the reaction mixture diligently, it has been possible, by and large, to eliminate the side reactions between the product D(-) phenylglycine and the nitrous acid. Enhancement in interfacial solubility has enhanced the overall rate of the reaction, the selectivity and hence the percent yield.

2.2 EXPERIMENTAL

2.2.1 Materials

AR grade sodium dodecyl sulfate (SDS) was obtained from Loba Chemicals and was used without further purification. Pentan-1-ol (AR grade) was a Fluka guaranteed material. Concentrated H_2SO_4 was obtained from SD chemicals and was diluted using distilled water. The exact concentration of H_2SO_4 was determined by titration with standardized 0.5 *N* and 1.0 *N* sodium hydroxide solutions. Sodium nitrite was AR grade Aldrich material. The D(-)-N-carbamoyl derivative of phenylglycine (denoted as N.Carb) was chemically synthesized in the laboratory and was purified by recrystallization [13]. AR grade of D(-) phenylglycine (denoted as PG) was obtained from Sigma and was used as standard material for the analysis.

2.2.2 Methods

2.2.2.1 Phase diagrams and solubilization studies

The ternary phase diagram for the system consisting SDS, water and pentan-1-ol has been reported earlier by Clausse et al. [17]. In the present study, isothermal (25 ^{o}C) pseudo-ternary phase diagrams were constructed experimentally for various systems incorporating SDS as the surfactant, H_2SO_4 of different concentrations as the aqueous phase, and pentan-1-ol as the water-insoluble component using the procedure described in the literature [18, 19]. The partial phase diagrams are shown in Figures 2.1 through 2.4. For determining the solubilities of D(-)-N-carbamoyl phenylglycine in micellar and microemulsions solutions of SDS in sulfuric acid, a few representative points were chosen from these phase diagrams to decide the optimum initial starting composition of the micellar/microemulsion mixtures. Referring to the insets of Figures 2.2 through 2.4, these points have been marked as mi_1 through mi_{14} representing different micellar solutions and me_1 through me_{10} representing different microemulsion solutions. Accurately weighed (slightly excess) amounts of D(-)-N-carbamoyl phenylglycine was added to 100 ml of each of these micellar and microemulsion solutions. The excess undissolved D(-)-N-carbamoyl phenylglycine was immediately removed by vacuum filtration using Whatman No. 1 filter paper. The same experiment was repeated for

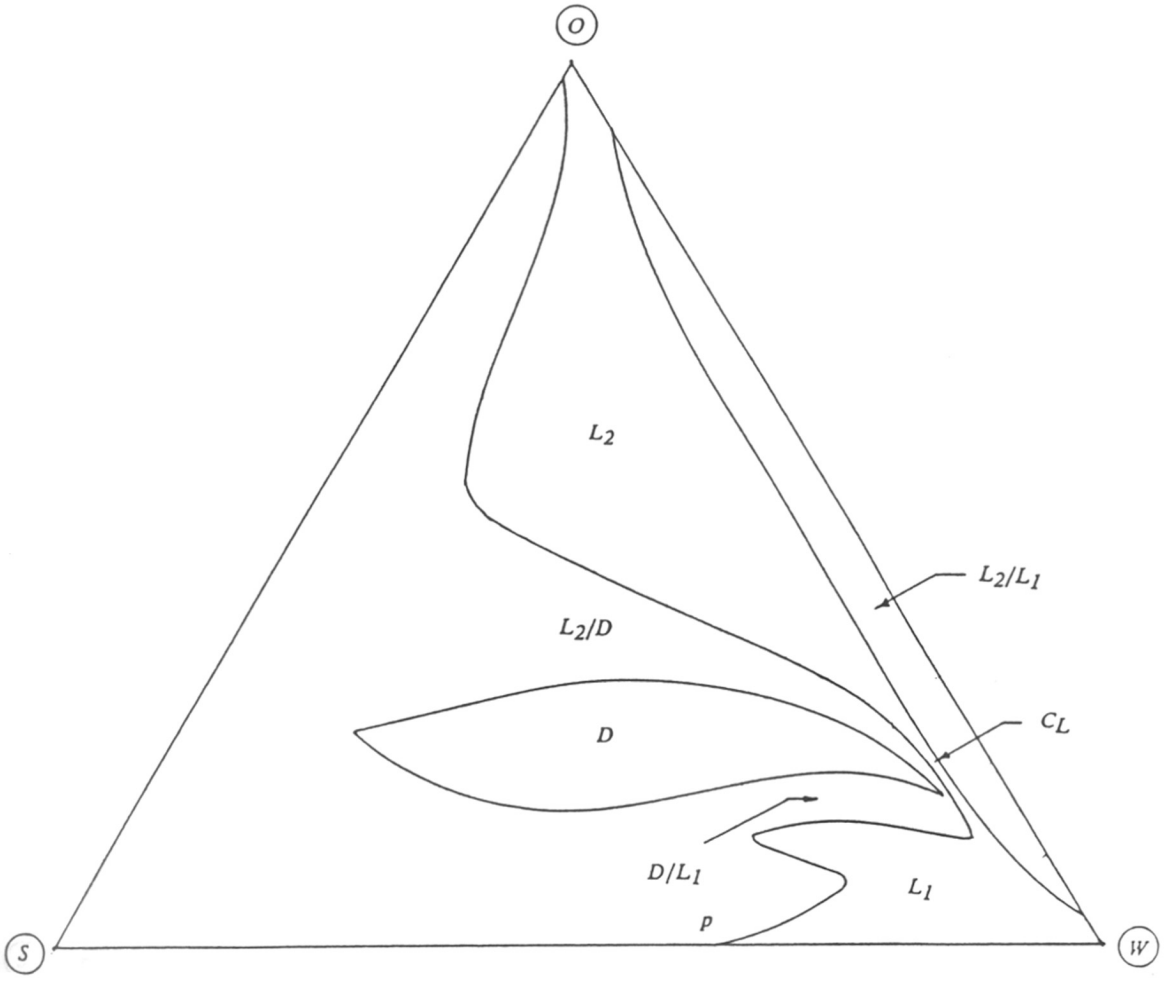

Figure 2.1 : Ternary phase diagram of the system SDS (S)/water (W)/pentan-1-ol (O). L_1 and L_2 are, respectively, the regions of "direct" and "indirect" solubilization. C_L is the channel connecting L_1 and L_2. D is the region of monophasic lamellar liquid crystals. (Adapted from Ref. 26).

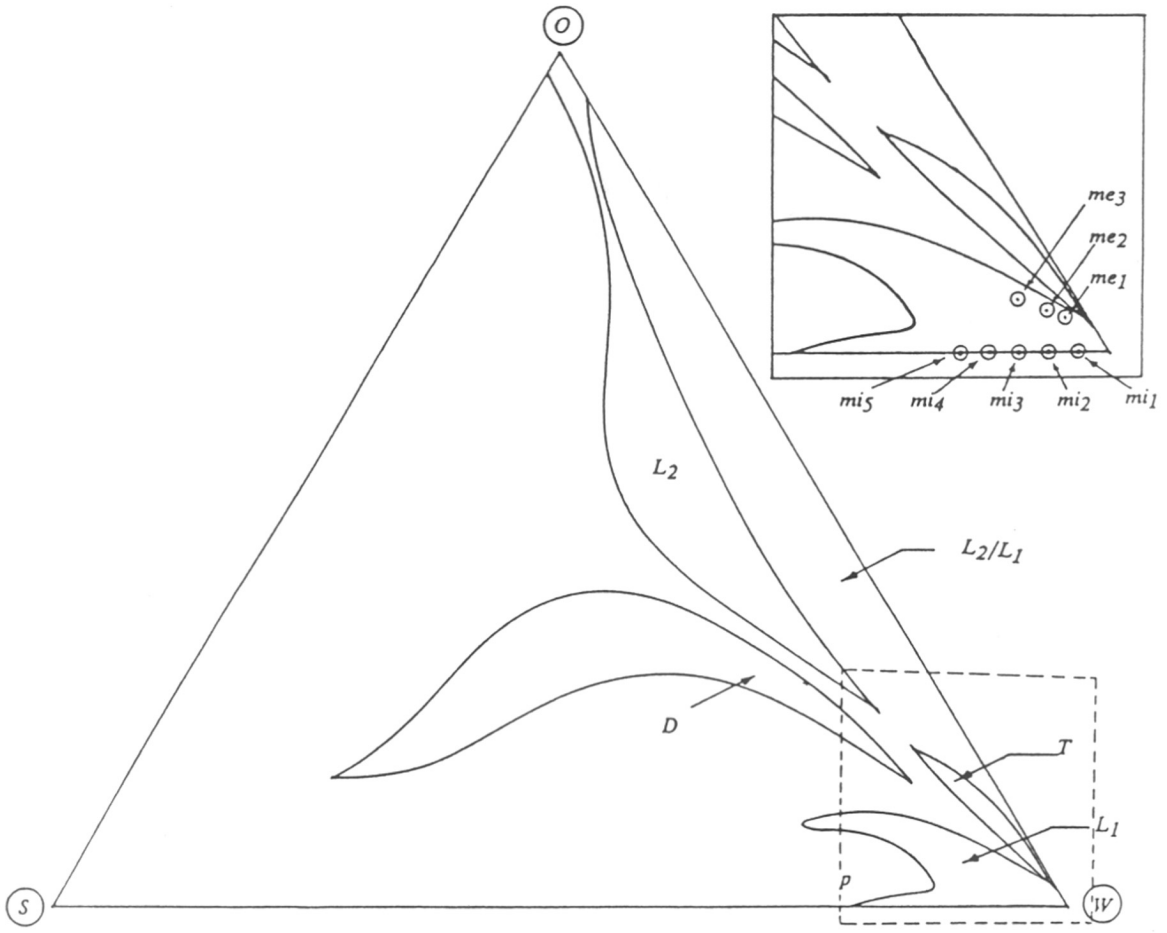

Figure 2.2 : Pseudoternary phase diagram of the system SDS (S)/0.54 *N* H_2SO_4 (W)/pentan-1-ol. L_1 and L_2 are, respectively, the regions of "direct" and "indirect" solubilization. *T* is the region of monophasic lamellar liquid crystals. (Inset: The aqueous corner showing the experimental points representing the compositions used in solubilization studies).

Table 1.1 : Representative Surfactants

Type	Chemical name	Molecular formula	Abbreviations
Anionic	Sodium dodecyl sulfate	$CH_3(CH_2)_{11}OSO_3^-Na^+$	SDS
	Sodium bis(2-ethylhexyl) sulfosuccinate	$CH_3(CH_2)_3CHCH_2OOC]_2CHSO_3^-Na^+$	Aerosol OT (AOT)
	Sodium p-dodecylbenzenesulfonate	$p\text{-}CH_3(CH_2)_{11}(C_6H_4)SO_3^-Na^+$	SDBS
Cationic	Cetyltrimethylammonium bromide	$CH_3(CH_2)_{15}N(CH_3)_3^+Br^-$	CTAB
	Didoceyldimethylammonium bromide	$[CH_3(CH_2)_{11}]_2N(CH_3)_2^+Br^-$	DDAB
	Hexadecylpyridinium bromide	$CH_3(CH_2)_{15}Py^+Br^-$	HDPB
Zwitterionic	Dodecyldimethylammonio acetate (dodecyl n- betaine)	$CH_3(CH_2)_{11}N^+(CH_3)_2CH_2COO^-$	DODAA (B-12)
	Tetradecyldimethylamine oxide	$C_{14}H_{29}\text{-}N(CH_3)_2O$	TDMAO (C_{14}DMAO)
	Hexadecylsulfo betaine	$C_{16}H_{33}N^+Me_2(CH_2)_3SO_3^-$	SB3-16
Non-ionic	Sorbitan monolaurate	$CH_3(CH_2)_9CH_2CO\text{-}OCH_2\text{-}CHOH\text{-}(C_4H_5O)\text{-}(OH)_2$	Span 20
	Polyoxyethylene (10)-cetyl ether	$CH_3(CH_2)_{15}(OCH_2CH_2)_{10}OH$	Brij-56
	Polyoxyethylene (23)-dodecyl ether	$CH_3(CH_2)_{11}(OCH_2CH_2)_{23}OH$	Brij-35
	1-(1,1-Dimethyl-3,3-dimethyl-butane) -4-polyoxyethylene (9.5)	$(CH_3)_3CCH_2C(CH_3)_2\text{-}(C_6H_4)\text{-}(C_2H_4O)_{9.5}OH$	Triton 100 (TX-100)

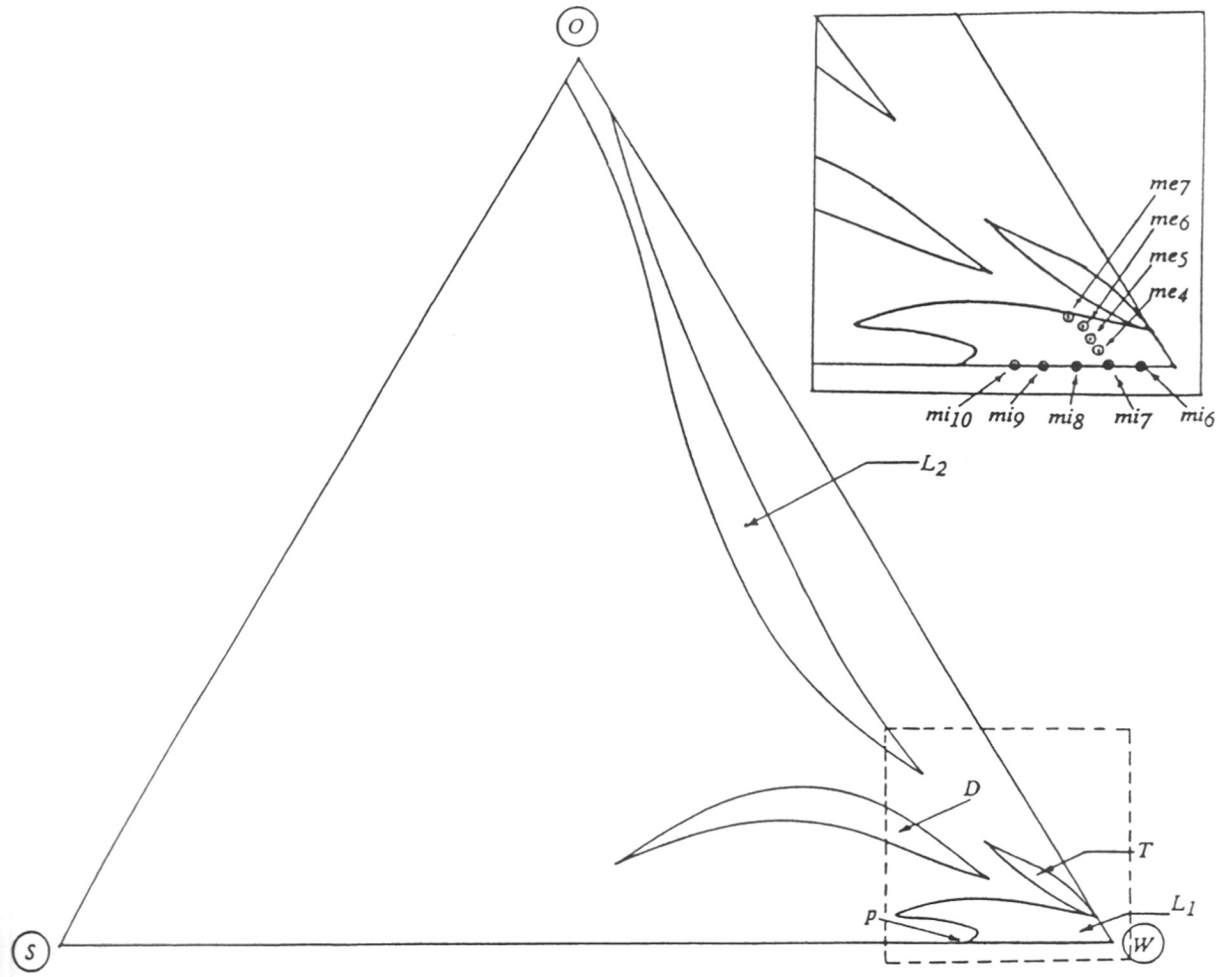

Figure 2.3 : Pseudoternary phase diagram of the system SDS (S)/1.08 *N* H_2SO_4 (W)/pentan-1-ol. L_1 and L_2 are, respectively, the regions of "direct" and "indirect" solubilization. *T* is the region of monophasic lamellar liquid crystals. (Inset: The aqueous corner showing the experimental points representing the compositions used in solubilization studies).

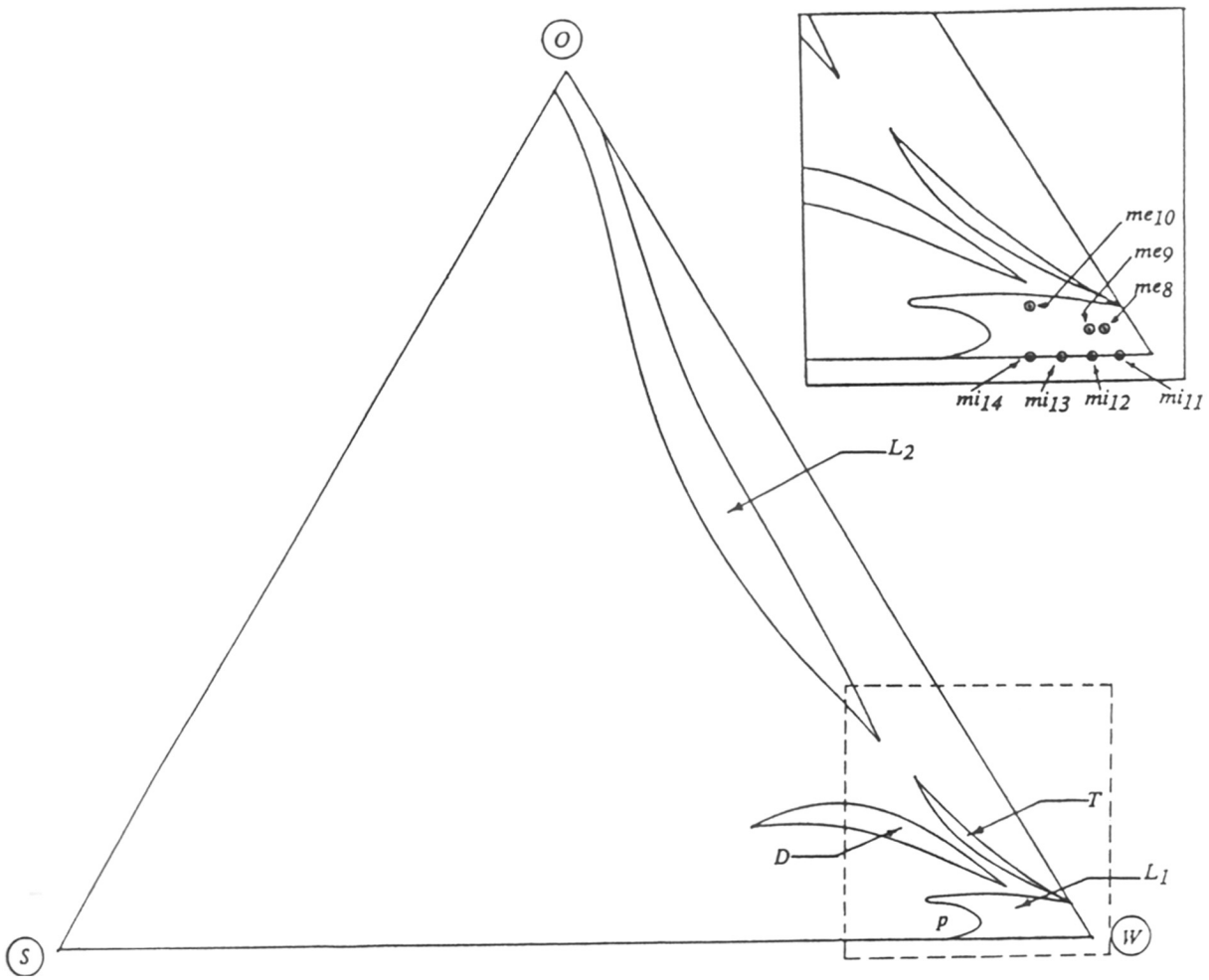

Figure 2.4 : Pseudoternary phase diagram of the system SDS (S)/2.16 *N* H_2SO_4 (W)/pentan-1-ol. L_1 and L_2 are, respectively, the regions of "direct" and "indirect" solubilization. *T* is the region of monophasic lamellar liquid crystals. (Inset: The aqueous corner showing the experimental points representing the compositions used in solubilization studies).

determination of solubilities of D(-)-N-carbamoyl phenylglycine in distilled water and aqueous solutions of H_2SO_4 of various strengths (that is, the composition representing the "W" vertex in each of the phase diagrams). This was done in order to compare the effect of micellar and microemulsion solutions on the solubilities of D(-)-N-carbamoyl phenylglycine. The solubility of D(-)-N-carbamoyl phenylglycine in each of the above solutions was measured by High Performance Liquid Chromatograph (HPLC) analysis of the filtrate. The amount of undissolved D(-)-N-carbamoyl phenylglycine was determined for mass balance by repeatedly washing the residue with minimum amount of distilled water, drying and finally, weighing the residue accurately. Table 2.1 gives the percent SDS content (wt/vol) of various micellar solutions and the solubility of D(-)-N-carbamoyl phenylglycine in each of these micellar solutions. Tables 2.2 gives the composition of various microemulsions and the solubility of D(-)-N-carbamoyl phenylglycine in each of these microemulsion solutions. Table 2.3 gives the solubility of D(-)-N-carbamoyl phenylglycine in aqueous solutions of sulfuric acid with varying normalities.

2.2.2.2 Optimizing the composition of the reaction mixture

Referring to Table 2.2 it can be noted that the maximum solubility of D(-)-N-carbamoyl phenylglycine is about 41.91 mg/ml in a microemulsion comprising 4% (wt/wt) SDS, 93% (wt/wt) 1.08 *N* H_2SO_4 and 3% (wt/wt) pentan-1-ol. This composition is represented by the point me_6 in Figure 2.3 and Table 2.2. We also observe a solubility of about 41.72 mg/ml in the case of a micellar solution of SDS in 1.08 *N* H_2SO_4 represented by point mi_7 in Figure 2.3 and Table 2.1. Since there is hardly any difference between these solubilities, the composition nearby that of the micellar solution denoted by point mi_7 was chosen as the starting composition of the reaction medium, thereby avoiding the inclusion of pentan-1-ol as extra component in the reaction mixture.

Table 2.1 : Solubility of D(-)-N-carbamoyl Phenylglycine in Various Micellar Solutions of Dilute Sulfuric Acid

% SDS	Solubility (mg/ml) in micellar solution		
(wt/vol)	0.54 *N* H_2SO_4	1.08 *N* H_2SO_4	2.16 *N* H_2SO_4
2	13.41 (mi_1)*	15.15 (mi_6)	11.01 (mi_{11})
4	16.07 (mi_2)	41.72 (mi_7)	36.20 (mi_{12})
6	15.75 (mi_3)	33.11 (mi_8)	20.94 (mi_{13})
8	10.23 (mi_4)	17.57 (mi_9)	15.13 (mi_{14})
10	8.07 (mi_5)	12.26 (mi_{10})	-

* mi_1 through mi_{14} represent various points on the corresponding phase diagrams.

Table 2.2 : Solubility of D(-)-N-carbamoyl phenylglycine in a Microemulsion System SDS/Pentan-1-ol/Sulfuric Acid

	Point	% SDS (wt/wt)	% Acid (wt/wt)	% Pentan-1-ol (wt/wt)	Volume /ml	% SDS (wt/vol)	Solubility (mg/ml)
	me_1*	1.4	96.1	2.5	98.1	1.43	9.21
0.54 *N*	me_2	2.0	95.0	3.0	97.3	2.05	13.88
H_2SO_4	me_3	4.0	92.0	4.0	98.2	4.07	19.25
	me_4	4.0	95.0	1.0	98.4	4.06	40.12
1.08 *N*	me_5	4.0	94.0	2.0	97.3	4.11	41.33
H_2SO_4	me_6	4.0	93.0	3.0	96.3	4.15	41.91
	me_7	4.5	91.0	4.5	96.1	4.68	37.24
	me_8	2.0	96.0	2.0	98.4	2.03	11.49
2.16 *N*	me_9	3.0	95.0	2.0	98.5	3.04	24.01
H_2SO_4	me_{10}	6.0	90.0	4.0	96.3	6.23	21.22

* me_1 through me_{10} represent various points on the corresponding phase diagrams.

Table 2.3 : Solubility of D(-)-N-carbamoyl Phenylglycine at 25 °C Measured as Function of the Normality of H_2SO_4

No.	Normality of H_2SO_4	Solubility (mg/ ml)
1	0.00	1.36
2	0.54	1.32
3	1.08	1.158
4	2.16	0.55

2.2.2.3 Micellar solution and decarbamoyaltion reaction

The initial composition of various reaction mixtures (Runs 1 through 7) is shown in Table 2.4. The general procedure for preparing the micellar solutions and conducting the decarbamoylation reaction is as follows. The micellar solution of SDS in 1.08 *N* H_2SO_4 was prepared by mixing an accurately weighed amount of SDS in the acid, and stirring well. To a fixed volume of this micellar solution, D(-)-N-carbamoyl phenylglycine was added so as to make the final concentration of D(-)-N-carbamoyl phenylglycine in the micellar solution to about 40 mg/ml. The micellar solution of D(-)-N-carbamoyl phenylglycine in H_2SO_4 was transferred to a stirred cell reactor and then cooled to 5 ^{o}C using ice-salt mixture. It was found that the micellar solution was quite stable even at this temperature. A concentrated aqueous solution of slight excess of acid-equivalent amount of sodium nitrite was introduced very slowly into the reaction mixture from the bottom of the stirred cell, is shown in Figure 2.5. Enough care was taken to maintain the reaction mixture temperature around 5 ^{o}C. The speed of rotations of the stirrer was maintained at 50 ± rpm. After 3 hours of the reaction the stirring was stopped, and the pH of the mixture was adjusted to around 6.5 using sodium hydroxide solution. The product was obtained as a precipitate (Crop I), which was removed by vacuum filtration using Whatman No. 1 filter paper. A further addition of the alkali to the filtrate solution ensured breaking of the micelles and hence the separation of the solubilized product from the micellar phase (Crop II). These two crops were mixed and purified by repeatedly washing with minimum amount of distilled water, drying the product and finally, weighing it accurately.

2.2.2.4 Product analysis by high performance liquid chromatograph (HPLC) and optical purity measurement

The product was then analyzed for its chemical purity by HPLC. The amount of unreacted D(-)-N-carbamoyl phenylglycine and the dissolved product D(-) phenylglycine remaining in the filtrate was also measured immediately by HPLC analysis to obtain the mass balance. The analysis method was developed on a Millipore-Waters (Milford, MA, USA) HPLC system consisting of a model 510 dual head reciprocating solvent delivery pump, a Rheodyne (Cotati,

Table 2.4 : Initial Composition of the Reaction Mixtures with 1.08 *N* H_2SO_4 (Run Nos. 1-7)

Run No.	Amount of the components					
	SDS / gm	Acid / ml	N.Carb / gm	$NaNO_2$ / gm	H_2O / ml	Total vol. / ml
1	2.0	50.0	2.2	0.79	10	63
2	2.0	50.0	2.0	0.79	10	62
3	5.1	125.0	5.0	2.00	25	156
4	20	500	20	8.0	100	635
5	20	500	20	8.0	100	634
6	50	1250	50	20	250	1540
7	80	2000	80	40	110	2240

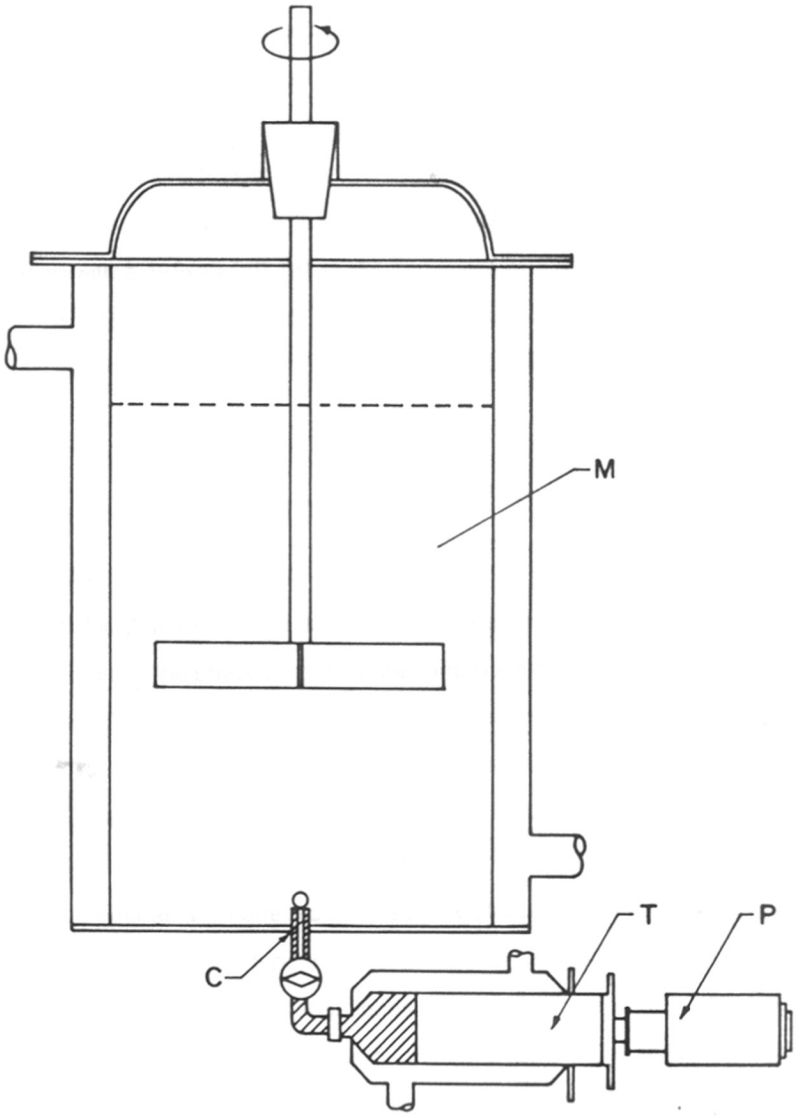

Figure 2.5 : Schematic diagram of the stirred cell reactor used for decarbamoylation of D(-)-N-carbamoyl phenylglycine. M :- micellar solution; C :- capillary of known diameter; P :-automatic plunger; T :- thermostatic syringe.

CA, USA) model 7125 injector and a Model 440 filter photometric absorbance detector operating at 254 nm. The analogue output of the detector was recorded and processed with a Hewlett-Packard (Avondale, CA, USA) model 3390A integrator. A Waters Radial-PAK μ Bondapak phenyl (1 dp 10 m μ) cartridge column (8 mm i.d. × 10 cm) with Waters Z-module radial compression mounting system was used. The mobile phase consisted of a mixture of methyl alcohol and 10 mmol triethyl ammonium phosphate buffer (pH 2.6) in the ratio of 10:80. The flow rate of the mobile phase was maintained at 2.0 ml/min.

The product was also analyzed for its steric configuration and optical purity by measuring the optical rotation with a JASCO DIP-181 make digital polarimeter. This was done by determining the specific rotation of sample of D(-) phenylglycine in 1.0 *N* hydrochloric acid. The obtained specific rotation was -158± 0.6° similar to the earlier reported value by Schawatrz et al. [20].

2.3 RESULTS AND DISCUSSION

2.3.1 Effect of acid concentration on phase behavior

Figures 2.1 through 2.4 show the partial phase behavior of various microemulsion and micellar systems studied. The phase diagrams are composed of various domains such as the *D* region composed of monophasic lamellar liquid crystals, the L_1 region composed of oil-in-water or "direct" type of solubilization, and the L_2 domain composed of water-in-oil or "reverse" type of solubilization. In the case of the system SDS/water/pentan-1-ol, a narrow channel C_L connects the L_1 and L_2 domains (Figure 2.1). The "direct" and "inverse" types of micellar domains appear as all-in-one block. In such a situation, no solubilization gap exists between these domains, and such type of behavior has been classified as type *U* by Clausse et al. [21]. Increasing the acid concentration leads to two separate and distinct regions of the "direct" and the "inverse" types (Figures 2.2 through 2.4). Such a situation has been classified as type *S*. Also, rather unexpectedly, a three phase domain denoted by *T* appears in the phase diagrams constituting sulfuric acid. These phase diagrams reveal various changes occurring in the phase behavior when the acid strength is increased. One of the most significant changes

micelles [11] (from the Latin <<micelle>> meaning small bit) formed beyond the CMC concentrations are of globular shape, in which the hydrocarbon chains are in the middle, avoiding contact with water, and the hydrophilic groups are at the surface. The driving force for the micelle formation is the hydrophobic interaction, which tries to minimize the energetically unfavorable contact between the hydrocarbon part and water while simultaneously retaining the polar part in aqueous environment [12]. The CMC's have been determined for numerous systems and are tabulated in various publications [13]. The critical concentration of surfactant molecules depends on the size of the hydrophobic part of the molecules and to some degree on the hydrophilic group, in particular whether it is ionic or nonionic [9, 12]. Aggregation behavior of surfactants is strongly co-operative and can, depending on conditions (concentration, temperature, electrolyte etc), give aggregate of various sizes and geometries [14, 15]. Figure 1.2 outlines the schematic configurations of surfactant aggregation in aqueous solution.

Various configurations of defined molecular architecture include micelles, reverse micelles, microemulsions, liquid crystals, black lipid membranes (BLMs) and vesicles etc [4]. Since the orientation and organization by solute molecules are common characteristics, these solutions (systems) are designated as organized solutions [16]. These systems are pseudophase systems and the solution properties as a function of concentration resemble those of two-phase mixtures (i.e., dilute solution of solvent + dispersed organized particles). They are not a random mixture of solute and solvent molecules, but a combination of solvent molecules and organized solute molecules (50-400) [17, 18]. Table 1.2 summarizes the various characteristics of the organized surfactant assemblies.

1.3 SOLUBILIZATION AND PHASE MAPS

One of the important properties of surfactant aggregates is their role in the solubilization process [19, 20]. Solubilization process has been defined by McBain and Hutchinson (1955) as *a particular mode of bringing into solution substances that are otherwise insoluble in a given medium, involving the previous presence of a colloidal solution whose particles take up and incorporate within or upon themselves the otherwise insoluble material* [21]. However, modern definition broadens the earlier definition of solubilization process and implies the preparation of

observed is that on increasing the normality of the acid the D, L_1, and the L_2 domains shrink in size. Another notable change is that the channel C_L disappears on increasing the acid strength. The solubility of SDS in the acid is represented by the point p on the phase diagram. The point p is found to move towards the W apex of the diagram on increasing the normality of the acid, indicating a decrease in the solubility of SDS in the acid.

2.3.2 Effect of surfactant concentration on the solubilities of D(-)-N-carbamoyl phenylglycine

Figures 2.6 through 2.8 show solubilities of D(-)-N-carbamoyl phenylglycine obtained as a function of the surfactant concentration. It is observed that the solubility of D(-)-N-carbamoyl phenylglycine in distilled water at 25 ^{o}C is 1.36 mg/ml. As it is evident from Table 2.3, the solubility decreases as a function of the H_2SO_4 concentration, from 1.36 mg/ml for distilled water to 0.55 mg/ml for 2.16 N H_2SO_4. A notable unusual feature of the solubilities of D(-)-N-carbamoyl phenylglycine as a function of the percent surfactant, observed in micellar and microemulsion solutions, is that the solubility initially increases and reaches a maximum at around 4% SDS (wt/vol). It then decreases as the concentration of the surfactant is increased further. In the case of 0.54 N H_2SO_4 micellar and microemulsion solutions (Figure 2.6), the microemulsion solubilizes more of the D(-)-N-carbamoyl phenylglycine than its micellar counterpart. The maximum solubility in these cases is about 19.25 mg/ml. The same trend is observed in the case of 1.08 N H_2SO_4, but the maximum solubilities obtained are almost comparable. However, in case of 2.16 N micellar and microemulsions, the micellar solution is found to solubilize D(-)-N-carbamoyl phenylglycine to a greater extent than their microemulsion counterparts.

The maxima observed in the interfacial solubilities of D(-)-N-carbamoyl phenylglycine as function of surfactant concentration in all the above cases can be explained as follows. Surfactants in solution are known to aggregate and they partition themselves at the oil-water interface, or at the surface of the micellar globule. The micellar aggregation occurs only above a certain concentration of the surfactant, called as the critical micelle concentration (CMC). In

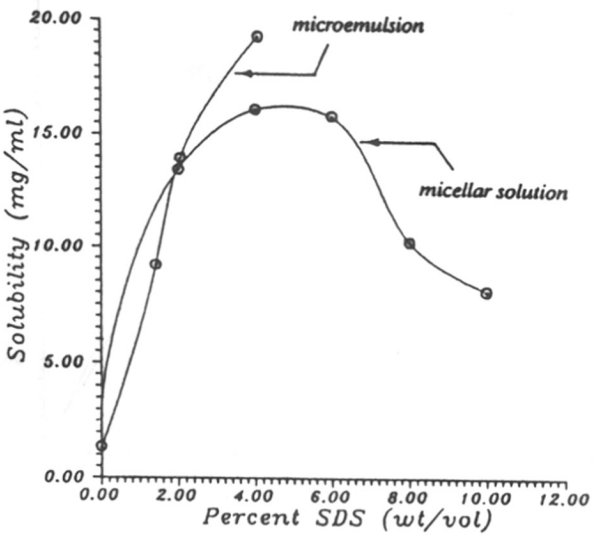

Figure 2.6 : Solubility of D (-)-N-carbamoyl phenylglycine (mg/ml) in 0.54 *N* H_2SO_4 micellar and micro-emulsion solutions as a function of the concentration of SDS expressed as percent (wt/vol).

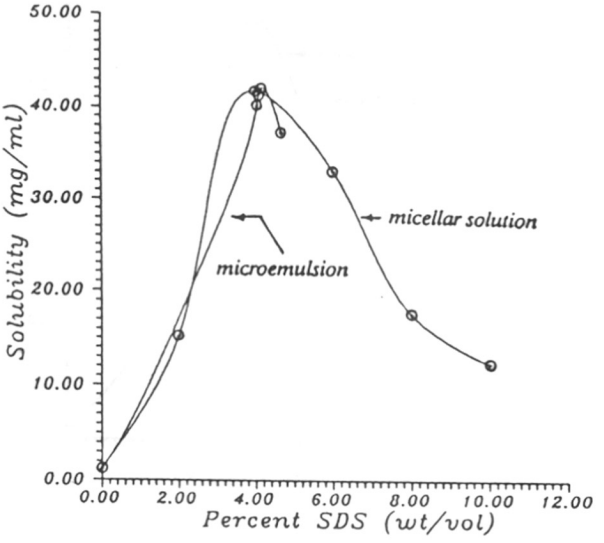

Figure 2.7 : Solubility of D (-)-N-carbamoyl phenylglycine (mg/ml) in 1.08 *N* H_2SO_4 micellar and microemulsion solutions as a function of the concentration of SDS expressed as percent (wt/vol).

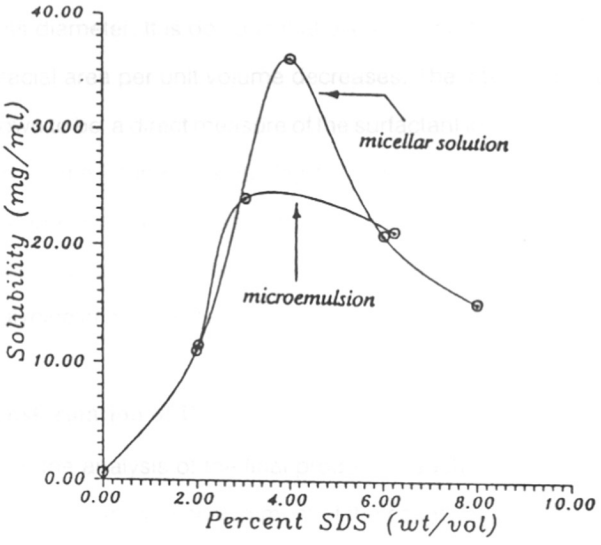

Figure 2.8 : Solubility of D (-)-N-carbamoyl phenylglycine (mg/ml) in 2.16 *N* H_2SO_4 micellar and microemulsion solutions as a function of the concentration of SDS expressed as percent (wt/vol).

case of aqueous SDS system, the CMC is about 8.3×10^{-3} mol/liter. The average aggregation number of SDS in water at 25 ^{o}C is about 64 [22] and the micelles are roughly spherical in nature [23]. Increasing the SDS concentration, the acidity or electrolyte concentration of the aqueous phase, leads to reduced intermicellar interactions and hence an increase in the aggregation number as proposed initially by Williams et al. [24] and later confirmed experimentally by Mazer et al. [25]. Increased aggregation numbers correspond to rod-like micelles [26]. When the surfactant concentration is increased, the length of a rod-like micelle increases without change in its diameter. It is obvious that even though the area of the rod-like micelle increases, its interfacial area per unit volume decreases. The interfacial area per unit volume of the micelle is known to be a direct measure of the surfactant interfacial concentration, which in turn is a measure of the interfacial solubility of the substrate (given in mg/ml). Hence we observe a decrease in interfacial solubility of D(-)-N-carbamoyl phenylglycine on increasing the SDS concentration above 4%. This also explains the decrease in solubility of D(-)-N-carbamoyl phenylglycine in micellar or microemulsion solutions having higher acid strengths.

2.3.3 Selective transformation of D(-)-N-carbamoyl phenylglycine to D(-) phenylglycine

Table 2.5 gives the analysis of the final product in each of the reaction runs. It is quite apparent from the product analysis that in most of the cases there is slight or no formation of side products like phenylglycine hydantoin, mandelic acid, benzoic acid and benzaldehyde. The isolated reaction product consists mainly of 99% D(-)-phenylglycine, with an optical purity of more than 98%. The phenomenon involved in obtaining such a remarkable product selectivity and product yield is explained as follows. D(-)-N-carbamoyl phenylglycine is a partly polar compound, practically insoluble in an aqueous acidic medium. When such a molecule is subject to interfacial conditions like those in micellar and microemulsion solutions, it gets solubilized at the interface and interior of the microglobule of the micellar solution, which in the cases studied here is of the L_1 type (oil-in-water). The reactant molecule re-orients itself at the interface in a fashion similar to the one reported earlier [27]. The relatively more polar part of the molecule protrudes in the aqueous surroundings, whereas the relatively less polar portion

Table 2.5 : Product Composition of the Reaction Mixtures with 1.08 *N* H_2SO_4 (Run Nos. 1-7)

Run No.	Total PG isolated/ gm	Unreacted N.Carb/ gm	% Unreacted N.Carb	Other products
1	1.61	0.12	5.4	Hydantoin: traces
2	1.54	0.01	0.5	Nil
3	3.71	Nil	-	Hydantoin: traces
4	15.28	0.36	1.8	Nil
5	15.19	0.31	1.55	Hydantoin: traces
6	34.62	1.13	2.26	Hydantoin and Benzoic acid: traces
7	55.2	3.7	4.6	Nil

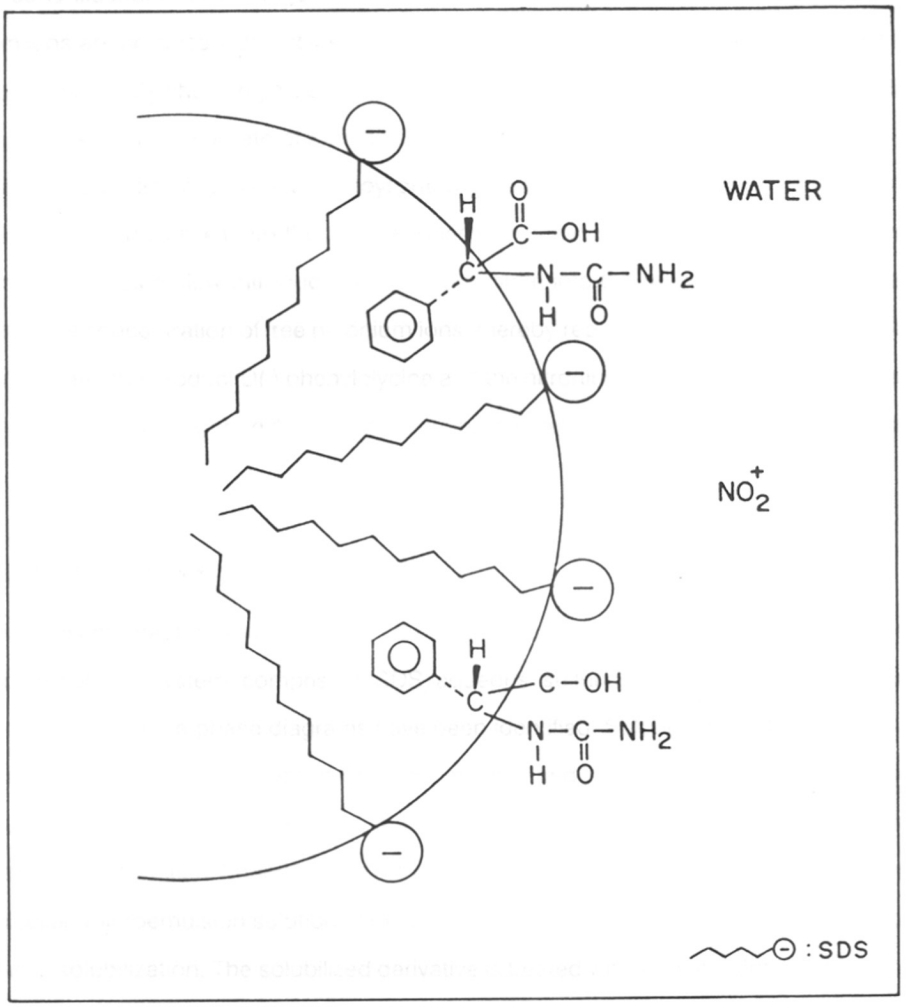

Figure 2.9 : Orientation of D(-)-N-carbamoyl phenylglycine at the microscopic interface.

of the D(-)-N-carbamoyl phenylglycine molecule extends into the interior nonpolar core of the micelle, as is illustrated in the Figure 2.9. On addition of $NaNO_2$ into the acidic medium, nitronium ions are produced almost instantaneously, and react with the derivative very fast at the micelle surface. By choosing a slow rate of addition of aqueous sodium nitrite to the acidic medium one can control the rate of formation of the nitronium ions. This therefore leads to a selective transformation of D(-)-N-carbamoyl phenylglycine to D(-) phenylglycine. The product immediately distributes itself into the micellar phase, thus avoiding any further attack of the nitronium ions. Thus a slow introduction of sodium nitrite into the reaction mixture ensures minimum local concentration of free nitronium ions, thereby reducing the danger of any other reaction between the product D(-) phenylglycine and the nitronium ions, which may otherwise form by-products such as phenylglycine hydantoin, mandelic acid, benzoic acid, or benzaldehyde.

2.4 CONCLUSIONS

The present chapter reports isothermal phase behavior of the pseudo-ternary micellar and microemulsion system comprising SDS/aqueous sulfuric acid/pentan-1-ol. Various important regions on the phase diagrams have been identified. Solubilization studies of D(-)-N-carbamoyl phenylglycine in various selected micellar and microemulsion solutions have been carried out with a view to use these solutions as a reaction medium for the decarbamoylation reaction. Enhancement in the solubilities of D(-)-N-carbamoyl phenylglycine in the micellar/microemulsion solution of dilute sulfuric acid is attributed to the phenomenon of interfacial solubilization. The solubilized derivative is treated with sodium nitrite as a limiting component to produce quantitative yields of D(-) phenylglycine, selectively. This study provides optimism for exploiting the important regions on the phase diagram for conducting several chemical reactions.

NOTATIONS

m_i	micelle
m_e	microemulsion
D	lamellar liquid crystal
L_1	oil in water or "direct" type
L_2	water in oil or "reverse" type
C_L	narrow channel
T	three phase

REFERENCES

[1] P. G. de Gennes and C. Taupin, *J. Phys. Chem.*, **86** (1982) 2294.

[2] E. B. Leodidis and T. A. Hatton, *J. Phys. Chem.*, **94** (1990) 6400.

[3] M. Adachi, M. Harada, A. Shioi and Y. Sato, *J. Phys. Chem.*, **95** (1991) 7925.

[4] P. Lianos and J. K. Thomas,, *J. Colloid. Interface. Sci.*, **117** (1987) 505.

[5] A. Mehra and M. M. Sharma, *Chem. Eng. Sci.*, **41** (1986) 2455.

[6] P. D. I. Fletcher and J. Parrot, *J. Chem. Soc. Faraday Trans.* I, **84** (1988) 1131.

[7] M. Menger and A. R. Elrington, *J. Am. Chem. Soc.*, **113** (1991) 9621.

[8] M. L. Moya, C. Izquierdo and J. Casado, *J. Phys. Chem.*, **95** (1991) 6001.

[9] R. Schomacker, K. Stickdorn and W. Knoche, *J. Chem. Soc. Faraday Trans.* I, **87** (1991) 847.

[10] K. Martinek, A. V. Levashov, N. Klyachko, Y. L. Khmelnitski and I. V. Berezin, *Euro. J. Biochem.*, **155** (1986) 453.

[11] M. R. Lemert, R. A. Fuller and K. P. Johnston, *J. Phy. Chem.*, **94** (1990) 6021.

[12] H. T. Bucherer and W. Steiner, *J. Prakt. Chem.*, **140** (1934) 291.

[13] S. Takahashi, T. Ohashi, Y. Kii, H. Kumagai and H. Yamada, *J. Ferment. Technol.*, **57** (1979) 328.

[14] S. Takahashi, Microbial Production of D-p-Hydroxyphenylglycine. In *Biotechnology of Amino Acid Production*: *Progress in Industrial Microbiology*; K. Aida, I. Chibata, K. Nakayama, K. Takinami and H. Yamada, Eds.; Elsevier: New York, 1986; Vol. **24**, pp 269-279.

[15] S. Shimizu, S. Shimada, S. Takahashi, T. Ohashi, Y. Tani and H. Yamada, *Agric. Biol. Chem.*, **44** (1980) 2233.

[16] H. Yamada, S. Shimizu, H. Shimada, Y. Tani, S. Takahasi and T. Ohashi, *Biochimie*, **62** (1980) 395.

[17] M. Clausse, A. Zradba and L. Nicolas-Morgantini, Water/Sodium Dodecyl Sulfate/pentan-1-ol/N-Dodecane Microemulsions. Realm-of-Existence and Transport Properties. In *Microemulsion Systems: Surfactant Science Series*; H.L. Rosano and M. Clausse, Eds.; Dekker: New York, 1987; Vol. **24**, Chapter 25, pp 387-425.

[18] A. M. Bellocq and D. Roux, In *Surfactants in Solutions*; K. L. Mittal and P. Bothorel, Eds.; Plenum: New York, 1987; Vol. **4**.

[19] A. S. Chhatre and B. D. Kulkarni, *J. Colloid. Interface Sci.*, **150** (1992) 528.

[20] J. Schawartz and G. Eibel, *Chem. and Ind.*, **48** (1968) 1698.

[21] M. Clausse, J. Peyrelasse, C. Boned, J. Heil, L. Nicolas-Morgantini and A. Zradba, Influence of the Cosurfactant Chemical Structures Upon the Phase Diagram Features and Electrical Conductive Behavior of Winsor IV Type Media (so-called Microemulsions). In *Surfactants in Solutions*; K. L. Mittal and B. Lindman, Eds.; Plenum: New York, 1984; Vol. 3, pp 1583-1626.

[22] E. A. G. Aniansson, S. N. Wall, M. Almgren, H. Hoffmann, I. Kielmann, W. Ulbricht, R. Zana, J. Lang and C. Tondre, *J. Phys. Chem.*, **80** (1976) 905.

[23] M. Bourrel and R.S. Schechter, The Phase Behavior and Properties of Solutions Containing Amphiphiles, Organic Liquids and Water: Micellar Solution. In *Microemulsions and Related Systems*: *Surfactant Science Series*; Dekker: New York, 1988; Vol. **30**, Chapter 4, pp 127-205.

[24] R. J. Williams, J. N. Phillips and K. J. Mysels, *Trans. Faraday Soc.*, **51** (1955) 728.

[25] N. A. Mazer, G. B. Benedek and M. C. Carey, *J. Phys. Chem.*, **80** (1976) 1075.

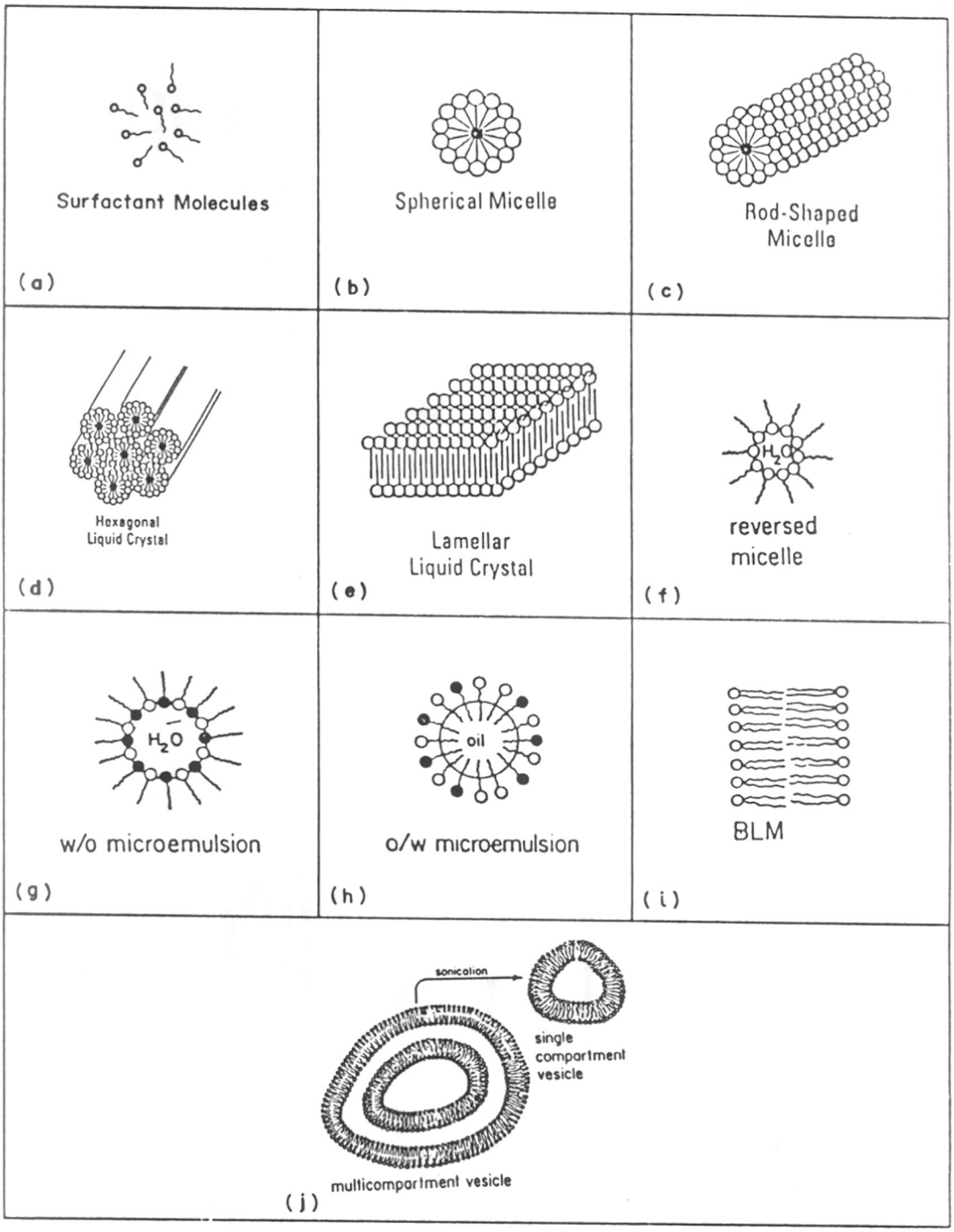

Figures 1.2(a-j) : Schematic representation of organized colloidal aggregates that may form in aqueous solution of surfactants.

[26] C. Y. Young, P. J. Missel, N. A. Mazer, G. B. Benedek and M. C. Carey, *J. Phys. Chem.*, **82** (1978) 1375.

[27] A. S. Chhatre, R. A. Joshi and B. D. Kulkarni, *J. Colloid Interface Sci.*, **158** (1993) 183.

CHAPTER 3

CYCLIZATION AND MOLECULAR REARRANGEMENT REACTIONS

3.1 INTRODUCTION

Micelles and other association colloids have been used as a media for conducting numerous organic and inorganic reactions [1-9]. Micelles have been shown to provide a solubilizate with at least three environments (fully aqueous, interfacial and hydrophobic core) depending on its localization. Solubilization of nonpolar organic molecules and inorganic salts in such a phase brings about variation in rates that can be attributed to electrostatics, hydrophobic, electrophilic and/or nucleophilic interactions resulting in changing the free energy of activation of the process [10-16]. Similarly microemulsions by virtue of their large interfacial area reduce transport limitations fostering the rates of chemical reaction. In addition to its use as a medium for reactions, other properties such as ease of preparation, stability, low viscosity and interfacial tension and molecularly ordered interface have proven to be useful in various applications. It is well recognised that micelles and microemulsions can catalyse the reaction by concentrating the reagents in the interfacial region or "Stern" layer (i.e., an interface between the hydrocarbon like interior and solvent and regarded as the slipping plane of micelles possessing a powerful field gradient) having a width about the size of the surfactant head group, and contains the ionic head group of the amphiphiles, a fraction of counterions and water [10, 17-20]. As the micelles have highly mobile structures, the various reactants solubilized in the micelles may meet through hydrophobic and electrostatic interactions (which bring together the reagents in the micelle and lead to an increase of their local concentration) and thus react at the microscopic interface with significant improvements in the product yield, conversion, and rate of reactions [21-24]. It is also suggested that the reactions associated with the participation of H^+-ions either as reactants or as catalytic species can substantially benefit in such media due to an increase in the local concentration of H^+-ions at the microscopic interface [25, 26]. Under these conditions, the rate of bimolecular reactions mainly depends on the concentrations of micellar bound H^+-ions rather than on the total H^+-ion concentration. Therefore the molecular scale reactors offered by these organized assemblies are of interest from a technological viewpoint [27-29].

Reports of micelles and microemulsions effect on nonphotochemical cyclization/rearrangement reactions have been sparse despite the importance [30, 31]. A few acid-catalyzed reactions such as rearrangement of the benzidine molecule [32, 33] and cyclization of terpenoids [34, 35] have shown significant improvements in the rate of reaction in micellar media. Recent studies of organized assembly-localized cyclization reactions include lactonization in reverse micelles [36, 37] and cyclization of o-(w-bromoalkaoxy)-phenoxides in aqueous direct micelles [38]. Lennox et al. [39] observed enhanced cyclization rates due to looping the substrates at the interface of the micelles, an effect similar to a "2D tempelate effect". Normally if the substrate is poorly soluble in the solvent, it will be solubilized at the interface where the reactive polar moities occupy the quasi-two dimensional (2D) suraface of finite thickness rather than having them occupy a three dimensional (3D) volume as occurs in homogeneous solution environment.

The question of determining the strength of an acid or a base in micelles and microemulsions has been vigorously pursued in the past years and the problem is complicated due to changes in the acid dissociation constants [40]. The lack of accurate information about the hydrogen ion concentration in such systems has often hindered interpretation of many experimental results [41]. Notwithstanding the developments and the difficulties in the accurate determination of acid concentration, the fact remains that anomalous changes in acid strengths do occur in certain phase volumes of the system. We focus on the exploitation of anomalous H^+-ions concentration in certain region of the phase space and effect of micellar orientation of substrate on the magnitude of micellar catalysis.

We elucidate these points and examine the influence of micelles/microemulsions on the cyclization and molecular rearrangement reactions. More specifically, in the present chapter we report the cyclization of D(-)-N-carbamoyl phenylglycine to phenylhydantoin (**Case study A**) and Beckmann rearrangement of cyclohexanone oxime to caprolactam (**Case study B**) under mild acidic conditions.

3.1.A Cyclization of D(-)-N-carbamoyl phenylglycine

Phenylhydantoin is an important intermediate in the chemico-enzymatic process for D(-) phenylglycine production. It is known that phenylhydantoin is synthesized by the reaction of benzaldehyde, ammonium bicarbonate, and sodium cyanide, according to Bucherer-Berg's method [42]. It may be noted that the conventional D(-)-N-carbamoyl phenylglycine is usually obtained from phenylhydantoin using a microbial route [43]. Most often phenylhydantoin is completely transformed into D(-)-N-carbamoyl phenylglycine by the action of microbial hydantoinases, which is then transformed into D(-) phenylglycine by reaction with nitrous acid. The overall process is summarized in Scheme 3.1.

Scheme 3.1

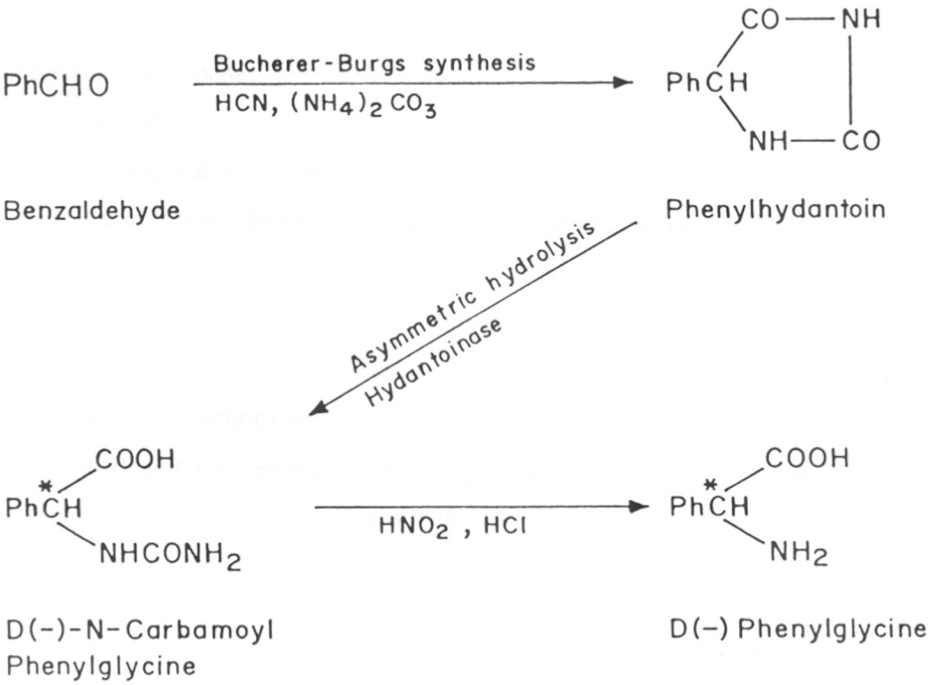

Scheme 3.2 presents the cyclization of D(-)-N-carbamoyl phenylglycine at the interface of micelle/microemulsion droplets, which accomplishes the reverse step.

Scheme 3.2

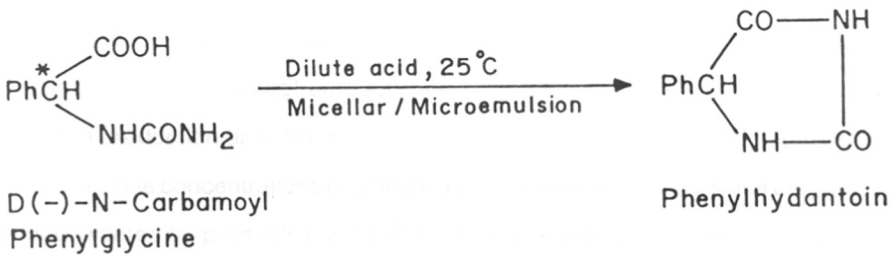

3.1.B Beckmann rearrangement of cyclohexanone oxime

Caprolactam (2-oxohexamethylenimine, hexahydro-2H-azepin-2 one) is one of the most widely used chemical intermediates. It is used as the monomer for nylon-6 fibres, plastics and also used for the preparation of L-lysine which is an essential ingredient in animal food. Conventional methods of preparation of caprolactam involves treating cyclohexanone oxime with concentrated sulfuric acid followed by neutralization with liquid ammonia [44, 45]. Other process involves reaction of cyclohexanone oxime with phosphoric acid. These processes yield caprolactam along with equally large quantities of ammonium sulfate or ammonium phosphate. Other commercial processes use the high pressure reaction of caprolactone and ammonia at elevated temperatures or nitration of cyclohexanone in acetic anhydride with acetyl nitrate to produce 1-nitrocyclohexanone. Base-catalysed hydrolysis of this product gives ϵ-nitrohexanoic acid which on reduction yields ϵ-aminohexanoic acid. This is then thermally cyclised to caprolactam. In yet another approach hexahydroxide acid is reacted with nitrosyl sulfuric acid in oleum to produce caprolactam. This process yields appreciable amount of ammonium sulfate as by-product. One

of the more recent methods to produce caprolactam includes production of hexahydro benzoic acid and treating it with nitrosyl sulfuric acid. This reaction yields nitrobenzene as a by-product [46, 47].

Most of the customary methods of producing caprolactam use either oleum or concentrated sulfuric acid as reaction medium. The reactions are usually carried out at higher temperatures ranging from 50 - 150 ^{o}C with a control over the temperature. In some cases where gaseous catalysts are used, pressures ranging from 2000 to 5000 psi or even more are required for improving the capacity of the production unit. The residence time in the reactor (or reactors) ranges from 1 to 5 hours. Control of the concentrations of ammonia and water is very critical since they determine the amount of unwanted by-products such as δ-methyl δ-valerolactam. Operation in presence of excess ammonia or low quantity of water results in formation of large quantities of reaction intermediates that makes it very difficult to recycle these even though they are convertible to caprolactam [48]. In batch process of preparation of caprolactam under oleum or concentrated sulfuric acid, a large quantity of ammonium sulfate or bisulfate ranging from 2 to 5 times the quantity of caprolactam is formed as by-product. Using concentrated sulfuric acid or oleum may also lead to certain operational problems such as corrosion and environmental problems like waste stream pollution.

The overall reaction of Beckmann rearrangement of cyclohexanone oxime can be represented as follows:

Scheme 3.3

Caprolactam preparation

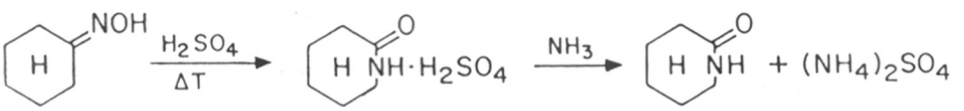

(2-5 tons AS / ton of caprolactam)

3.2 EXPERIMENTAL

Case study A

3.2.A.1 Materials

Sodium dodecyl sulfate (SDS) obtained from Loba Chemicals (Analytical reagent grade) was used as a surfactant. Fluka guaranteed pentan-1-ol (Analytical reagent grade) was used as a co-surfactant. Concentrated H_2SO_4 was obtained from SD chemicals and was diluted to the required strength using distilled water. The exact concentration of H_2SO_4 was determined by titration with standardized 0.5 mol dm^{-3} sodium hydroxide solution. The D(-)-N-carbamoyl phenylglycine was chemically synthesized in the laboratory and was purified by recrystallization [49].

3.2.A.2 Methodology

The phase behavior of the micelle/microemulsion system comprising sodium dodecyl sulfate (SDS), pentane-1-ol and aqueous sulfuric acid is reported in previous chapter. The aqueous sulfuric acid vertices of each of these triangular phase diagrams are of interest to us in the present investigation, and these have been shown in Figures 3.1(a-c). As can be appreciated from these figures, in a region close to the transition from a single phase to a two phase to a three phase region (marked as A in the figure) the local concentration of the reactants are relatively high in some of the colloidal assemblies. We carried out the cyclization of the D(-)-N-carbamoyl phenylglycine to phenylhydantoin in this region.

We have selected a set of compositions of various micellar or microemulsion solutions from the above mentioned phase diagrams, for carrying out the cyclization of D(-)-N-carbamoyl phenylglycine to phenylhydantoin (Runs 1-20) in the first part of the experiments. The different micellar/microemulsion systems studied and the percentage composition of various media used in the present work are reported in Table 3.1. Runs 1-6, 8-13 and 15-19 correspond to micellar/microemulsion solutions containing SDS and pentane-1-ol in 0.27, 0.54 and 1.08 mol dm^{-3} H_2SO_4 respectively. Runs 7, 14 and 20 correspond to aqueous solutions of 0.27, 0.54 and 1.08

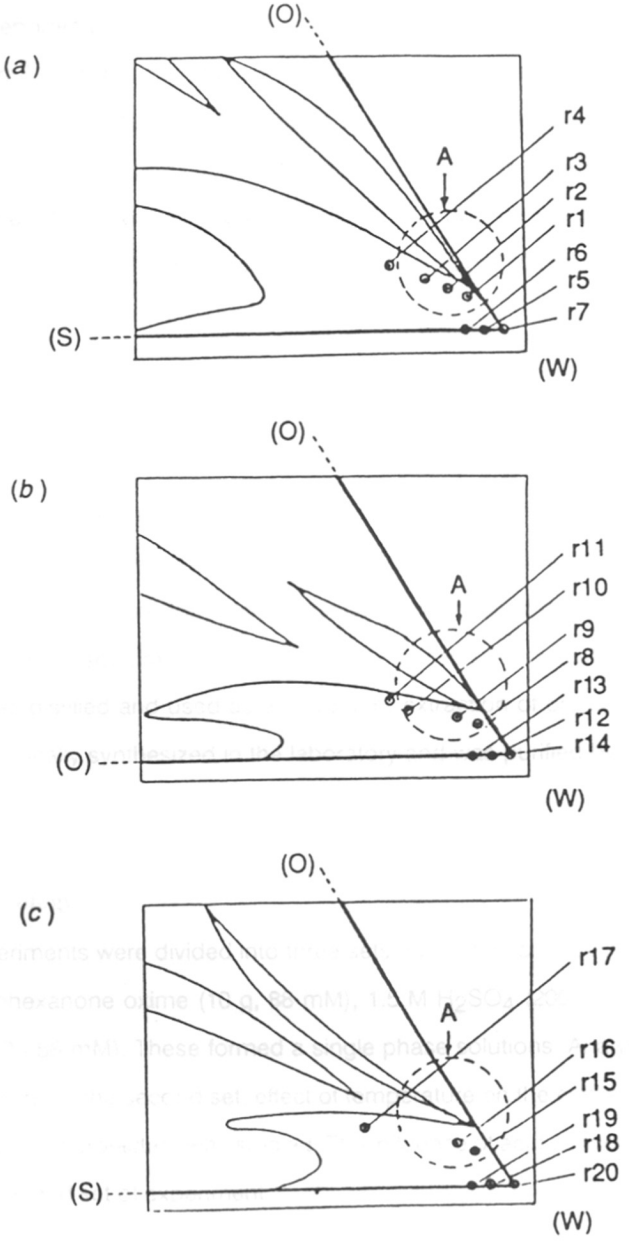

Figures 3.1(a-c) : Sulfuric acid apex of the pseudoternary diagram of the micellar/microemulsion system comprising SDS (S), aqueous H_2SO_4 (W) and pentan-1-ol (O). Experimental points r1 through r20 represent the compositions used in Runs 1 through 20 respectively. Strength of aqueous H_2SO_4 (a) 0.27, (b) 0.54, (c) 1.08 mol dm^{-3}.

mol dm^{-3} H_2SO_4 containing no surfactant or the co-surfactant. Taking into consideration the solubility data reported in the previous chapter, 4.00 gm of D(-)-N-carbamoyl phenylglycine was added to 100 cm^3 of each of the above mentioned solutions so that the reaction mixture in most of the runs was always saturated with respect to D(-)-N-carbamoyl phenylglycine. The reaction mixture was maintained at 25 ^oC under stirring for 24 hours after which the solution was vacuum filtered to remove the solid undissolved D(-)-N-carbamoyl phenylglycine. The filtrate was analyzed quantitatively by High Performance Liquid Chromatograph (HPLC) technique as described in the previous chapter.

Case study B

3.2.B.1 Materials

Sodium dodecyl sulfate (SDS) obtained from Loba chemicals (Analytical reagent grade, 99.5%) was used as surfactant without further purification. Sulfuric acid procured from SD chemicals was used in dilute form and the exact concentration of H_2SO_4 was determined by titration with standard sodium hydroxide solution. Benzene (Analytical reagent grade) procured from Sigma was distilled and used as a solvent for extraction of products. The cyclohexanone oxime was chemically synthesized in the laboratory and was purified by recrystallization (mp = 88 ^oC) [50].

3.2.B.2 Methodology

The experiments were divided into three sets. In the first set, reaction mixtures were composed of cyclohexanone oxime (10 g, 88 mM), 1.5 M H_2SO_4 (200 mL) and various SDS concentrations (0.0 - 56 mM). These formed a single phase solutions. Analysis of the reaction was done after 2 hours. In the second set, effect of temperature on the conversion of cyclohexanone oxime and yield of caprolactam was studied. The influence of acid concentration on reaction was examined in the third set of experiment.

Table 1.2 : Properties of Organized Surfactant Assemblies

Feature	Aqueous micelles	Reversed micelles	Microemulsions	Vesicles	Monolayers	BLMs
Constituents	Surfactants	Surfactants	Surfactants, cosurfactants, polar and apolar solvents	Lipids and surfactants	Surfactant and polar or apolar solvents	Mostly lipids of biological origin
Method of Preparation	Dissolve appropriate concentration (above CMC) of surfactant in water	Dissolve appropriate concentration in an apolar solvent adding small amounts of water	Dissolve appropriate concentration of surfactant and cosurfactant in suitable solvent	(a) Shake or vortex thin lipid films with aqueous solution; (b) Inject ether or alcoholic solution of the lipid into a aqueous solution	Spread surfactant dissolved in an organic solvent on water surface	Paint surfactant dissolved in an organic solvent on a pinhole
Weight-average molecular weight	2000-6000	2000-6000	10^5-10^6	$>10^7$	Depends on area covered and density of coverage	Depends on area covered and density of coverage
Hydrodynamic diameter, Å	30-60	40-80	50-1000	300-10,000	Depends on area covered and density of coverage	Depends on area covered and density of coverage
Stability	Weeks, months	Weeks, months	Weeks, months	Weeks	Hours, days	Hours
On dilution by H_2O	Destroyed	Water pool enlarges: W/O microemulsions	O/W + water --> aqueous micelle; W/O + water --> phase separation	Unaltured	Destroyed	Destroyed
Number of Solubilizate taken up per aggregate	Few	Few	Large	Large	Large	Large
Available solubilization sites	Surface, Stern layer, vicinity of headgroups	Aqueous pool, inner surface, surfactant tail	Inner pool, inner surface, surfactant tail	Aqueous pool, inner and/or outer sides of the surface, among the bilayer	On surface, around the hydrocarbon	Either or both sides of the surface

Reaction products were extracted with benzene and quantitatively analyzed by an automated Chemito 3800 gas chromatograph using a flame ionization detector (FID). A 3 m long, 0.8 mm internal diameter stainless steel column was packed with 10% SE 30 on Chromosorb W (HP) 80/100 mesh, and was used for separation. The oven temperature was set at 150 ^{o}C and a flow rate of ≈35 mL/min of nitrogen was employed as carrier gas. The injector and detector were maintained at 250 ^{o}C and 310 ^{o}C respectively. The internal standard and response factors were determined from respective authentic compounds of known purity. Analysis was performed in duplicate for each sample.

3.2.B.3 Phase diagram study

A ternary phase diagram was constructed using varying extents of SDS, aq. H_2SO_4 and cyclohexanone oxime at three different temperatures 15 ^{o}C, 30 ^{o}C and 40 ^{o}C. The sample tubes used in the phase diagram study was maintained at the desired temperature with an accuracy of ±0.1 ^{o}C. The different domains namely the micellar L_1 (single-phase) and macroemulsion (two-phase) were determined using the standard method [51, 52].

3.3 RESULTS AND DISCUSSION

Case study A

3.3.A.1 Selective formation of phenylhydantoin

The analysis of 100 cm^3 of the filtrate of the product mixture is reported in Table 3.1 The percent conversions are calculated on the basis of net D(-)-N-carbamoyl phenylglycine solubilized at the end of 24 hours. It can be seen from Table 3.1 that the conversion of D(-)-N-carbamoyl phenylglycine to phenylhydantoin after 24 hours of the reaction is much better in the case of microemulsions (Runs 1-4, 8-11 and 15-17) than those in the case of micellar solutions (Runs 5

Table 3.1 : Composition of Reaction Medium[a] and Analysis of 100 cm^3 of the Filtrate of the Product Mixture After 24 h Reaction Time

Conc. H_2SO_4 mol dm^{-3}	Run No.	S (%)	W (%)	O (%)	N-Carbamoyl phenylglycine unreacted/g	Net phenylhydantoin formed/g	Conversion (%)
0.27	1	0.67	97.10	2.23	0.601	2.843	83.9
	2	1.40	96.10	2.50	0.924	2.610	75.7
	3	2.00	95.00	3.00	1.426	2.183	62.8
	4	4.00	92.00	4.00	1.988	1.089	37.6
	5	1.00	99.00	0.00	0.988	traces	-
	6	2.00	98.00	0.00	1.349	traces	-
	7	0.00	100.0	0.00	0.132	nil	-
0.54	8	0.67	97.10	2.23	0.680	2.547	80.5
	9	1.40	96.10	2.50	1.381	1.966	61.1
	10	4.00	93.00	3.00	2.792	1.091	30.1
	11	4.50	91.00	4.50	2.808	1.077	29.7
	12	1.00	99.00	0.00	0.728	0.062	8.7
	13	2.00	98.00	0.00	1.538	0.084	5.7
	14	0.00	100.0	0.00	0.116	traces	-
1.08	15	0.67	97.10	2.23	0.344	2.903	90.3
	16	1.40	96.10	2.50	0.791	2.891	80.1
	17	6.00	90.00	4.00	2.240	1.588	43.8
	18	1.00	99.00	0.00	0.441	0.079	16.5
	19	2.00	98.00	0.00	1.116	0.086	7.8
	20	0.00	100.00	0.00	0.056	0.031	37.8

[a] At 25 °C; percentage by weight: SDS (S); H_2SO_4 (W); pentane-1-ol (O).

and 6, 12 and 13, 18 and 19) or pure aqueous sulfuric acid (Runs 7, 14 and 20). The analysis also indicates selective formation of phenylhydantoin, besides unreacted solubilized D(-)-N-carbamoyl phenylglycine in the product filtrate.

3.3.A.2 Effect of pentan-1-ol

All of the above micellar/microemulsions are of oil-in-water type. Monomeric surfactant SDS and added solutes D(-)-N-carbamoyl phenylglycine diffuse into the microscopic droplets, and in view of their interfacial area it is anticipated that the transfer of material between water and droplets is much faster than the activated thermal reactions. Reaction typically occurs at the interface or at the Stern layer which contain specially bound counterions. The underlying mechanism in obtaining such an improvement depends on the concentration of micellar bound hydrogen ions rather than on the total H^+ concentrations [53-55]. D(-)-N-carbamoyl phenylglycine which is poorly soluble in the aqueous continuous phase and so is completely localized at the interface of the micelles/microemulsion droplets. Molecules at the interface orient themselves with their carbamoyl groups and the acid groups extended into the Stern layer of the droplet (illustrated in Figure 3.2), where the reaction proceeds more efficiently, and then favour the cyclization. The product phenylhydantion may partition itself between the droplet interface and the bulk aqueous phase. Enhancement of the conversions can also be attributed to the increased concentration of reactants at interface. The addition of pentan-1-ol molecules, which are usually inserted between the SDS molecules by means of hydrophobic interactions changes the electric double layer. It provides more stabilty to the interface by forcing apart the ionic heads of the surfactants, reduces the surface charge density of the micelle and also increases the degree of ionization [56-58]. Thus a higher concentration of positive ions are obtained in the Stern layer with corresponding increase of the reaction rates in microemulsion.

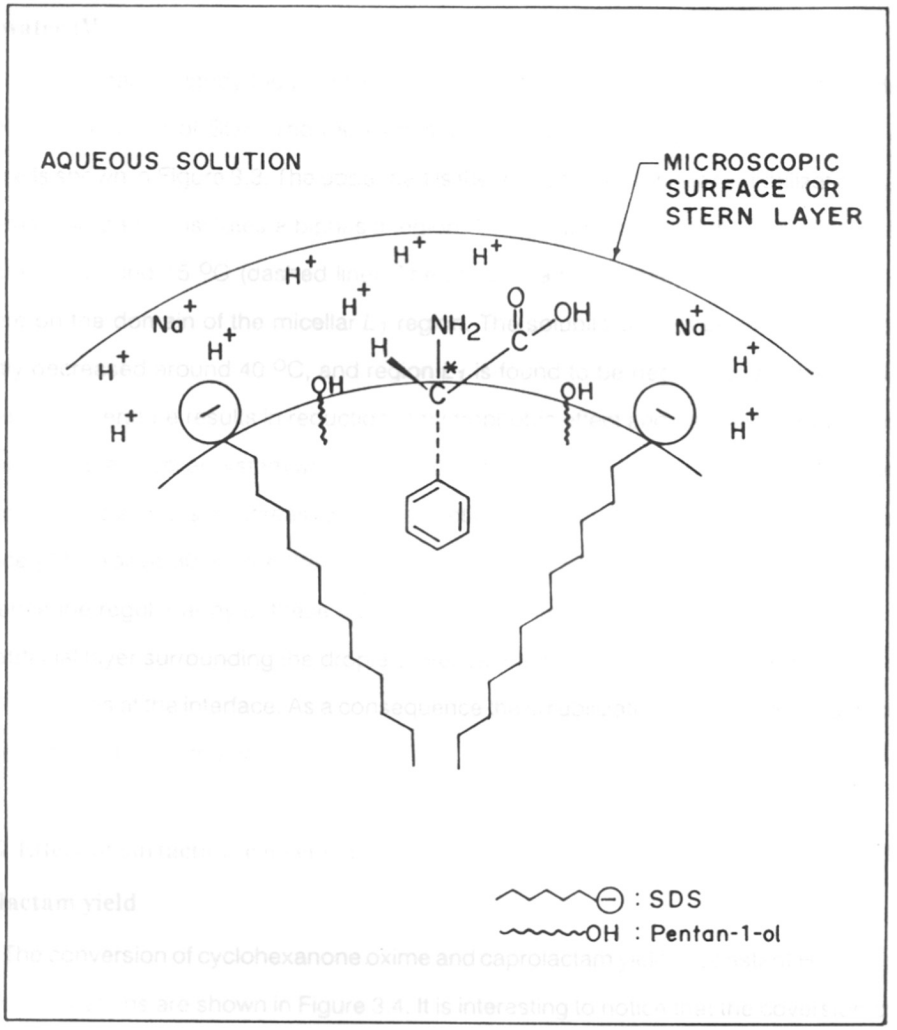

Figure 3.2 : Orientation of D(-)-N-carbamoyl phenylglycine at the interface.

Case study B

3.3.B.1 Effect of temperature on phase behavior of system SDS (S)/cyclohexanone oxime (O)/ water (W)

It is important to study the phase diagram at different temperatures in order to understand the solution behavior of SDS. The representative ternary phase diagram as a function of temperature is shown in Figure 3.3. The upper part is the monophasic micellar solubilization, L_1 zone. The remaining part constitutes a biphasic region. The monophasic region covers larger area for temperature around 15 ^{o}C (dashed line). The phase diagram clearly reveals the effect of temperature on the domain of the micellar L_1 region. The solubilization of cyclohexanone oxime is abruptly decreased around 40 ^{o}C, and region L_1 is found to be negligible (solid line). Normally the rise in temperature results in reduction in hydrophobic effect and entropic contribution to the free energy of the micellar system which minimize the adsorption driving force [59-62]. An increase of temperature also causes increased thermal motion of the adsorbed surfactant molecules at the interface [63]. Above 30 ^{o}C the thermal motion of the surfactant molecules become dominant, and hence the regular array of these molecules at the interface gets distorted and moves out of the inetrfacial layer surrounding the droplets. Hence there will be a decreased number of surface active molecules at the interface. As a consequence the solubilization capacity of SDS decreases, thus decreasing the L_1 region.

3.3.B.2 Effect of surfactant concentration on the conversion of cyclohexanone oxime/caprolactam yield

The conversion of cyclohexanone oxime and caprolactam yield at constant H^+ and various SDS concentrations are shown in Figure 3.4. It is interesting to notice that the coversion of oxime in the absence of SDS is 28 % with negligible caprolactam yield. The conversion increases with increasing SDS concentration and displays a maximum. The phenomenon involved can be rationalized by considering the way molecules get solubilized and reoriented at the interface [15,

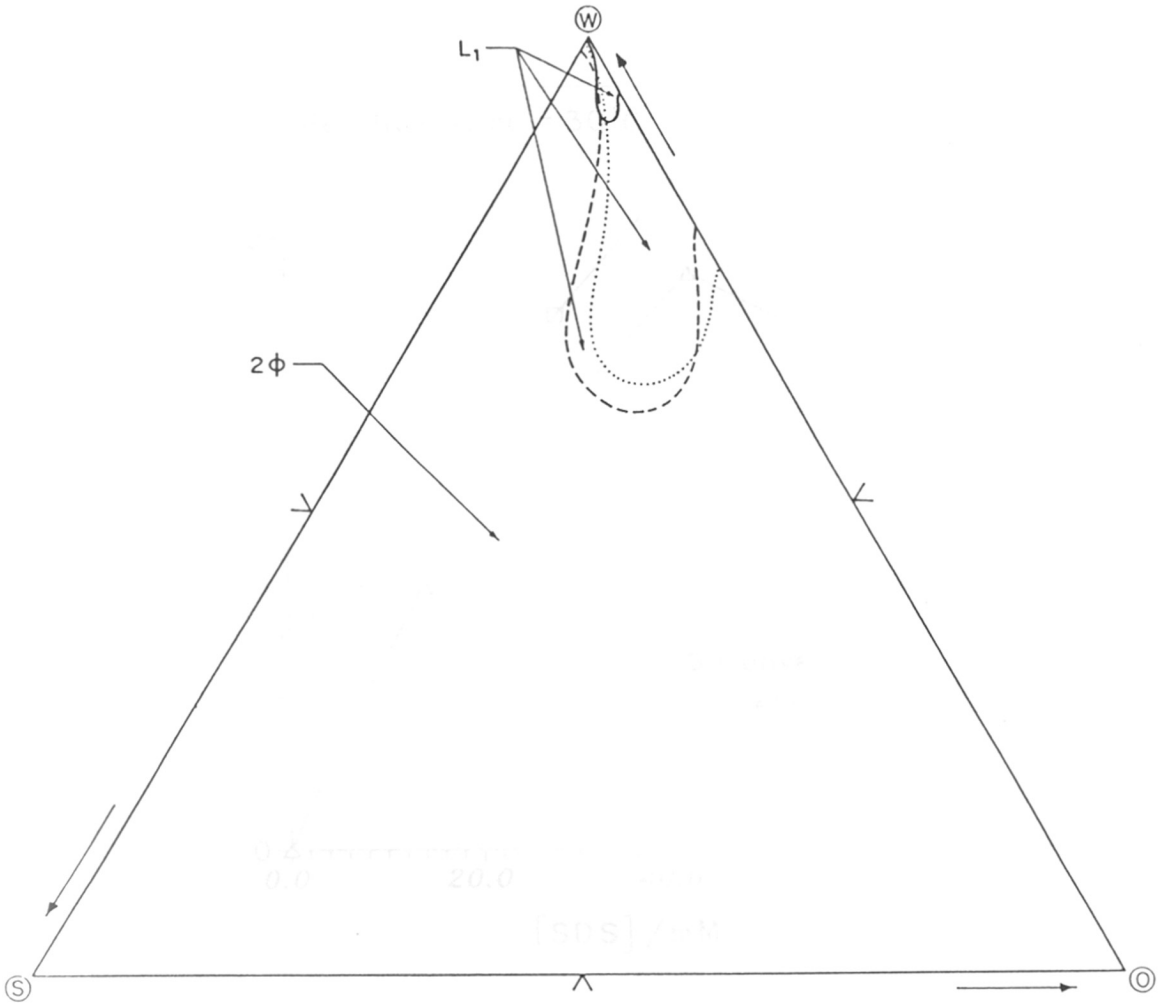

Figure 3.3 : Ternary phase diagram of the system cyclohexanone oxime (O)/SDS (S)/ 1.5 mol dm^{-3} H_2SO_4 (W) at 15 °C (dashed line), 30 °C (dotted line) and 40 °C (solid line). Concentrations are in weight percent. L_1 is monophasic solubilization region. 2ϕ is two-phase region.

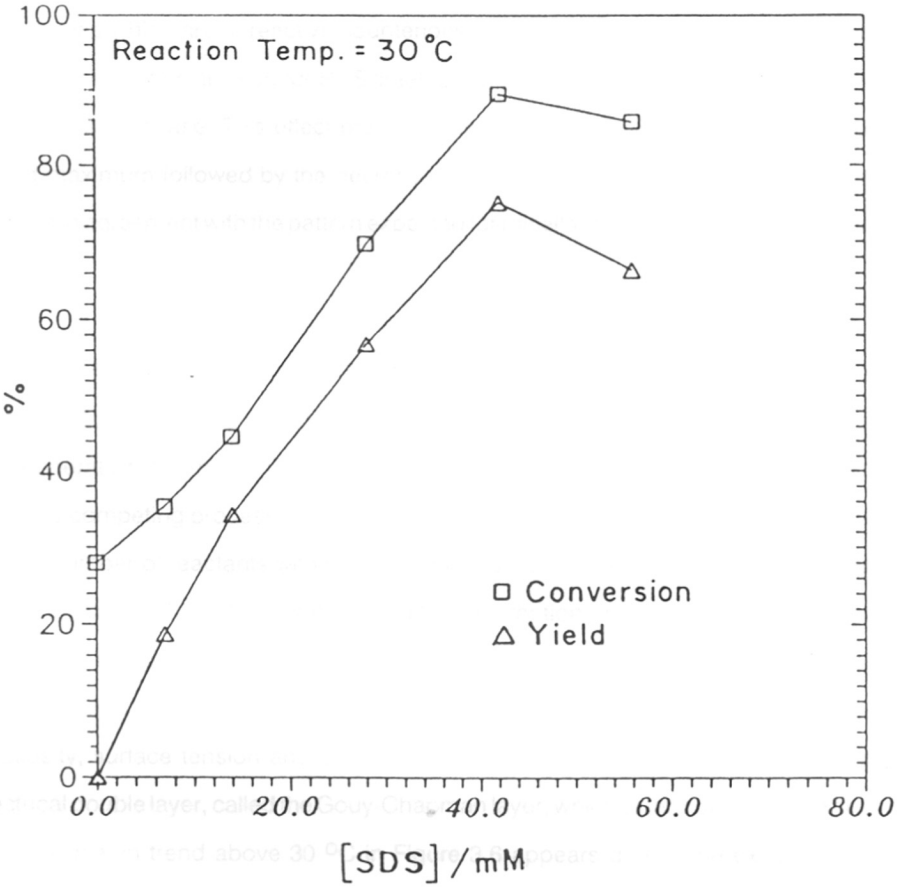

Figure 3.4 : Effect of SDS concentration on the conversion of cyclohexanone oxime and on the yield of caprolactam. $[H_2SO_4]$ = 1.5 mol dm^{-3}; [cyclohexanone oxime] = 88 mM.

20, 64] as is illustrated in Figure 3.5. The existence of maximum conversion of cyclohexanone oxime and caprolactam yield can be explained in terms of two competing effects. Cyclohexanone oxime is hydrophobic in nature and so is completely localized at the interface of the micelles. The presence of SDS increases the relative concentration of cyclohexanone oxime and H^+-ion in the Stern layer. However, further increase in SDS concentration causes an increase in the concentration of Na^+-ions which are unreactive counterions competing with protons for available sites in the Stern layer. In addition, the surplus SDS creates more micelles and hence dilutes the reagents in the micellar pseudophase. This effect predominates at higher SDS concentration producing the observed maximum followed by the decrease in rate of reaction. Thus the observed experimental trend is in agreement with the pattern expected for micellar catalyzed bimolecular reactions [7, 11, 15, 65].

3.3.B.3 Effect of temperature on the conversion of cyclohexanone oxime/caprolactam yield

Figure 3.6 illustrates the effect of temperature on the conversion of cyclohexanone oxime. An otimal temperature around 30 ^{o}C for better performance can be noticed. The optimum is a result of the two competing processes. The reaction rate-constant increases with the temperature while the total number of reactants within the proximity of each other decrease due to change in micellar chracteristics with the temperature. The thermal motion produces a disruptive effect on the packing of surface active molecules. This disruptive effect causes an increase in the intermolecular distance between the surfactant molecules at the interface, which in turn influences the surface viscosity, surface tension and stability of micelles. Normally thermal motion creates a diffuse electrical double layer, called the Gouy-Chapman layer, which extends out into the aqueous phase. The reversal in trend above 30 ^{o}C in Figure 3.6 appears due to the exclusion of ionic reagents or decrease in counterions binding at the interface as a result of the conformational changes that are possible within the micelles [66, 67]. This leads to the suggestion that favourable

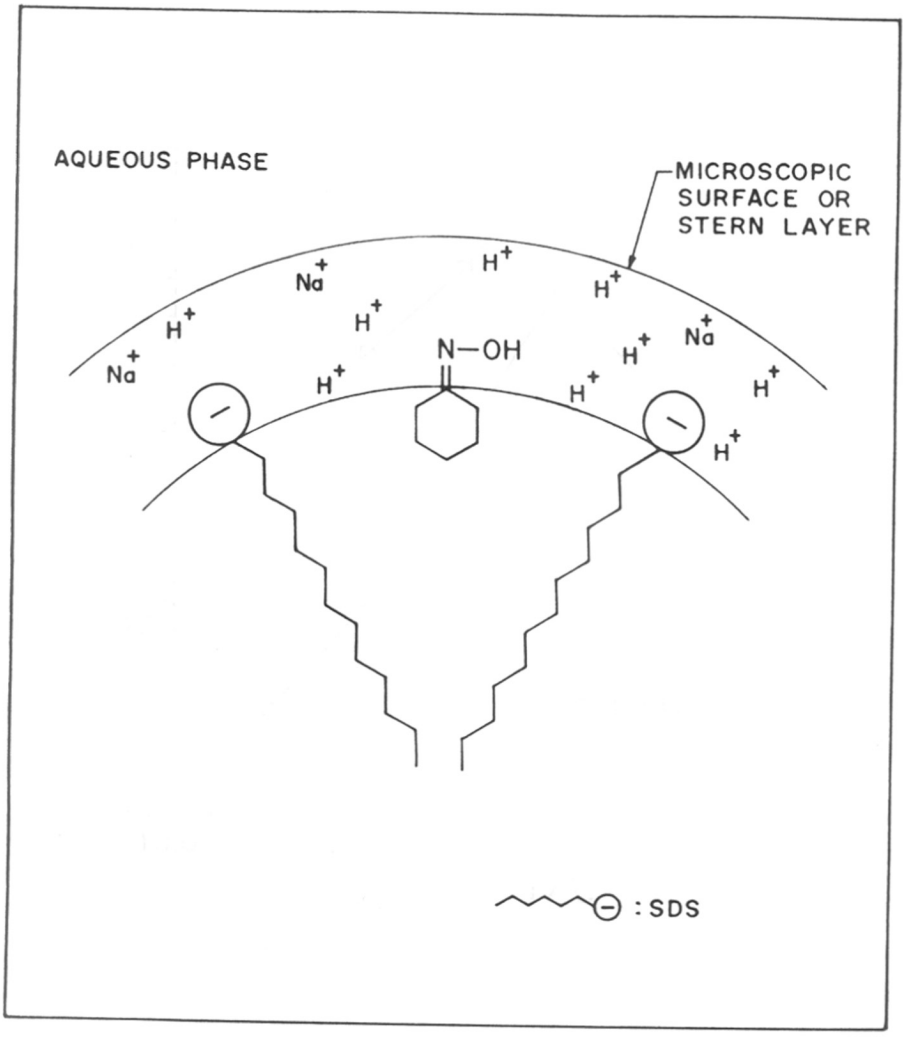

Figure 3.5 : Orientation of cyclohexanone oxime at the interface.

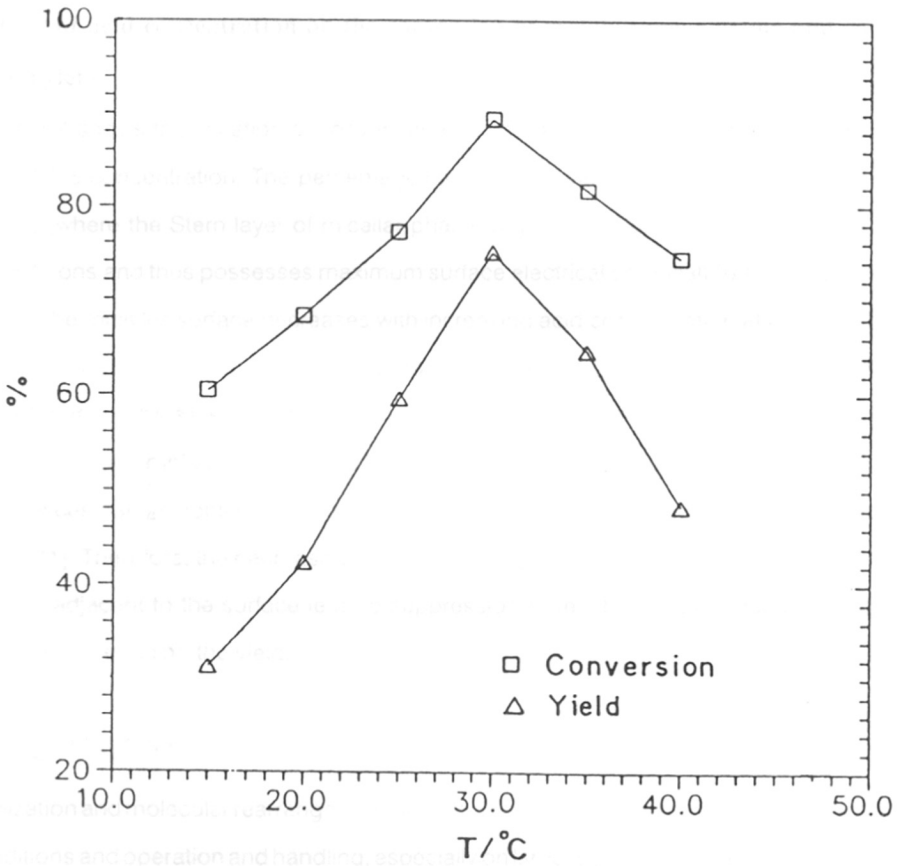

Figure 3.6 : Effect of temperature on the conversion of cyclohexanone oxime and on the yield of caprolactam. $[H_2SO_4]$ = 1.5 mol dm^{-3}; [cyclohexanone oxime] = 88 mM; [SDS] = 42 mM.

thermodynamically stable solution of a substance normally insoluble or sparingly soluble in a given solvent, by the addition of an amphiphilic component or components. According to Hartley [22] the solubilization phenomenon is related to the CMC of the surfactant and led to the determination of numerous CMC values. The increased solubility of a solubilizate in a surfactant solution is due to some form of attachment of the solubilizate to the exterior of the micelle or solution in it [23-25]. The presence of hydrophobic cores in micelles act as compatible medium for the location of hydrophobic solubilizates. Generally, three solubilization sites are available in surfactant aggregates (as shown in Figure 1.3) [26-28]. In the first site, the solubilizates are located among the hydrocarbon tails of the surfactant thus allowing for mixing between all the solubilizates and surfactant molecules (Figure 1.3(a)). In this case, the radius of the micelle can not exceed the length of the surfactant molecule and micelle can grow from sphere to cyllinder. In the second site, the solubilizate is partially located in the region among the surfactant tails and partially in a core where there is no contact with the surfactant tails (Figure 1.3(b)). The radius of the micelles can be larger than the length of surfactant tail. In this case, structure is swollen micelles or microemulsions. Whereas in the third site, polar solubilizate molecules may adsorb at the micellar surface (Figure 1.3(c)).

Micellar solubilization is sensitive to the nature of the solubilizate as well as on the solvent [19, 29]. Other parameter which affect solubilization include temperature, counterion, added electrolytes and non-electrolytes etc [30]. The solubilization capacity of micellar systems, generally follow the order: nonionics > cationics > anionics for the amphiphiles with the same hydrophobic moiety. Similarly, the solubilization of reactants in the microemulsions is affected by factors that influence the interfacial properties such as surface pressure and bending moment of the globules [31]. In addition to these, the stability of microemulsions droplets also influences solubilization [12]. Strong interactions among microemulsion droplets can cause an instability of the system, leading to phase separation or structural changes [33-35].

Data from the solubilizaion measurements are expressed either as solubility curves or phase diagrams [36]. The basic informations on the phase diagram of the system is prerequisite for meaningful investigations and are of both theoretical and technical interest [37]. A very large number of two component systems have been studied with respect to the influence of composition

orientation of the reactants is a factaor of prime importance for micellar catalyzed reaction, similar to enzymatic rate acceleration which utilize their ability to substrate binding force to act as "entropy trap" [68].

3.3.B.4 Effect of acid concentration on the conversion of cyclohexanone oxime and caprolactam yield

Figure 3.7 shows the variation of conversion of oxime and caprolactam yield with H_2SO_4 for the fixed SDS concentration. The percentage caprolactam yield exhibits maxima at 1.5 mol dm^{-3} H_2SO_4 (where the Stern layer of micellar phase may be considered to be saturated with respect to H^+-ions and thus possesses maximum surface electrical potential) [69]. The presence of H^+-ions at the micelles surface decreases with increasing acid concentration at constant SDS concentration once the threshold acid concentration is reached [70]. The reduction in surface electrical potential of micelles that follows when acid concentration increases results into the decrease in both coulombic attraction of H^+-ions and repulsion of SO_4^{2-} ions. In addition, the presence of excess SO_4^{2-} ions can also reduce the electrical potential and coulombic attraction for H^+-ions [71]. Therefore, the decreased repulsion of SO_4^{2-} ions along with an increase in their concentration adjacent to the surface lead to suppression of reaction of cyclohexanone oxime with H^+-ions thus reducing the yield.

3.4 CONCLUSIONS

Cyclization and molecular rearrangenet reactions as carried out conventionally require highly acidic conditions and operation and handling, especially on larger scales often prove to be difficult. Results reveal that the interfaces and supramolecular aggregates exert dramatic effects on the selectivity and rates of cyclization/rearrangement reactions in more complex ways than via simple medium (i.e., solvent polarity). Results obtained in the present studies suggest that micelles amd microemulsions of anionic surfactants in dilute acids can be looked upon as an alternative medium

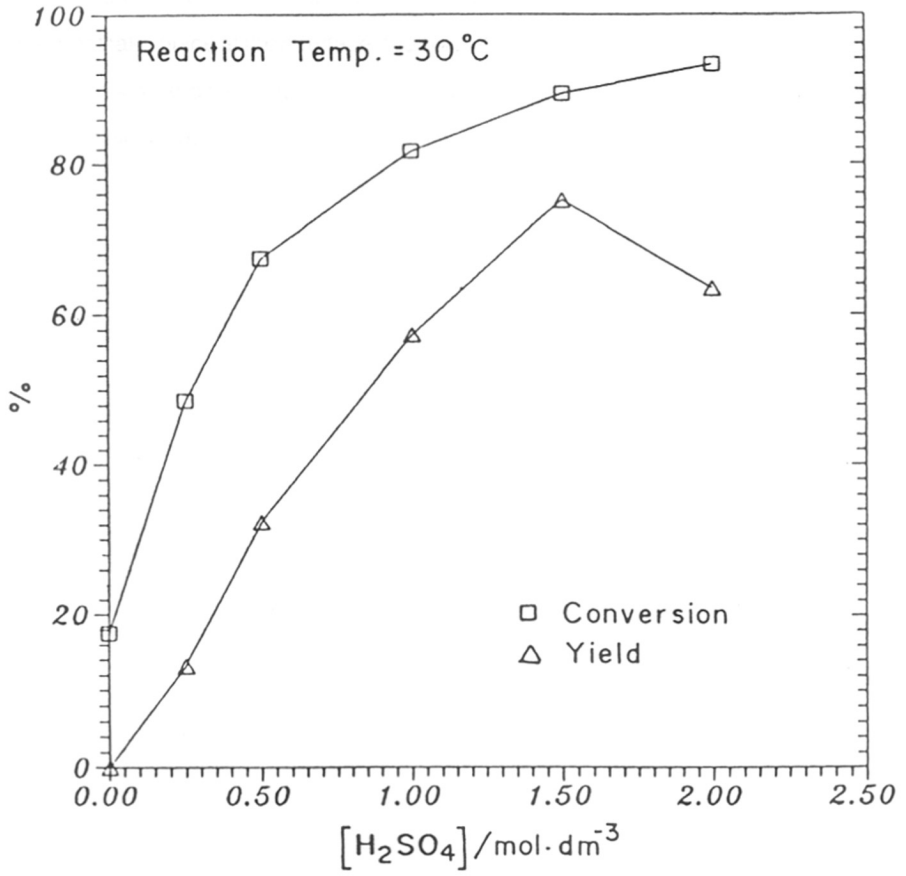

Figure 3.7 : Effect of H_2SO_4 concentration on the conversion of cyclohexanone oxime and on the yield of caprolactam. [cyclohexanone oxime] = 88 mM; [SDS] = 42 mM.

for these reactions which otherwise require drastic conditions. Eventually the reaction reported here are generic in character and demonstrate that other similar reactions can substantially benefit from this mode of operation. In general it is anticipated that all those reactions which occur at the microscopic interface or at Stern layer and involve the participation of hydrogen ions either as a reactant or as a catalytic species can benefit substantially in such media. Since cyclization and rearrangement take place at the interface, the solubility of the substrate in the solvent is of particular importance. This method would be especially suited to cyclization of peptide which are poorly soluble in organic solvents.

REFERENCES

[1] E. J. Fendler and J. H. Fendler, Micellar Catalysis of Miscellaneous Ionic Reactions. In *Catalysis in Micellar and Macromolecular Systems*; Academic Press: New York, 1975; Chapter 7.

[2] J. H. Fendler, Reactivity Control and Synthetic Applications. In *Membrane Mimetic Chemistry*; Wiley : New York, 1982; Chapter 11.

[3] R. A. Mackay, *Adv. Colloid Interface Sci.*, **15** (1991) 131.

[4] C. A. Bunton, *Catal. Rev. Sci. Eng.*, **20** (1979) 1.

[5] R. Leung, M. J. Hou and D. O. Shah, Micromeulsions: Formation, Structure, Properties and Novel Applications. In *Surfactants and in Chemical/Process Engineering: Surfactant Science Series* ; D. T. Wasan, M. E. Ginn and D. O. Shah, Eds.; Dekker: New York, 1988; Vol. **28**, Chapter 9, pp 315-367.

[6] L. N. Lewis, *Chem. Rev.*, **93** (1993) 2693.

[7] C. A. Bunton, Micellar Rate Effects Upon Organic Reactions. In *Kinetics and Catalysis in Microheterogeneous Systems: Surafactant Science Series*; M. Gratzel and K. Kalyanasundaram, Eds.; Dekker: 1991; Vol. **38**, Chapter 2, pp 13-62.

[8] F. M. Menger and H. Park, *Recl. Trav. Chim. Pays-Bas*, **113** (1994) 176.

[9] K. Holmberg, *Adv. Colloid Interface Sci.*, **51** (1994) 137.

[10] E. H. Cordes and R. B. Dunlop, *Accts. Chem. Res.*, **2** (1969) 329.

[11] C. A. Bunton and G. Savelli, *Adv. Phys. Org. Chem.*, **22** (1986) 213.

[12] K. Shinoda and B. Lindman, *Langmuir*, **3** (1987) 134.

[13] G. Gunnarsson, B. Johnsson and H. Wennerstrom, *J. Phys. Chem.*, **84** (1980) 3114.

[14] C. J. Drummond and F. Grieser, *J. Colloid Interface Sci.*, **127** (1989) 281.

[15] C. A. Bunton, F. Nome, F. H. Quina and L. S. Romsted, *Accts. Chem. Res.*, **24** (1991) 357.

[16] L. Garcia-Rio, E. Iglesias and M. E. Pena, *Langmuir*, **9** (1993) 1263.

[17] D. Stigter, *J. Phys. Chem.*, **68** (1964) 3603.

[18] K. A. Dill, D. E. Koppel, R. S. Cantor, J. D. Dill, D. Bendedouche and S. -H. Chen, *Nature*, **309** (1984) 42.

[19] D. W. R. Gruen, *Prog. Colloid Polym. Sci.*, **70** (1985) 6.

[20] N. Muller, *Accts. Chem. Res.*, **23** (1990) 23.

[21] L. Sepulveda, E. Lissi and F. Quina, *Adv. Colloid Interface Sci.*, **25** (1986) 1.

[22] T. Kunitake, S. Shinkai, *Adv. Phys. Org. Chem.*, **17** (1980) 435.

[23] L. S. Romsted, *J. Phys. Chem.*, **89** (1985) 5107.

[24] L. S. Romsted, Micellar Effects on Reaction Rates and Equilibria. In *Surfactants in Solutions*; K. L. Mittal and B. Lindman, Eds.; Plenum: New York, 1984;, Vol. **2**, pp 1015-1068.

[25] C. A. Bunton, K. Ohmenzetter and L. Sepulveda, *J. Phys. Chem.*, **81** (1977) 2000.

[26] C. A. Bunton, Micellar Rate Effects: What We Know and What We Think We Know. In *Surfactant in Solution*; K. L. Mittal and D. O. Shah, Eds.; Plenum: New York, 1991; Vol. **11**, pp 17-40.

[27] M. A. Mosset and C. O. Bizziogotti, *J. Am. Chem. Soc.*, **103** (1981) 6512.

[28] F. Candau, Y. S. Leong, G. Pouyet and S. Candau, *J. Colloid Interface Sci.*, **101** (1984) 167.

[29] G. D. Rees and B. H. Robinson, *Adv. Mater.* **5** (1993) 608.

[30] C. A. Bunton, Micellar Reactions. In *Application of Biochemical System in Organic Chemistry*; J. B. Jones, C. J. Sih and D. Perlman, Eds.; Wiley: New York, 1976; Part **2**, pp 731-814.

[31] G. Cerichelli, G. Mancinni, L. Luchetti, G. Savelli and C. A. Bunton, *J. Phys. Org. Chem.*, **4** (1991) 71.

[32] C. A. Bunton and R. J. Rubin, *Tetrahedron Letters*, **1** (1975) 55.

[33] C. A. Bunton, L. S. Romsted and H. J. Smith, *J. Org. Chem.*, **43** (1978) 4299.

[34] B. C. Clark, Jr., T. S. Chamblee and G. A. Iacobucci, *J. Org. Chem.*, **49** (1984) 4557.

[35] B. C. Clark, Jr., T. S. Chamblee and G. A. Iacobucci, *J. Org. Chem.*, **54** (1989) 1032.

[36] D. A. Jager, J. T. Ippoliti, *J. Org. Chem.*, **46** (1981) 4964.

[37] I. Rico, K. Halvorsen, C. Dubrule and A. Lattes, *J. Org. Chem.*, **59** (1994) 415.

[38] G. Cerricelli, L. Luchetti, M. N. Muzzioli, R. Germani, P. D. Ponti, N. Spreti, G. Savelli, C. A. Bunton, *J. Chem. Soc., Perkin Trans.* 2, (1989) 1801.

[39] I. Wei, A. Lucas, J. Yue and R. B. Lennox, *Langmuir*, 7 (1991) 1336.

[40] C. A. Bunton and B. Wolfe, *J. Am. Chem. Soc.*, **95** (1973) 3742.

[41] O. A. Amire, *J. Colloid Int. Sci.*, **126** (1988) 508.

[42] R. Bogner, *Aantibiotiki*, **9** (1964) 875.

[43] S. Takahashi, Microbial Production of D-p-Hydroxy phenylglycine. In "*Biotechnology of Amino acid Production: Progress in Industrial Microbiology*; K. Aida, I. Chibata, K. Nakayama, K. Takinami and H. Yamada, Eds.; Elsevier: New York, 1986; Vol. **24**, Chapter 24, pp 269-279.

[44] A. H. De Rooij, Chr. Dijkhuis and J. T. J. Van Goolen, *Chemtech*, **7** (1977) 309.

[45] J. H. Ottenheym, and J. W. Gielkens, *Hydrocarbon Process*, **47** (1968) 176.

[46] J. H. Bonfield and J. Northeott, Caprolactam. In *Encyclopedia of Industrial Chemical Analysis*; F. D. Snell and L. S. Ettre, Eds.; Wiley: New York, 1969; Vol. **8**, pp 114-129.

[47] W. H. Haberstroh, D. E. Collins, Synthetic Organic Chemicals. In *Reigel's Handbook of Industrial Chemistry*; J. E. Kent, Ed.; Van Nostrand: New York, 1974, Chapter 25.

[48] M. Sitting, Caprolactam and Its Derivatives. In *Combine Hydrocarbons and Nitrogen for Profits*; Noyes Dvelopment Corp.: Park Ridge, NJ; Chemical Process Review No. **8**, 1967; pp 177-187.

[49] T. Satomi, T. Ohashi, Y. Kii, H. Kumagai and H. Yamada, *J. Ferment. Technol.*, **57** (1979) 328.

[50] A. I. Vogel, The Praparation of Derivatives. In *A Text Book of Practical Chemistry*, 3rd Ed., ELBS/Longmann: London, 1971; pp 343.

[51] M. Bourrel and R. S. Schechter, The Phase Behavior and Properties of Solutions Containing Amphiphiles, Organic Liquids and Water: Micellar Solution. In *Microemulsions and Releted Systems: Surafactant Science Series*; Dekker: New York, 1988; Vol. **30**, Chapter 4, pp 127-205.

[52] A. S. Chhatre and B. D. Kulkarni, *J. Colloid Interface Sci.*, **150** (1992) 528.

[53] C. J. Garnett, A. J. Lambie, W. H. Beck, and M. Liler, *J. Chem. Soc., Faraday Trans.* 1, **79** (1983) 953.

[54] C. J. Drummond and F. Grieser, *J. Colloid Int. Sci.*, **127** (1989) 281.

[55] C. J. Garnett, A. J. Lambie, W. H. Beck and M. Liler, *J. Chem. Soc., Faraday Trans.* 1, **79** (1983) 965.

[56] R. Zana, S. Yiv, C. Strazile and P. T. Lianos, *J. Colloid Interface Sci.*, **80** (1981) 208.

[57] M. Abu-Hamdiyyah and K. Kumari, *J. Phys. Chem.*, **94** (1990) 2518.

[58] B. Carlos, J. R. Leis and M. E. Pena, *J. Phys. Chem.*, **96** (1992) 1957.

[59] E. D. Goddard and G. C. Benson, *Can. J. Chem.*, **35** (1957) 986.

[60] H. Kunieda and S. E. Friberg, *Bull. Chem. Soc. Jpn.*, **54** (1981) 1010.

[61] D. F. Evans and P. J. Wightman, *J. Colloid Interface Sci.*, **86** (1982) 515.

[62] C. Tanford, The Effect of Temperature: Anomalous Entropy and Heat Capacity. In *The Hydrophobic Effect: Formation of Micelles and Biological Membranes*; Wiley: New York, 1980; Chapter 4.

[63] D. O. Shah, S. Y. Shaio, *Adv. Chem. Ser.*, **144** (1975) 153.

[64] U. Tonellato, *Colloid Surf.*, **35** (1989) 121.

[65] F. H. Quina and H. Chaimovich, *J. Phys. Chem.*, **83** (1979) 1844.

[66] B. W. Barry and R. Wilson, *Colloid Polym. Sci.*, **256** (1978) 251.

[67] C. J. Garnett, A. J. Lambie, W. H. Beck and M. Liler, *J. Chem. Soc., Faraday Trans.* 1, **79** (1983) 953.

[68] M. I. Page and W. P. Jencks, *Proc. Nat. Acad. Sci.*, U.S.A, **68** (1971) 1678.

[69] D. G. Hall, *J. Phys. Chem.*, **91** (1987) 4287.

[70] L. S. Romsted, A General Kinetic Theory of Rate Enhancement for Reactions Between Organic Substrates and Hydrophilic Ions in Micellar Systems. In *Micellization, Solubilization, and Microemulsions*; K. L. Mittal, Ed.; Plenum: New York, 1977; Vol. **2**, pp 509-530.

[71] C. A. Bunton, M. A. Mhala and J. R. Moffatt, *J. Phys. Chem.*, **93** (1989) 7851.

CHAPTER 4

ELECTROCHEMICAL INVESTIGATION IN MICELLES AND MICROEMULSIONS : A CYCLIC VOLTAMMETRY STUDY WITH ULTRAMICROELECTRODE

This chapter presents a cyclic voltammetric investigation of electrochemical behavior of potassium ferricyanide, a water soluble probe, in aqueous anionic surfactant solution (**Section A**) to obtain information pertaining to micellization. **Section B** of this chapter shows the usefulness of ultramicroelectrode ability in exploring the coupled chemical reaction in aqueous microemulsion systems.

Section A : Electrochemistry of potassium ferricyanide in anionic surfactant solutions

4.1.A INTRODUCTION

Microheterogeneous assemblies such as micelles and microemulsions have been used in a wide range of applications which include catalysis [1, 2], solar energy conversion [3], electroenzymatic catalysis [4] and many others [5,6]. The presence of surface active agents in these systems brings about several variations in the system properties which are characterized by special features such as lowering of interfacial tension, formation of micelles above a certain critical concentration and ability to solubilize water-insoluble substances. It is now known that these effects arise as a result of the association complexes (micelles) containing a large number of molecules of surface active agents. This phenomenon is normally accompanied by a sharp change in system properties such as intensity of light scattering, surface tension, viscosity and electrical conductivity. These properties in turn can be used to characterize the organized assemblies. Many techniques have been used to study the association of surfactant and a large number of papers have been devoted to the experimental study of critical phenomena in micellar solutions and microemulsions [7].

The different electrochemical techniques such as polarography, tensametry and ion-selective electrodes have been found to be useful in determining the *critical micelle concentration* (CMC) [8-11]. The cyclic voltammetry with conventional size macroelectrode has been used successfully in determining the CMC of surfactant, translation diffusion coefficient of micelles and solution microstructure [12-14]. Kaifer and Bard [15] in a cyclic voltammetric (CV) study of methylviologen in micellar systems, noted that the CMC of SDS could be estimated from changes in

adsorption-desorption patterns of the cation radical. Recently Mandal et al. [16] have shown that CV peak currents of ferrocyanide can be used to detect CMC in a variety of micellar systems. However recent developments in voltammetry using ultramicroelectodes (UMEs) offers a promising route to minimize some of the disadvantages of CV with macroelectrode [17, 18] and facilitate their use in resistive solution or solution with low dielectric constant [19, 20].

4.2.A EXPERIMENTAL

4.2.A.1 Materials

Analytical grade sodium dodecyl sulfate (SDS) obtained from Loba Chemicals was recrystallized from ethanol in order to remove the traces of long chain alcohol and used as a surfactant. $K_3Fe(CN)_6$ from Sarabhai Merck Limited was used as a redox-active probe and analytical grade NaCl of BDH Chemicals was used as a supporting electrolyte. Doubly distilled conductivity water having a specific conductance 2×10^{-6} to 3×10^{-6} ohm^{-1} was used as a solvent throughout the experiment.

4.2.A.2 Methods

4.2.A.2.1 Cyclic voltammetric measurements

Cyclic voltammetric experiments were carried out using a conventional three electrode-cell with a *Pt* gauze ($2.5 \times 4 cm^2$) as counter electrode and a reference electrode of saturated calomel. The UME was fabricated from platinum wire of 10 μm diameter which was washed with 30% nitric acid, etched in aqua regia, dried overnight, and then placed in a 10 cm long 1 mm Pyrex tube. After high temperature vacuum cleaning the wire was sealed and etched in hydrofluoric acid, polished with graded alumina poder (down to 0.05 μm) on a polishing microcloth. Electrical connection to the platinum wire was made by immersing copper wire through mercury column in the capillary. All measurements were performed with a PAR (Princeton Applied Research Princeton,

NJ) Model 175 Universal Programmer and PAR Model 173 Potentiostat coupled with a Houston Instrument Model RE 0091 X-Y Recorder. In the electrochemical measurement, solutions were deoxygenated by bubbling argon for at least 10 minutes. Cyclic voltammograms were typically scanned at 200 mV/s from a potential +0.7 to -0.1 volt (vs SCE) for a series of SDS solutions prepared with definite concentration of redox active material and supporting electrolyte (1.0 mM $K_3Fe(CN)_6$ and 0.1 M NaCl) at 25 °C. Peak currents were measured from *i-E* curves by the method described elsewhere [21]. A remarkable change in CV behavior and also an abrupt change in peak current, I_p, was considered as the CMC.

4.2.A.2.2 UV-VIS measurements

UV-visible spectral measurements were made on Shimadzu spectrophotometer (Model UV-260) using a matched pair of stoppered quartz cells of 1 cm path length placed in a thermostated cell holder at 25 °C. Spectrometric determinations of the transitions was performed by recording its spectra and plotting the absorbance at two different wavelengths against SDS concentration.

4.3.A RESULTS AND DISCUSSION

4.3.A.1 Diffusion of redox species

Derivation

For a disk-shaped UME, the steady-state diffusion controlled limiting current, I_l, irrespective of the degree of reversibility is given by equation [22]:

$$I_l = 4nFDCa \qquad (4.1)$$

where n is the number of electrons involved in the electrochemical reaction, F is the Faraday constant, a is the electrode radius and D is the diffusion coefficient for the electroactive species, and C is the concentration of the electroactive species. The diffusion coefficient of electroactive species can be estimated from limiting currents using Eq (4.1).

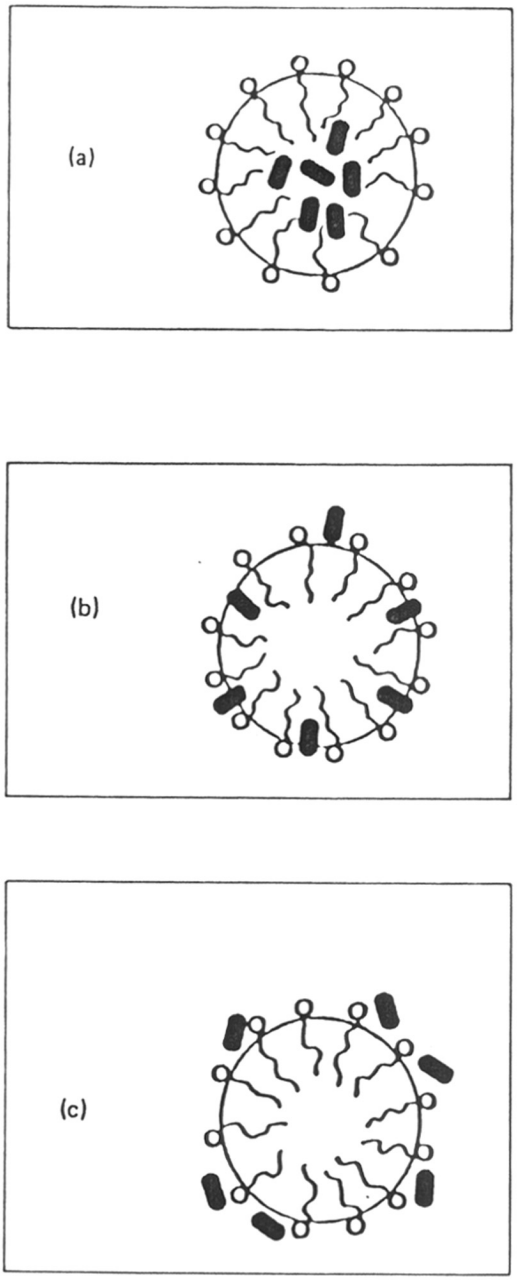

Figure 1.4 : Schematic view of the three possible solubilization sites in surfactant aggregates: (a) micelle interior; (b) palisade layer; (c) micellar surface.

In a micellar solution, where the electroactive probe is partitioned between micelles and continuous phase, the diffusion limited current may then be expressed as,

$$I_l = 4nF\alpha(D_m C_m + D_p C_p) \qquad (4.2)$$

where C_m and C_p are the concentration of probe in the micellar and the continuous phase respectively; D_m is the micelles diffusion coefficient and D_p is the probe diffusion coefficient in the bulk. The partition coefficient, K, is a function of surfactant concentration (C_S) and generally decreases with increasing C_S after CMC.

$$K = C_m / C_p(C_s - cmc) \qquad (4.3)$$

Substituting for C_m in Eq (4.2) and on rearrangement we get,

$$I_l = 4nF\alpha[D_m K C_p(C_s - cmc) + D_p C_p] \qquad (4.4)$$

Thus the apparent diffusion coefficient, D can be identified as,

$$D = \frac{D_m K(C_s - cmc) + D_p}{1 + K(C_s - cmc)} \qquad (4.5)$$

The above equation reveals the dependence of D in the micellar solution on the concentration of surfactant, CMC and partition coefficient respectively.

4.3.A.2 Effect of SDS concentration on the redox behavior of $K_3Fe(CN)_6$

Figures 4.1(A-G) show the cyclic voltammograms for 1 mM $K_3Fe(CN)_6$ in aqueous NaCl solution at a scan rate of 200 mV sec^{-1}. The peak potential separation (ΔE_p), the difference between the cathodic, E_{pc} and the anodic, E_{pa}, in all the voltammograms is greater than 59 mV. The anodic to cathodic current ratio (I_{pa}/I_{pc}) is more than one, indicating irreversibility in all solutions. Since SDS is ionic in nature and negatively charged it is expected that the adsorption increases with increasing positive potential and can result in more anodic peak current. In addition the remarkable change in peak currents can be explained by changes in diffusion coefficient of $Fe(CN)_6^{3-/4-}$ [23]. Although the SDS molecules do not take part in any charge-transfer reaction

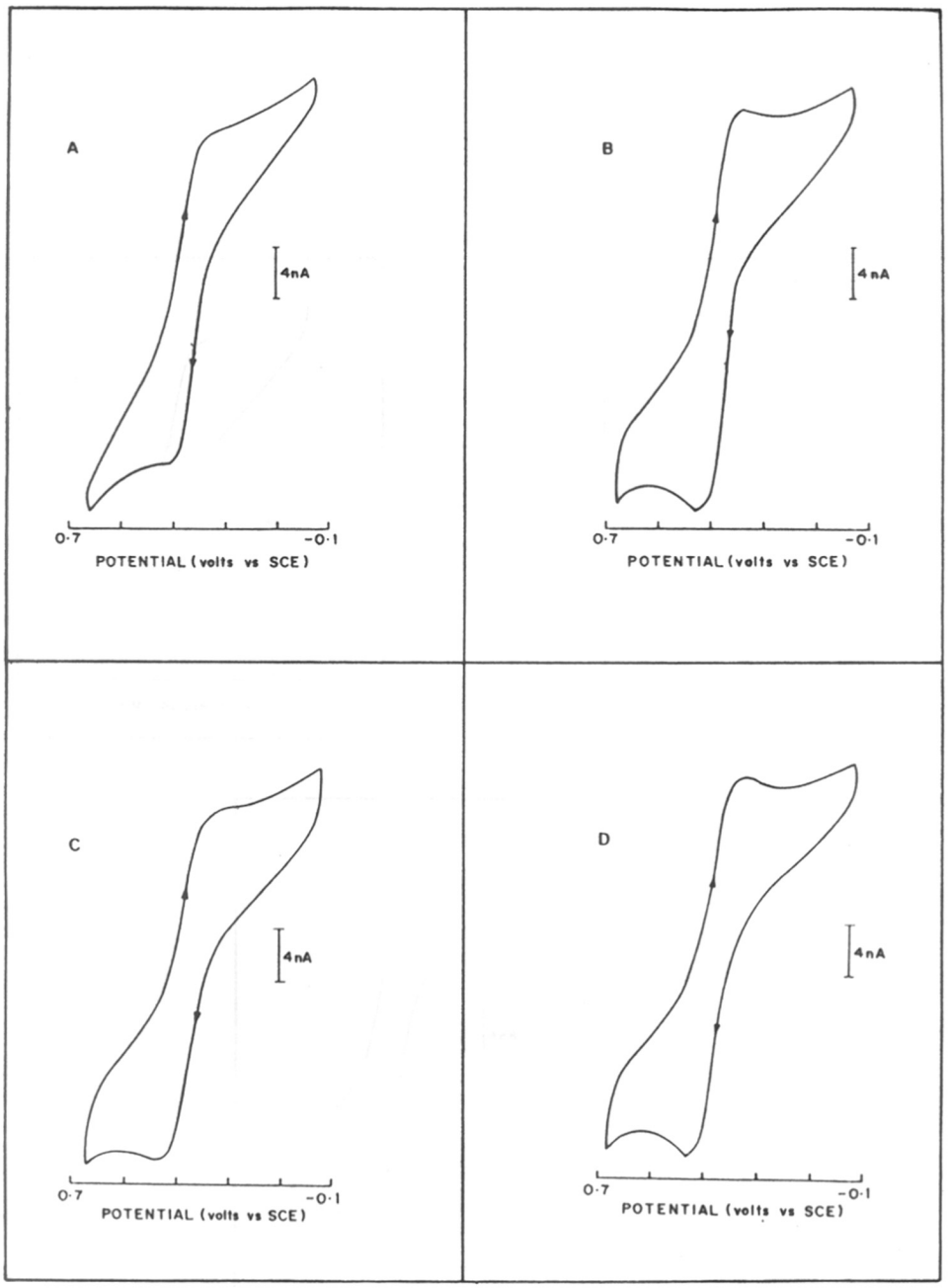

Figures 4.1(A-G) : Cyclic voltammograms of the 1 mM $K_3Fe(CN)_6$ in 0.1 M NaCl aqueous SDS solution at ultramicroelectrode. Concentrations of SDS : (A) 0 mM; (B) 0.5 mM; (C) 1.0 mM; (D) 1.5 mM; (E) 2.0 mM; (F) 3.0 mM; (G) 4.0 mM.

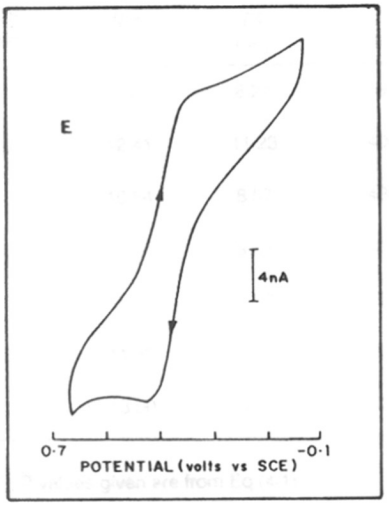

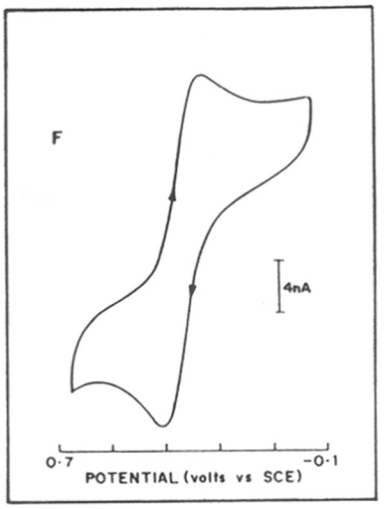

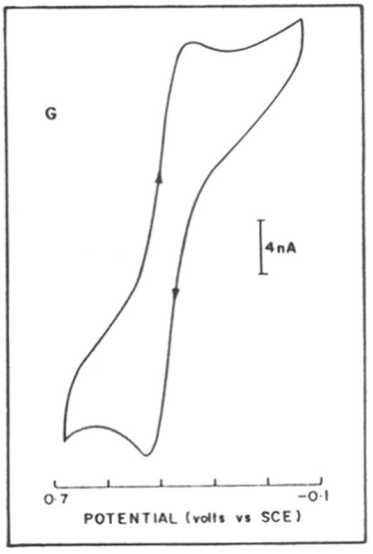

Figure 4.1 : (continued).

Table 4.1 : Electrochemical Data for $K_3Fe(CN)_6$ in 0.1 M NaCl as a Function of SDS Concentration[a]

SDS (mM)	I_{pa} (nA)	I_{pc}. (nA)	E_{pa} (mV)	E_{pc} (mV)	D_{pa} ($cm^2\ s^{-1}$)[b]	D_{pc} ($cm^2\ s^{-1}$)[b]
0.0	9.46	8.27	396	284	0.49×10^{-7}	0.43×10^{-7}
0.5	12.41	11.23	400	280	0.64×10^{-7}	0.58×10^{-7}
1.0	10.84	8.57	436	272	0.56×10^{-7}	0.44×10^{-7}
1.5	12.61	9.85	432	272	0.65×10^{-7}	0.51×10^{-7}
2.0	8.27	7.09	420	276	0.43×10^{-7}	0.37×10^{-7}
3.0	11.62	11.43	392	268	0.60×10^{-7}	0.59×10^{-7}
4.0	13.50	12.31	424	276	0.70×10^{-7}	0.64×10^{-7}

[a] 25 °C; [b] values given are from Eq (4.1).

at the interface (conventionally known as electro-inactive), it can modify the interfacial charge transfer as well as the mass transfer characteristics of the probe in various ways. These include blocking effects due to effective area variation, electrostatic effects due to adsorbed surfactant moieties and specific chemical interactions with the reactant or product of the probes. All these factors can cause changes in the structures of electrical double layer (ψ effects) [24]. Accordingly, the behavior of SDS anion may be attributed to the way these adsorbed ions influence the structure of the electrode-electrolyte interface. Thus reorganization of the electrical double layer on the electrode surface and presence of micelles in the bulk solution regulate the rate of diffusion of probe towards the electrode surface.

The results of electrochemical investigation with potassium ferricyanide as a probe are summarized in Table 4.1, wherein the diffusion coefficient, calculated from the Eq (4.1) (limiting currents are taken from the CV data of Figures 4.1(A-G)) shows a considerable dependence on SDS concentration reflecting the unequal mobility of oxidized and reduced forms even below CMC ($\approx$ 1.39 - 1.7 mM). This can be attributed to the polydispersion/heterodispersion of SDS [25, 26] and also to the dimer formation by step-wise association leading to the formation of premicellar aggregates [27, 28]. Normally the ionic head groups are kept far apart by electrostatics repulsions and only a small portion of the total area of the hydrocarbon chains is in intimate contact. Typically, the electroactive species $Fe(CN)_6^{3-/4-}$ demonstrates the limiting case where both oxidized and reduced forms reside in the aqueous phase [29]. However, the preferential association of the $Fe(CN)_6^{3-}$ form of the probe over $Fe(CN)_6^{4-}$ form with SDS can be visualized as follows. Association of the two forms with SDS monomer and micelles is determined by a combination of the hydrophobic attractions and the electrostatic repulsion. In the present case, with the anionic micelles of SDS it appears that electrostatic repulsion dominate for $Fe(CN)_6^{4-}$ form whereas the hydrophobic attraction dominate for the $Fe(CN)_6^{3-}$. Further it is seen that diffusion coefficient of $Fe(CN)_6^{3-/4-}$ increases with increasing SDS concentration after CMC. Such an increase may be caused by percolation [30] or due to micellar/monomer equilibrium [31, 32].

4.3.A.3 Spectroscopic evidence of micellization

There is a great deal of evidence for some form of association of SDS molecules. To explore the extent of micellization in present system and to assess the effects, absorption spectra for the same compositions were examined. Figure 4.2 shows the uv-visible spectra for 0.5 - 1.5 mM SDS concentration and exhibits absorption maxima at 305 and 417 nm which are identical to those reported earlier [33]. The absorption spectra also reflect the change in intensity as SDS concentration varies and is maximum for 0.5 mM SDS. In addition, the plots of absorbance against SDS concentration shows a break point between 1.5 - 2.0 mM, which is ascribed to be the CMC (Figure 4.3) of SDS in 0.1 M NaCl aqueous solution at 25 ^{o}C, and is in accordance with the values of 1.39 - 1.7 mM reported earlier [34-38]. Inspection of the data in Table 4.1 also shows a change in the peak current and diffusion coefficient of probe in the above region of SDS concentration and thus support our interpretation.

4.4.A CONCLUSIONS

In summary, the work reported in section A of this chapter shows that the movement of probe is sensitive to the surfactant concentration. The minimum of probe diffusion coefficient that accompany micellization is in good agreement with uv-visible spectrophotometeric study, and suggests an additional utility of ultramicroelectrode for determining the CMC of surfactant. The measurement also provides a qualitative insight into the existence of premicellar aggregates.

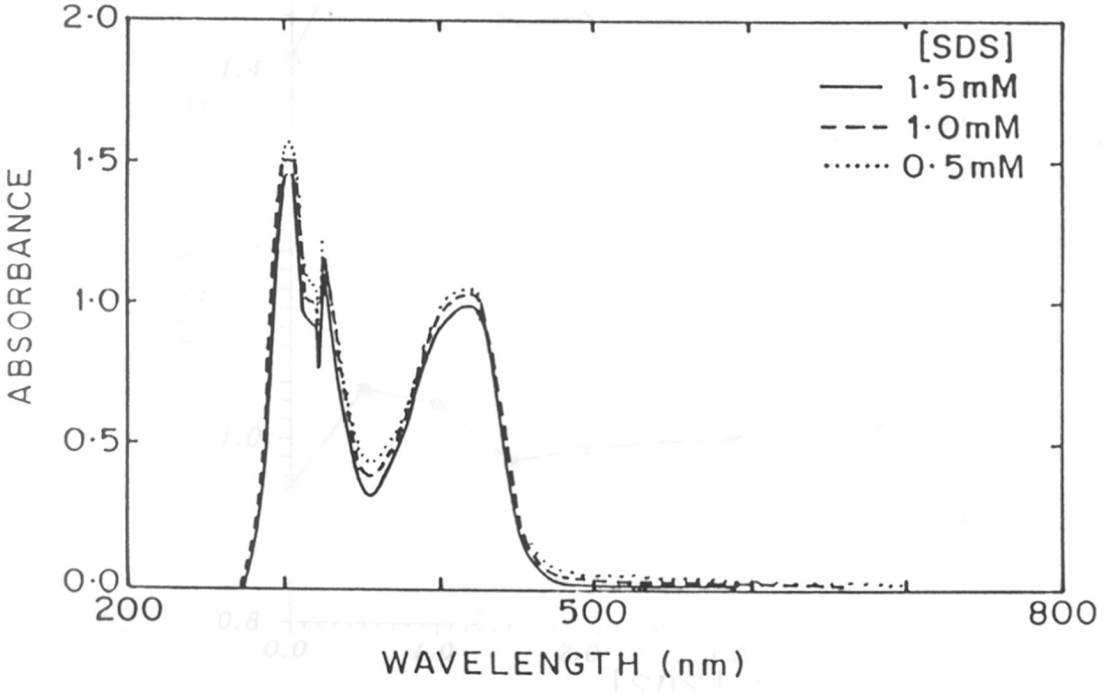

Figure 4.2 : UV-visible absorption spectra of 1 mM $K_3Fe(CN)_6$ in 0.1 M NaCl aqueous SDS solution in a quartz cell of path length 1 cm.

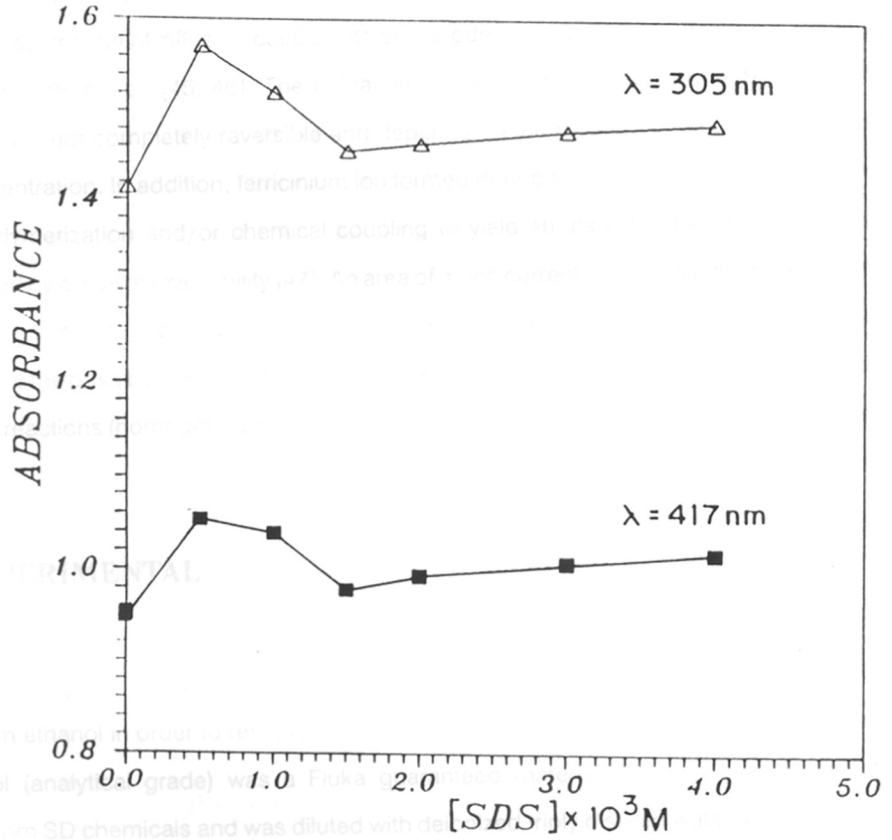

Figure 4.3 : Plot of absorbance of 1 mM $K_3Fe(CN)_6$ in 0.1 M NaCl aqueous solution vs SDS concentration.

Section B : Electrochemistry of ferrocene solubilized in O/W microemulsions

4.1.B INTRODUCTION

Microheterogeneous systems provide a multifunctional environment for the solubilization and partitioning of aqueous solute and insoluble molecules [39-42]. The electrochemistry of ferrocene solubilized in organized assemblies has been the subject of several studies [43, 44] as a probe for the estimation of diffusion coefficients of microdroplets and also to explore the changes in microscopic structures [45, 46]. The oxidation of ferrocene at Pt electrode in micelles/microemulsions is not completely reversible and depends on the medium of electrolysis and also on the concentration. In addition, ferricinium ion formed during the oxidation has been shown to undergo polymerization and/or chemical coupling to yield an insoluble film on *Pt* electrodes accompanied by a loss of reversibility [47]. An area of much current interest is that of the dynamics of electron-transfer that occurs between a micelle/microemulsion solubilized ferrocene and UME surface where the possibilty of film formations is generally minimal, and also to probe the possibilty of chemical reactions (homogeneous) associated with electrochemical reactions (heterogeneous) at UMEs.

4.2.B EXPERIMENTAL

4.2.B.1 Materials

Analytical grade sodium dodecyl sulfate (SDS) obtained from Loba Chemicals was recrytallized from ethanol in order to remove the traces of long chain alcohol and used as surfactant. Pentan-1-ol (analytical grade) was a Fluka guaranteed material. Concentrated H_2SO_4 was obtained from SD chemicals and was diluted with deionized triply distilled water. Analytical grade Ferrocene (Fc) was purchased from BDH. The exact concentration of H_2SO_4 was determined by titration with standardized 0.5 M NaOH solution. Microemulsion investigated was composed of pentan-1-ol (1.78 % by wt), SDS (1.0 % by wt) and aq. H_2SO_4 (97.22 % by wt). This ternary mixtures correspond to a limiting case of microemulsion [48].

4.2.B.2 Methods

4.2.B.2.1 Cyclic voltammetric measurements

The electrochemical behavior of 10^{-3} M of ferrocene solubilized in the microemulsion has been examined using conventional *Pt* disk electrode of diameter $1.0\,mm$ as well as ultramicro-electrode of $10\,\mu m$ diameter. Cyclic voltammetric (CV) measurements were performed with a PAR (Princeton Applied Research, Princeton, NJ) Model 175 Universal Programmer and PAR Model 173 Potentiostat coupled with a Houston Instrument Model RE 0091 X-Y recorder. A *Pt* foil counter electrode and precalibrated Hg/Hg_2SO_4 reference electrode were used in argon atmosphere during the voltammetric experiments. CV results were confirmed by at least two replicates and separate experiments were conducted to avoid both the possibility of any instrumental artifact and reactions involving surface species on the electrode surface. All the experiments were conducted at room temperature, ca. $25 \pm 1\,^{o}C$.

4.2.B.2.2 Controlled potential coulometry (CPC) study

Controlled potential coulometry is a very useful method for studying the mechanism of electrode reactions and also for determining the n_{app} (number of electrons involved in electro-chemical process). In order to examine the effects of chemical reactions coupled to electron transfer, the CPC of 10^{-3} M ferrocene at a large carbon electrode, and at a potential of about + 1.30 V vs SCE near the first oxidation peak (**AI**) was performed, as described by Bard et al. [49] The total number of coulombs consumed in electrolyses durations ($t \approx 10$ hrs) was 53.50.

4.3.B RESULTS AND DISCUSSION

4.3.B.1 Cyclic voltammetric behavior

Figure 4.4 shows the cyclic voltammograms of ferrocene at conventional electrode for two representative scan rates namely 10 and 500 mV/s respectively over the range of -0.47 to + 1.26 volt. Unlike the well known reversible voltammograms observed for ferrocene in nonaqueous

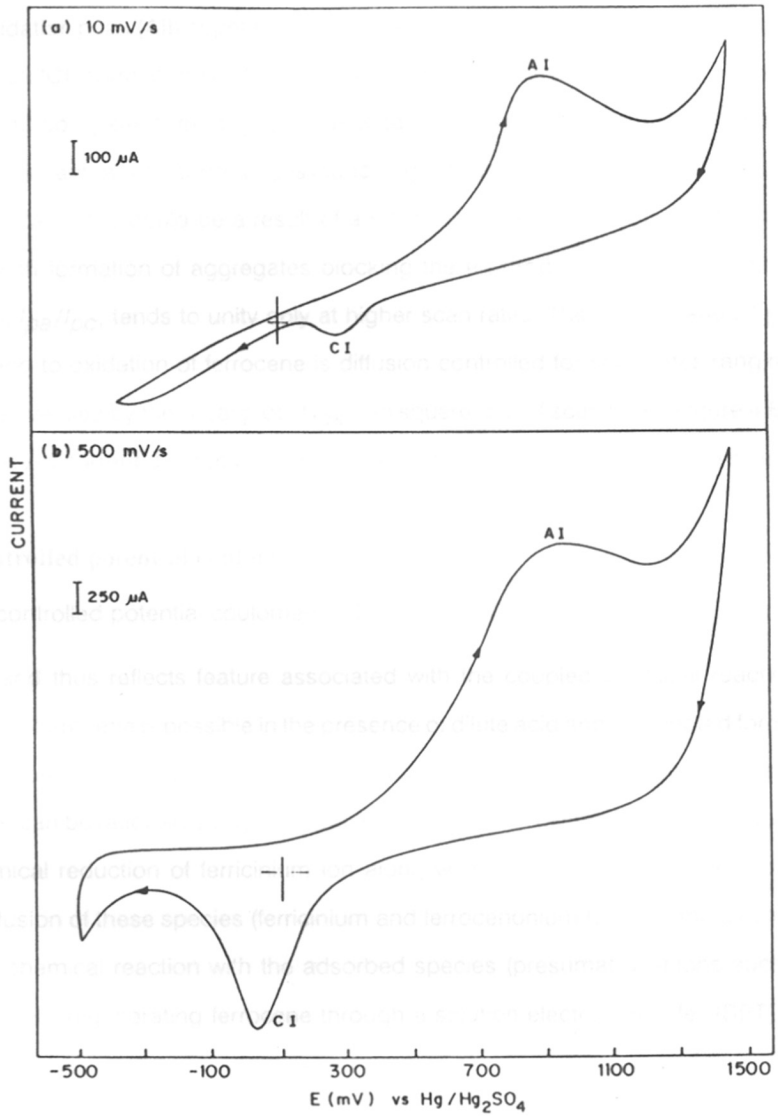

Figure 4.4 : Cyclic voltammograms of 1.0 mM ferrocene solubilized in the microemulsion system of pentan-1-ol/SDS/0.5 M H_2SO_4 on a conventional Pt disk electrode of diameter 4.0 mm versus Hg/Hg_2SO_4 for two scan rates, namely (a) 10 mV/s and (b) 500 mV/s over the range -0.47 to +1.26 V.

systems, the cathodic and anodic peak potential varies with scan rates indicating irreversibilty in the microemulsion. This is further confirmed by the I_{pa}/I_{pc} ratio and peak separation (ΔE_p) with high as well as low scan rates. In sharp contrast to voltammograms obtained using larger electrode a second oxidation peak (**AII**) appears during the reverse scan at low scan rates (Figures 4.5(a-h)), where the peak (**CI**) corresponding to ferricinium ion reduction is almost absent. However, gradual increase in cathodic peak current, I_{pc}, with a negative shift in peak potential is observed at higher scan rates and eventually no current dip is found (e.g., at scan rate 1000 mV/s). The lack of intensity of **CI** at low scan rates could be a result of a slow cation exchange between Na^+ of SDS and ferricinium with formation of aggregates blocking the electrode surface. In addition, the peak current ratio, I_{pa}/I_{pc}, tends to unity only at higher scan rates. The forward anodic peak current corresponding to oxidation of ferrocene is diffusion controlled for scan rates ranging from 5 to 2000 mV/s as verified by the linear plot of I_{pa} with square root of scan rates (Figure 4.6). However, the magnitude of current dip does not show any such apparent correlation with scan rate.

4.3.B.2 Controlled potential coulometry

The controlled potential coulometry (CPC) at +1.30 V vs SCE gives n_{app} as 0.55 ($n/2 < n_{app} < n$) and thus reflects feature associated with the coupled chemical reactions [50-54]. Protonation of ferrocene is possible in the presence of dilute acid and protonated form may prefer to stay in the continuous phase of microemulsion solution [55]. The above competing trend during reverse scan can be rationalized by invoking a second step of oxidation process suppressing the electrochemical reduction of ferricinium ion along with the regeneration of ferrocene. Consequently, diffusion of these species (ferricinium and ferrocenonium towards the electrode surface causes the chemical reaction with the adsorbed species (presumably anions such as HSO_4^-, SO_4^{2-} and OH^-) regenerating ferrocene through a solution electron transfer (SET) [56]. These

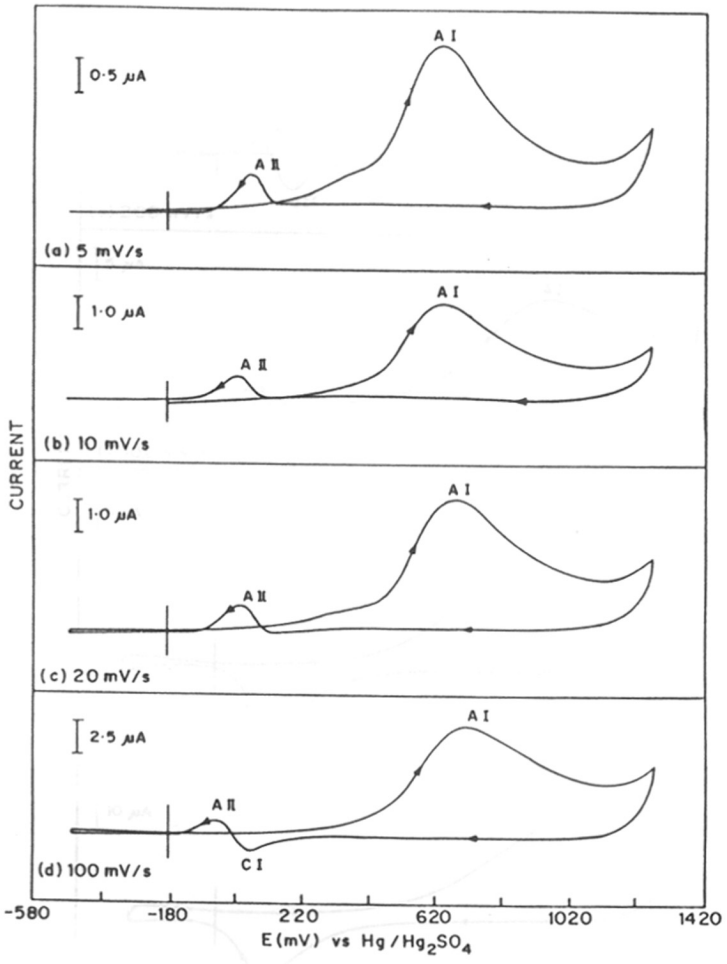

Figure 4.5 : Cyclic voltammograms of 1.0 mM ferrocene solubilized in the microemulsion of pentan-1-ol/SDS/0.5 M H_2SO_4 on a Pt ultramicroelectrode of 10 μm diameter versus Hg/Hg_2SO_4; Scan rates: (a) 5 mV/s; (b) 10 mV/s; (c) 20 mV/s; (d) 100 mV/s; (e) 200 mV/s; (f) 500 mV/s; (g) 1000 mV/s; (h) 2000 mV/s. The peak (CI) corresponding to ferricinium ion reduction is nearly absent at low scan rates.

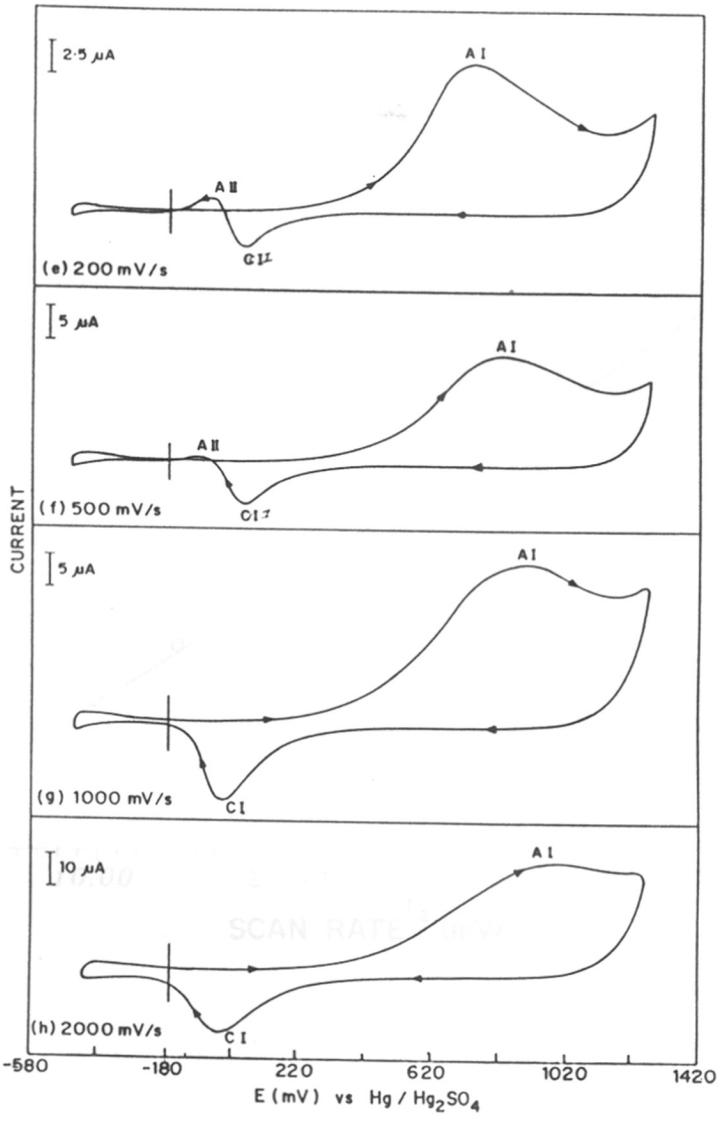

Figure 4.5 : (continued).

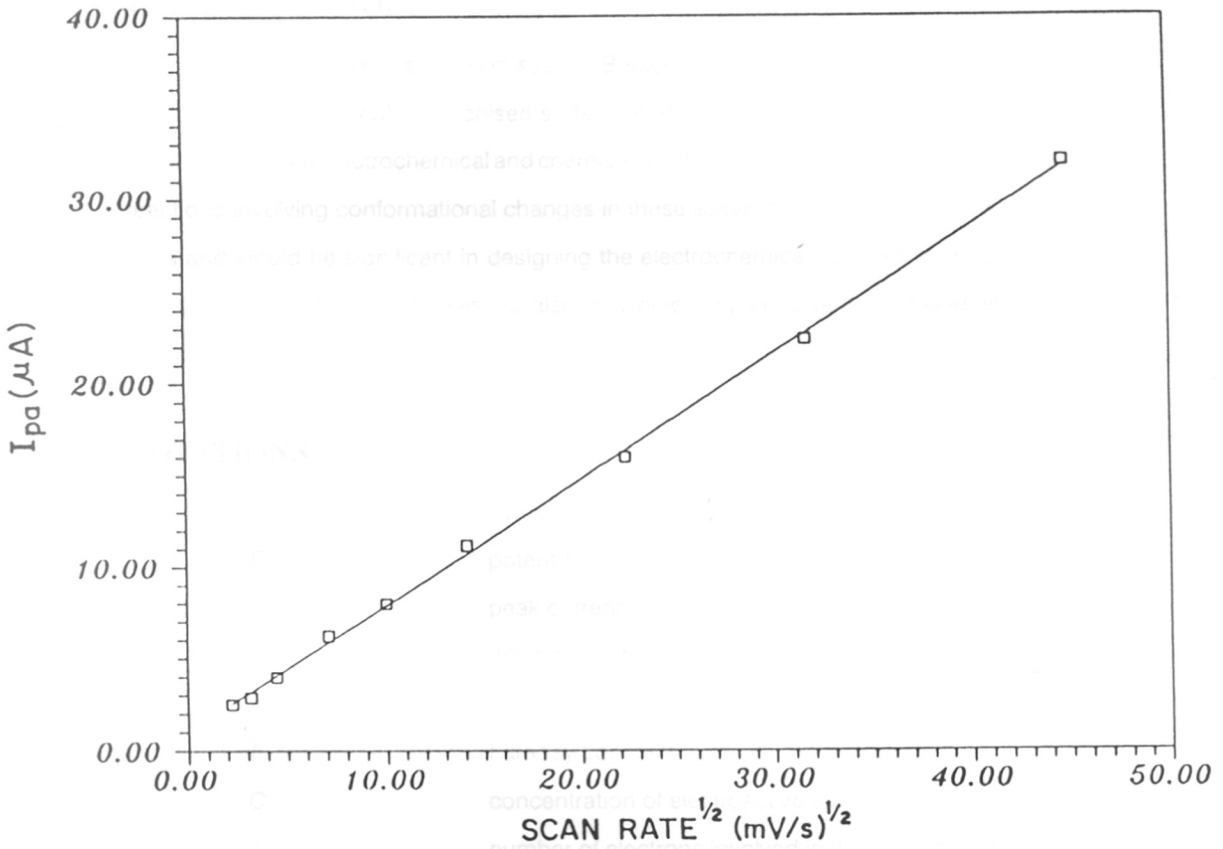

Figure 4.6 : Scan rate dependence of the forward anodic peak current, I_{pa}, for the oxidation of 1.0 mM ferrocene solubilized in the microemulsion system of pentan-1-ol/SDS/0.5 M H_2SO_4.

side reactions also mask the reduction of ferricinium ions at lower scan rates. But at higher scan rates, the chemical steps do not have ample time to occur and reaction becomes a nearly reversible one-electron process.

4.4.B CONCLUSIONS

The phenomena described in section B exemplifies a class of reactions where electrocatalytic rate enhancement in organised surfactant assemblies are observed due to an interesting coupling between electrochemical and chemical reactions. An understanding of coupled chemical reactions involving conformational changes in these assemblies may have far reaching implications and would be significant in designing the electrochemical reactors for electrosynthesis of inorganic and organic materials as also in biologically important mediated electron-transfer process.

NOTATIONS

i	current
E	potential
I_p	peak current
I_l	diffusion limited current
a	electrode radius
F	Faraday constant
C	concentration of electroactive species
n	number of electrons involved in the electrochemical process
D	apparent diffusion coefficient
C_m	probe concentration in micelles
C_p	probe concentration in bulk
D_m	micellar diffusion coefficient

D_p	probe diffusion coefficient in bulk
K	partition coefficient of probe between micelle and bulk
C_s	surfactant concentration
I_{pa}	anodic peak current
I_{pc}	cathodic peak current
E_{pa}	anodic peak potential
E_{pc}	cathodic peak potential
ΔE_p	peak potential separation
n_{app}	number of electrons involved in the electrochemical process
AI	first oxidation peak
AII	second oxidation peak
CI	first reduction peak

REFERENCES

[1] J. H. Fendler and E. J. Fendler, In *Catalysis in Micellar and Macromolecular Systems*; Academic: New York, 1975.

[2] R. Leung, M. J. Hou and D. O. Shah, Microemulsions: Formation, Structure, Properties and Novel Applications. In *Surfactants in Chemical/Process Engineering: surfactant Science Series*; D. T. Wasan, M. E. Ginn and D. O. Shah, Eds.; Dekker: New York, 1988; Vol. **28**, Chapter 9, pp 315-367.

[3] M. Gratzel, In *Heterogeneous Photochemical Electron Transfer*; CRC: Boca Raton, 1989.

[4] G. F. Hall and A. P. F. Turner, *Electroanalysis*, **6** (1994) 217.

[5] J. F. Rusling, *Acc. Chem. Res.*, **24** (1991) 75.

[6] A. S. Chhatre, N. K. Yadav and B. D. Kulkarni, *Sep. Sci. Technol.*, **28** (1993) 1465.

[7] M. J. Rosen, Micelle Formation by Surfactants. In *Surfactants and Interfacial Phenomena*; Wiley: New York, 1978; chapter 3, pp 83-121.

[8] E. L. Colichman, *J. Am. Chem. Soc.*, **72** (1950) 4036.

[9] B. J. Birch, D. E. Clarke, R. S. Lee and J. Oakes, *Anal. Chim. Acta*, **70** (1974) 417.

[10] T. Fujinaga, S. Okazaki and H. Freiser, *Anal. Chem.*, **46** (1974) 1842.

[11] N. Shinozuka and S. Hayano, Electrochemical Investigations in Micellar Media. In *Solution Chemistry of Surfactants*; K. L. Mittal, Ed.; Plenum: New York, 1979; Vol. **2**, pp 599-623.

[12] K. R. Chokshi, S. Qutubuddin and A. Hussam, *J. Colloid Interface Sci.*, **129** (1989) 315.

[13] R. A. Mackay, S. A. Myers, L. Bodalbhai and A. Brajter-Toth, *Anal. Chem.*, **62** (1990) 1084.

[14] A. B. Mandal and B. U. Nair, *J. Chem. Soc. Faraday Trans.*, **87** (1991) 133.

[15] A. E. Kaifer and A. J. Bard, *J. Phys. Chem.*, **89** (1985) 4876.

[16] A. B. Mandal and B. U Nair, *J. Phys. Chem.*, **95** (1991) 9008.

[17] R. M. Wightman, *Science*, **240** (1988) 415.

[18] R. J. Forster, *Chem. Soc. Rev.*, **23** (1994) 289.

[19] J. D. Norton, W. E. Benson, H. S. White, B. D. Pendley and H. D. Abruna, *Anal. Chem.*, **63** (1991) 1909.

[20] R. C. Engstrom, M. Weber, D. J. Wunder, R. Burgess and S. Winquist, *Anal. Chem.*, **58** (1986) 844.

[21] A. Owlia, Z. Wang and J. F. Rusling, *J. Am. Chem. Soc.*, **111** (1989) 5091.

[22] R. M. Wightman, D. O. Wipf, In *Electroanalytical Chemistry*; A. J. Bard, Ed.; Dekker: New York, 1988; Vol. **16**, pp 267-353.

[23] J. R. Kirchhoff, J. D. Skelton, Jr., and K. T. Brooks, Electrochemical and Spectroelectrochemical Measurements in Sodium Dodecyl Sulfate Micellar Solutions as a Function of Electrolyte Concentration. In *Electrochemistry in Colloids and Dispersions*; R. A. Mackay and J. Texter, Eds.; VCH: New York, 1992; Chapter 4, pp 119-235.

[24] A. J. Bard and L. R. Faulkner, In *Electrochemical Methods: Fundamental and Apllications*; A. J. Bard, Ed.; Wiley: New York, 1980.

[25] J. F. Rusling and C. Shi, *Anal. Chem.*, **60** (1988) 1260.

[26] A. B. Mandal, B. U. Nair and D. Ramaswamy, *Langmuir*, **4** (1984) 736.

[27] C. Tanford, In *The Hydrophobic Effect: Formation of Micelles and Biological Membranes*; Wiley: New York, 1980.

[28] P. Mukerjee, K. J. Mysels and C. I. Dulin, *J. Phys. Chem.*, **62** (1985) 1390.

[29] S. A. Myers, R. A. Mackay and A. Brajter-Toth, *Anal. Chem.*, **65** (1993) 3447.

[30] M. T. Carver, E. Hirsch, J. C. Whittmann, R. M. Fitch and F. Candau, *J. Phys. Chem.*, **93** (1989) 4867.

[31] D. F. Evans, S. Mukherjee, D. J. Mitchell and B. W. Ninham, *J. Colloid Interface Sci.*, **93** (1983) 184.

[32] N. Mikati, *Chem. Phys. Lett.*, **123** (1986) 51.

[33] J. J. Alexander and H. B. Gray, *J. Am. Chem. Soc.*, **90** (1968) 4260.

[34] J. N. Phillips, *Trans Faraday Soc.*, **51** (1955) 561.

[35] R. J. Williams, J. N. Phillips and K. J. Mysels, *Trans Faraday Soc.*, **51** (1955) 728.

[36] E. W. Anacker, R. M. Rush and J. S. Johnson, *J. Phys. Chem.*, **68** (1964) 81.

[37] H. Schott, *J. Phys. Chem.*, **70** (1966) 2966.

[38] J. Texter, F. R. Horch, S. Qutubuddin and E. Dayalan, *J. Colloid and Interface Sci.*, **135** (1990) 263.

[39] J. H. Fendler, In *Membrane Mimetic Chemistry*; Wiley: New York, 1982.

[40] K. Shinoda and B. Lindman, *Langmuir*, **3** (1987) 134.

[41] R. S. Sarpal, M. Belletete and G. Durocher, *Chem. Phys. Lett.*, **180** (1994) 283.

[42] T. C. Franklin and S. Mathew, In *Surfactant in Solution*; K. L. Mittal, Ed.; Plenum: New York, 1989; Vol. **10**.

[43] J. F. Rusling, Electrochemistry in Micelles, Microemulsions, and Related Microheterogeneous Fluids. In *Electroanalytical Chemistry*; A. J. Bard, Ed.; Dekker: New York, 1994; Vol. **18**, pp 1-88.

[44] G. L. McIntire, *Crit. Rev. Anal. Chem.*, **21** (1990) 257.

[45] J. Texter, In Colloidal Electrochemistry - Genesis and Scope. In *Electrochemistry in Colloids and Dispersions*; R. A. Mackay and J. Texter, Eds.; VCH: New York, 1992; Chapter 1, pp 3-21.

[46] R. A. Mackay, S. A. Mayers, L. Bodalbhai and A. Brajter-Yoth, *Anal. Chem.*, **62** (1990) 1084.

[47] G. N. Kamau, T. M. Saccucci, G. Gounili, A. F. Nassar and J. F. Rusling, *Anal. Chem.*, **66** (1994) 995.

[48] B. K. Jha, A. S. Chhatre, B. D. Kulkarni, R. A. Joshi, R. R. Joshi and U. R. Kalkote, *J. Colloid Interface Sci.*, **163** (1994) 1.

[49] A. J. Bard and K. S. V. Santhanam, *Electroanal. Chem.*, **4** (1970) 215.

[50] J. M. Saveant, *Chem. Rev.*, **90** (1990) 723.

[51] W. Smith and A. J. Bard, *J. Am. Chem. Soc.*, **97** (1977) 5203.

[52] C. P. Andrieux, P. Hapiot and J. M. Saveant, *J. Phys. Chem.*, **92** (1986) 5987.

[53] A. J. Bard and K. S. V. Santhanan, In *Electroanalytical Chemistry*; A. J. Bard, Ed.; Dekker: New York, 1984; Vol. **4**.

[54] A. J. Bard and L. R. Faulkner, Electrode Reactions with Coupled Homogeneous chemical Reactions. In *Electrochemical method: Fundamental and Applications*; Wiley: New York, 1980; Chapter 11, pp 429-487.

[55] G. Cerichelli, G. Illuminati, G. Ortaggi and A. M. Giuliani, *J. Organometal. Chem.*, **127** (1977) 357.

[56] H. A. Kozlowska and B. E. Conway, *J. Electroanal. Chem.*, **95** (1979) 1.

CHAPTER 5

RHEOLOGICAL STUDY OF MICELLAR AND LIQUID CRYSTALLINE PHASES

5.1 INTRODUCTION

The rheology of organized surfactant assemblies such as micelles and microemulsions under shear flow has been a subject of considerable interest in recent years [1-6]. The interest in micelles and/or microemulsion, a fascinating complex fluid mixture, is due to its solution environment and the range of supermolecular-architectures which can occur as the composition or extent of hydrocarbon, aqueous media and surfactant varies [7, 8]. It is generally well known that micellar structures may be spherical, globular or rodlike or have the structure of spherical bilayers depending upon the various parameters like temperature, salinity and cosurfactant concentration [9-11]. The shape of these assemblies is also sensitive to shear. Thus for instance flow brings about structural changes which in turn may modify the extent and nature of reaction occurring in the complex fluid [12]. The flow characteristics of such systems are of-course dependent on properties such as volume fraction of disperse phase, viscosity of the disperse droplets, droplet size distribution, and viscosity and chemical composition of the medium. Typically, these solutions show viscoelastic behavior at high concentration of surfactant but complex and unusual rheological phenomena such as rheopexy and shear thickening at low concentration [13, 14].

The flow behavior of micelles and microemulsions is a direct manifestation of the various forces that occur in these systems. On studying the sodium dodecyl sulfate (SDS)/alkanol/water phase diagrams the presence of different regions is noticed [15, 16]. These regions are characterized as L_1, the region corresponding to alkanol solubilization in water (direct solubilization), L_2, the region corresponding to water solubilization (inverse solubilization) and D, the region corresponding to lamellar liquid crytalline phase. The phase diagram shows possibilities of occurence of different types of organized assemblies of SDS aggregates. In view of the different microstructure of their assemblies they are expected to exhibit interesting rheological properties.

A number of studies showing the effect of various parameters such as water/SDS ratio on the properties of SDS micelles and microemulsion systems have been reported. Thus light

scattering studies by Sjoblom and Friberg [17] and Forche and Bellocq [18] show that the scattering light intensity begins to increase rapidly when the microemulsion water content exceeds a certain value corresponding to a water/SDS molar ratio. It has been shown by Brunetti et al. [19] that the n-alkanol number of carbon atoms has a strong influence on the interactions between microemulsion inverse microdroplets. The inverse microdroplets in heptan-1-ol are associated with weak attractive interactions and behave like hard spheres. In contrast, with pentan-1-ol the interactions are strongly attractive and consequently the microdroplets tend to form extended clustures [20]. Although the structural features of these assemblies have been firmly established, a detailed understanding of their dynamical behavior and, in particular rheological behavior is not yet completely understood. Recently Rodens et al. [21] reported the flow behavior of SDS and CTAB reverse micelles in hexanol. It was observed that for both surfactants, the systems behave as non-Newtonian fluids and shear viscosity decreases with the shear rate until a constant value is reached.

The present chapter reports the result related to the rheological behavior of L_2 and L_2/D phases of the ternary systems SDS/pentan-1-ol/water and SDS/heptan-1-ol/water using steady state (shear stress as a function of shear rate) and constant shear rate techniques (stress as a function of time at constant shear rate) and its dependence on composition and temperature.

5.2 EXPERIMENTAL

5.2.1 Materials

Sodium dodecyl sulfate (SDS) was purchased from Loba chemie. Pentan-1-ol and heptan-1-ol were of analytical grade from Sigma chemicals. All the materials were of high purity and used as received. Water used was deionised and distilled. The samples were prepared by through mixing of the components in a sealed containers.

5.2.2 Methods

5.2.2.1 Rheological measurements

The rheological measurements were performed using Ferranti-Shirley rheometer with cone and plate configuration (4 cm, 1°). The geometry was thermostated at 25 °C and sealed to prevent evaporation of the samples. The apparatus was caliberated using Newtonian caliberation oil (silicone oil) of known viscosity. The samples were introduced into the geometry and allowed to thermostate while shearing.

5.2.2.2 Quasielastic light scattering (QELS) measurements

Quasielastic light scattering (QELS) measurements were performed using a Malvern 4700 commercial light scattering system. The relevant components of this system were the temperature-controlled index matched scattering cell, the control computer including a 64-channel correlator and the photomultiplier tube which is mounted on the goniometer. All light scattering experiments were performed at a constant temperature of 25 ± °C. All data were collected during the run by the computer and were also printed out. The mean intensity and hydrodynamic radius of disperse particles were determined at 90° [22].

5.3 RESULTS AND DISCUSSION

5.3.1 Phase diagram

The phase diagrams of SDS/pentan-1-ol/water and SDS/heptan-1-ol/water systems shown in Figures 5.1 (a-b) clearly show three distinct regions and exhibit a large L_2 region covering a wide region of alkanol content. Rheological measurements of samples from both L_2 and L_2/D regions have been carried. The specific compositions are given in Table 5.1.

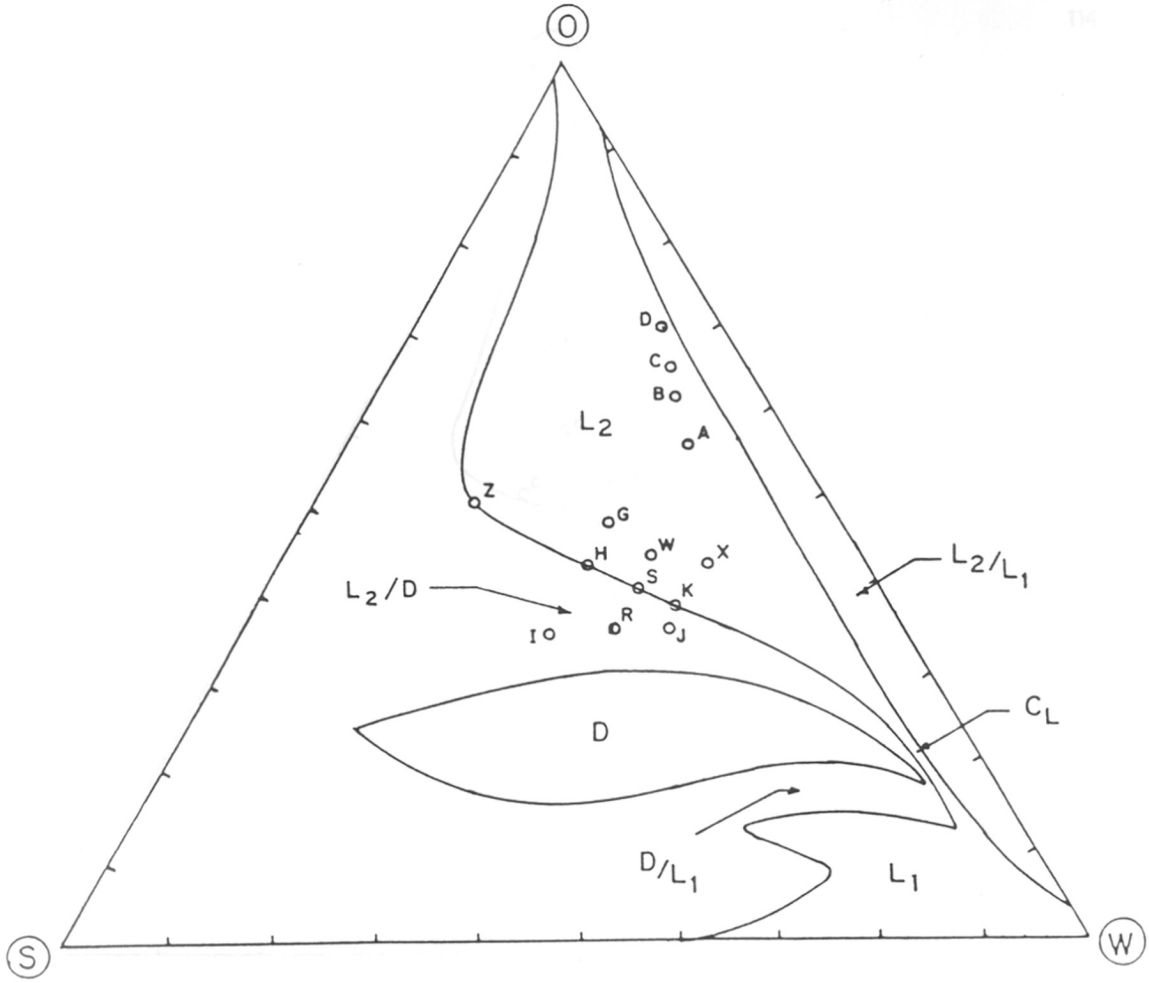

(a)

Figure 5.1 : Phase diagram of water (W)/sodium dodecyl sulfate (SDS) (S)/alkanol (O) system at 25 °C. (a) 1-pentanol; (b) 1-heptanol (Adapted from Refs. 15, 16).

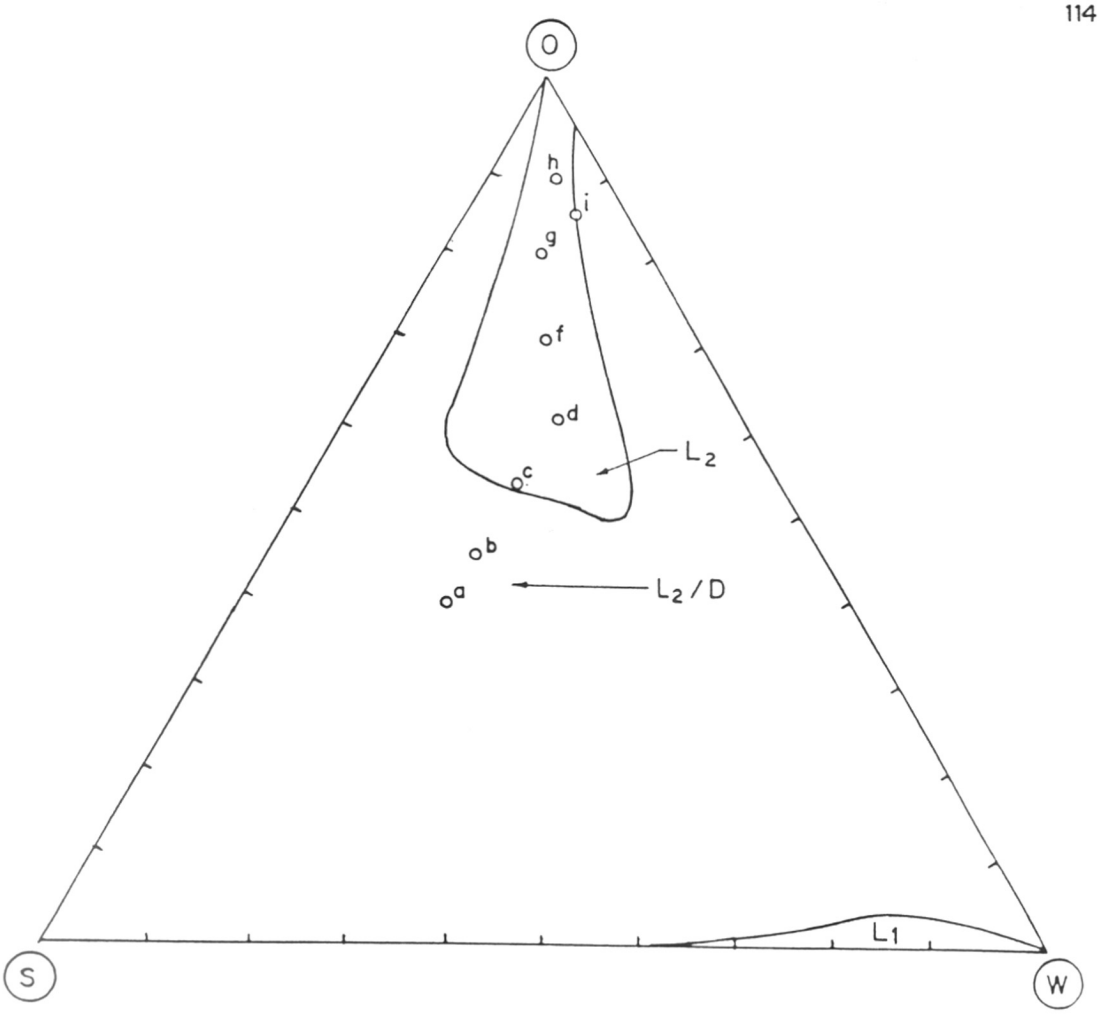

(b)

Figure 5.1 : (continued).

Table 5.1 : Composition (by Weight) of the Samples used in the Rheological Measurements*

Sample	% surf[ii] wt/wt	% alkanol[iii] wt/wt	% water[v] wt/wt	[alkanol]/[SDS]	[water]/[SDS]
A	10.0	56.4	33.6 (L_2)	18.45	53.77
B	8.4	61.6	30.0 (L_2)	23.99	57.15
C	7.2	64.0	28.8 (L_2)	29.08	64.01
D	6.0	70.0	24.0 (L_2)	38.17	64.01
G	22.0	46.8	31.2 (L_2)	6.96	22.70
H	26.4	42.4	31.2 (L_2)	5.25	18.91
I	34.0	34.8	31.2 (L_2/D)	3.35	14.69
J	22.2	34.8	43.0 (L_2/D)	5.13	31.00
K	20.6	36.4	43.0 (L_2)	5.78	33.41
R	28.2	34.8	37.0 (L_2/D)	4.04	21.00
S	23.0	40.0	37.0 (L_2)	5.69	25.74
W	20.0	43.2	36.8 (L_2)	7.07	29.45
X	15.0	42.0	43.0 (L_2)	9.16	45.88
Z	34.4	50.0	15.6 (L_2)	4.76	7.26
a	42.5	37.5[iv]	20.0 (L_2/D)	2.19	7.53
b	35.0	45.0[iv]	20.0 (L_2/D)	3.19	9.14
c	26.25	53.75[iv]	20.0 (L_2)	5.08	12.19
d	17.5	62.50[iv]	20.0 (L_2)	8.86	18.29
f	15.0	70.0[iv]	15.0 (L_2)	11.58	16.0
g	10.0	80.0[iv]	10.0 (L_2)	19.85	16.0
h	5.0	90.0[iv]	5.0 (L_2)	44.67	16.0
i	6.0	85.0[iv]	9.0 (L_2)	35.16	24.0

*All sample compositions are referred in weight percent. [ii]surf, sodium dodecyl sulfate (SDS). [iii]alkanol, pentan-1-ol; [iv]heptan-1-ol. [v]water, deionised distilled.

5.3.2 Effect of shear rate

Figures 5.2(a-e) show the dependence of shear viscosity on shear rate for samples taken from different phase regions. The strange upward curvature noted in Figures 5.2(a)/5.2(b) is a characteristic of non-Newtonian flow of dilatant type or the structural viscosity. The observed dilatant behavior arises due to shear induced coagulation. It is possible that deforming a material can cause rearrangement of its molecular structure such that the resistance to flow increases with shear rate [6]. It is also anticipated that micelles or microscopic droplets in different flow stream lines may colloid with each other in the flow directions and combine to grow in size through fusion mechanism [23-25]. As a result, larger micelles or larger micellar networks can form leading to increase in shear viscosity. It thus implies that substantial flow induced orientation takes place in these solutions and the orientation levels are consistently proportional to the shear rates.

Figure 5.2(c) shows the Newtonian type fluid behavior for those samples which are on the periphery of the L_2 phase. A gradual transition from an almost Newtonian behavior to a psuedo-plastic or shear thinning flow is observed for samples (I and R) as shown in Figure 5.2(d). It is conceivable that in the L_2/D region a lamellar liquid crystal phase is in equilibrium with a micellar solution. The lamellar liquid crystals have a highly developed structure in the quiescent state. When a liquid crystalline sample is sheared, its rheological response depends on the rearrangement of the structure during the flow [26]. The drop in viscosity of the samples within the L_2/D region with increasing shear rate may be attributed to the deformation and alignment of the liquid crystalline phase of SDS molecules which reduces their resistance to flow and gives rise to a reduction in the shear viscosity [27]. At higher shear rates, the structure is even more grossly oriented and separate layers of the continuous phase and micellar phase can be observed. The effect of shear rates can be rationalised by invoking the balance that results by considering the Brownian and shear motions [28-30]. Figure 5.2(e) shows the shear viscosity as a function of shear rate for solutions with different compositions in heptan-1-ol. The shear induced behavior for L_2 and L_2/D phases is similar to that observed in the earlier case using pentan-1-ol.

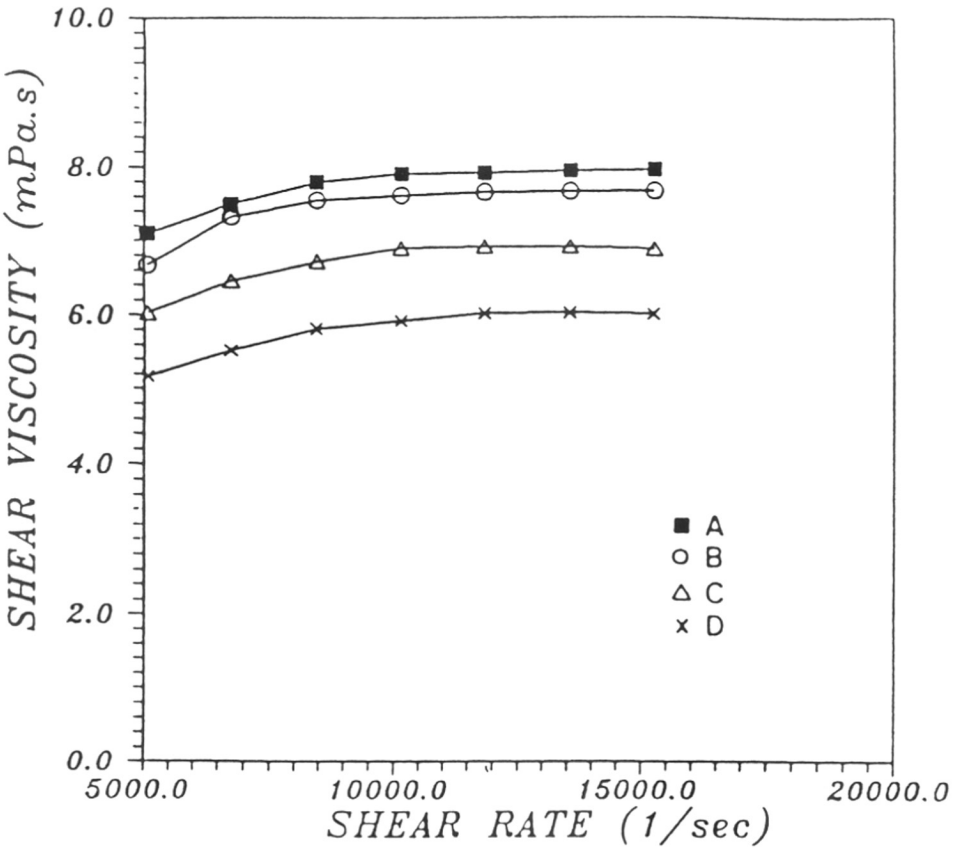

(a)

Figure 5.2 : Variation of shear viscosity as a function of shear rate at 25 °C.

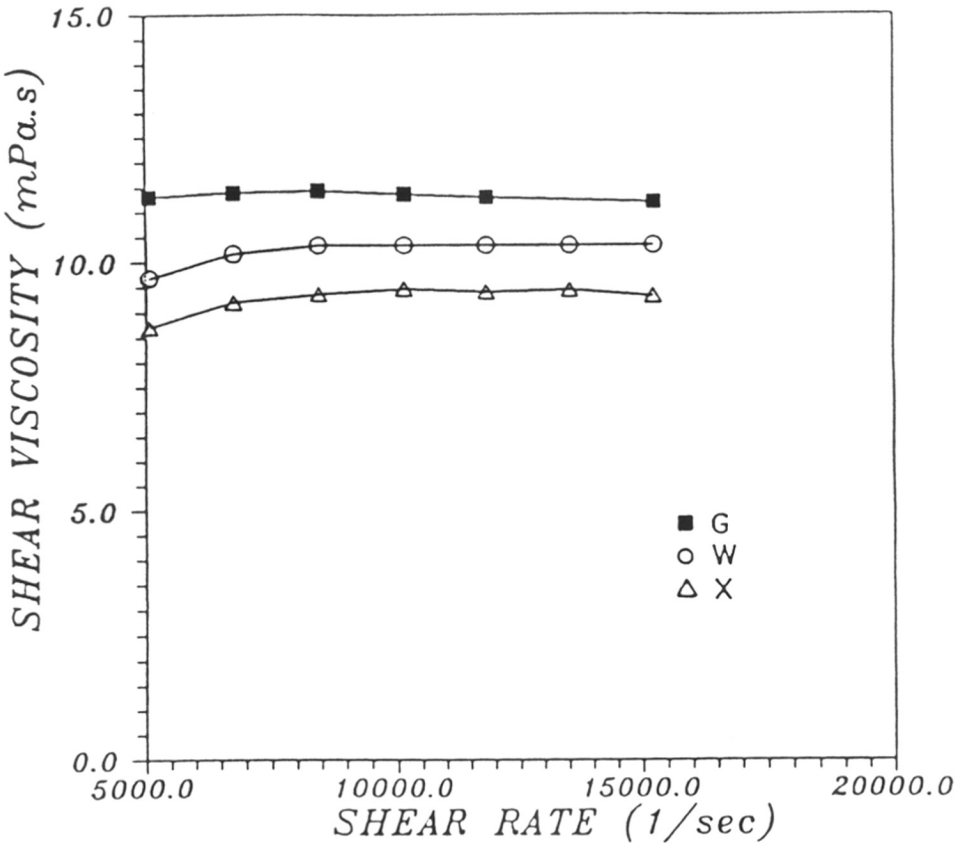

(b)

Figure 5.2 : (continued).

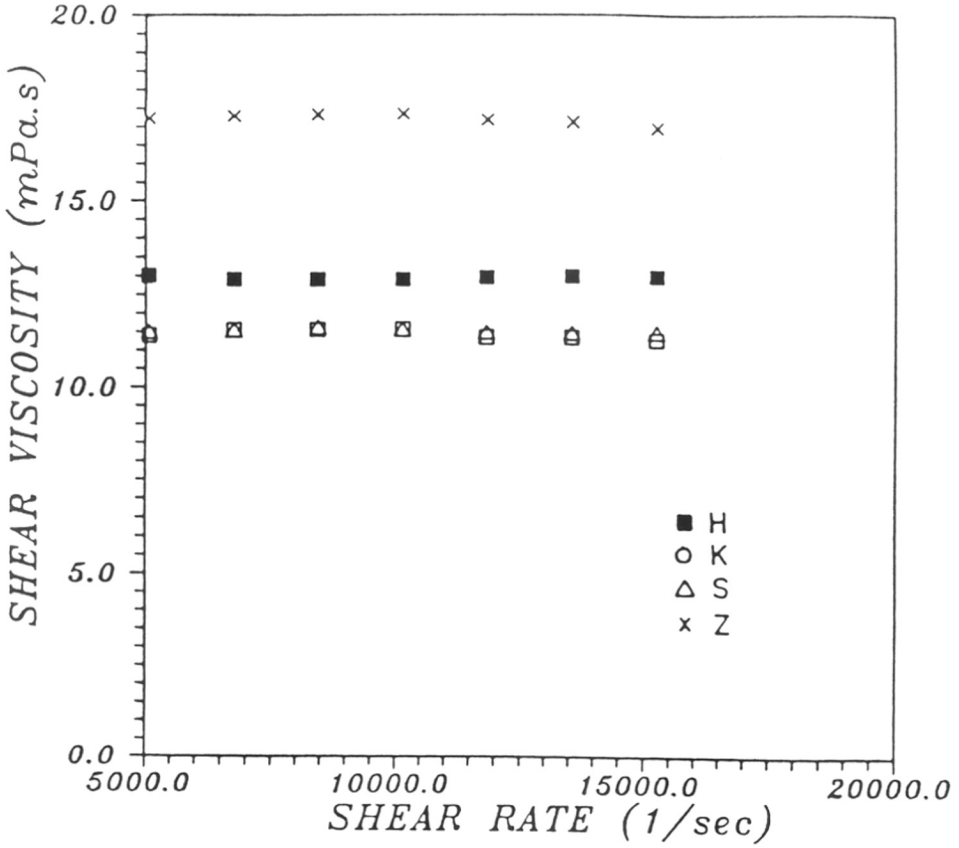

(c)

Figure 5.2 : (continued).

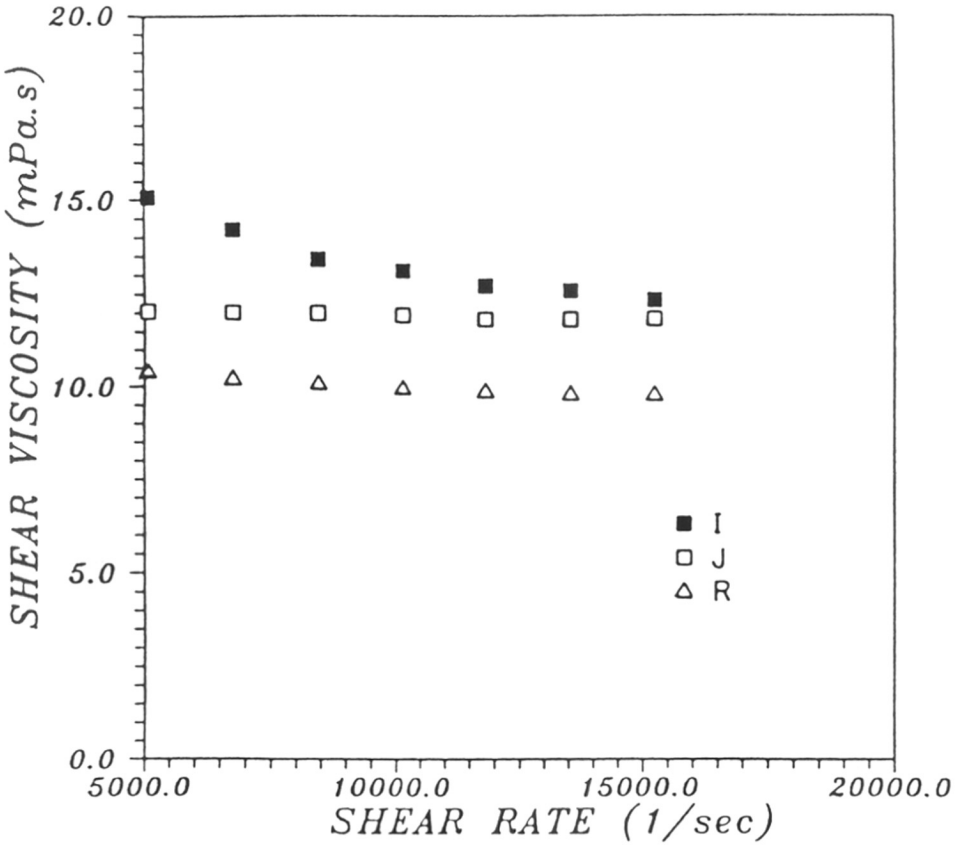

(d)

Figure 5.2 : (continued).

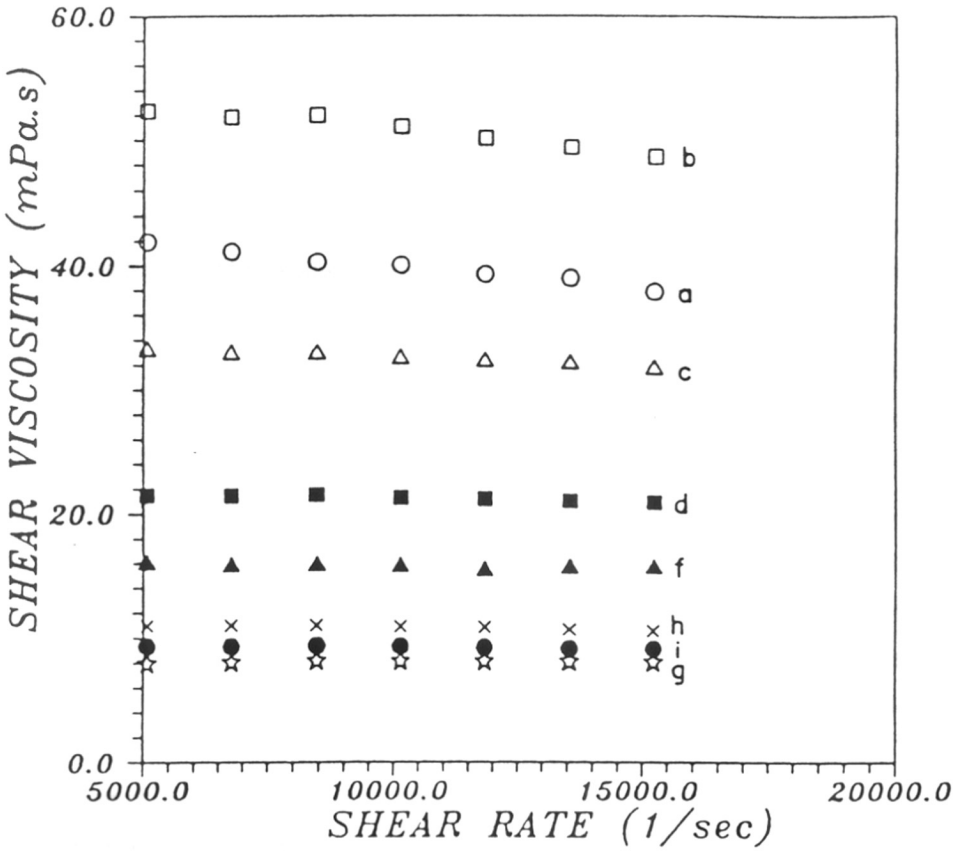

(e)

Figure 5.2 : (continued).

5.3.3 Transient studies

The transient behavior of the shear induced phase transitions can be investigated by measuring the time dependent rheological properties. In this experiment a high shear rate ($\dot{\gamma} \approx 11843.09 s^{-1}$) is applied to the solutions and shear stress is measured as a function of time. Typical results of this measurement are represented in Figures 5.3(a-e). Figure 5.3(a) shows the variation of viscosity with time of shearing at 25 ^{o}C. It is anticipated that the decrease of viscosity with time may be due to the breakdown of micellar structure which eventually reaches equilibrium. However rheological properties change drastically for some samples. The shear viscosity rises steeply to reach a plateau value as shown in Figures 5.3(b-e). This behavior is consistent with interpreting the phenomenon as due to the formation of shear induced micellar association and gain in energy [31, 32]. For the experimental determination of the resting time (t_R) behavior the sample I is first sheared at a high shear rate ($\dot{\gamma} \approx 11843.09 s^{-1}$) for sufficient time to build-up the state of structure. Then the sample is held in the state of rest for a resting time of 2 hrs. The shear stress is measured again at above shear rate. The shear viscosity remains unchanged and thus exhibits an irreversible shear induced structural build-up. Further in order to obtain the information pertaining to the dimension of disperse particles in the sample I, QELS study was performed before and after shearing. Solution was sheared nearly for one hour at constant shear rate. Figure 5.4 shows the results of QELS measurements. Measurements reveal that the shear induced structure (SIS) consists of globular aggregates or clusters of disperse particles (the mean z-average ≈ 1230 nm) whereas z-average hydrodynamic radius for the disperse particles before shearing was 210 nm. This suggests that the order of the system is increased when it is exposed to shear.

5.3.4 Effect of temperature

Rheological properties of solutions are expected to depend on the temperature and evaluating this dependence is important for practical applications [24, 33]. Blankshtein et al. [34] report the growth of micelles in aqueous solution as a function of surfactant concentration and

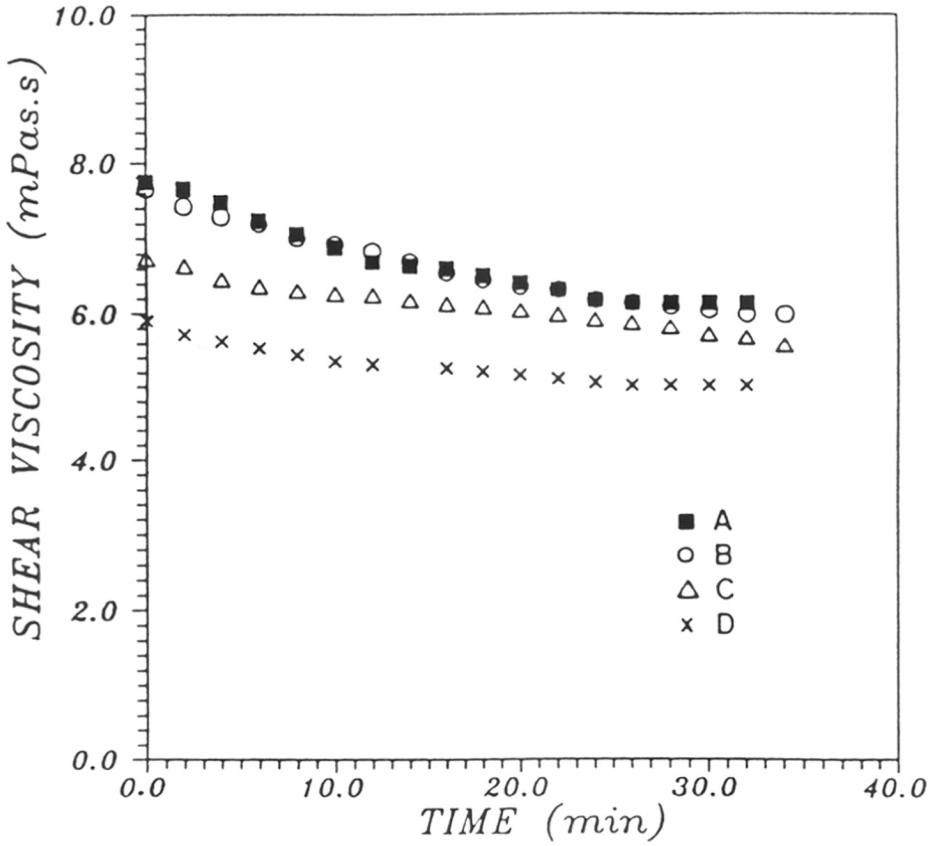

(a)

Figure 5.3 : Time dependence of the shear viscosity for a constant shear rate ($\gamma \approx 118\text{-}43.09 s^{-1}$) at 25 °C.

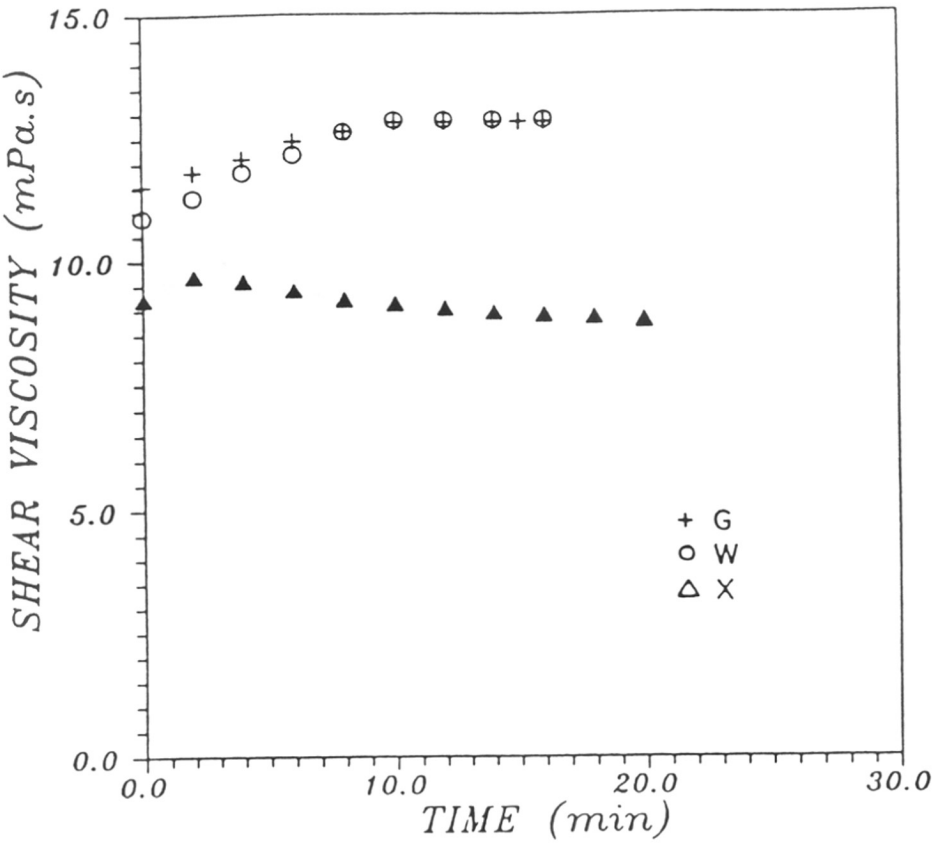

(b)

Figure 5.3 : (continued).

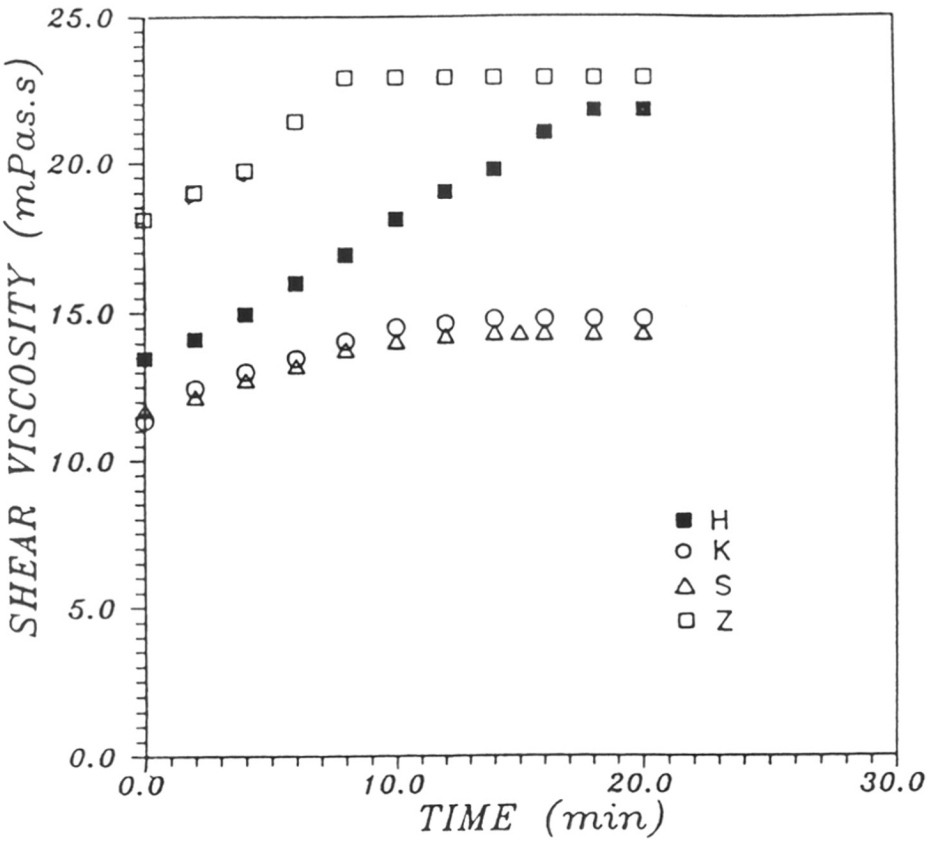

(c)

Figure 5.3 : (continued).

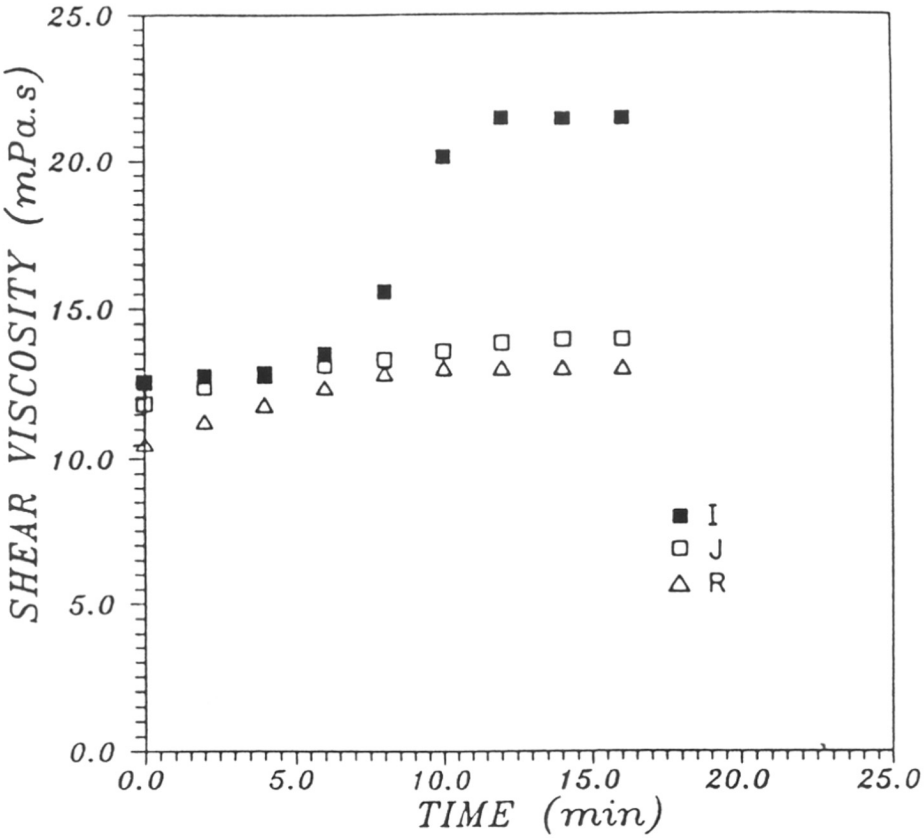

(d)

Figure 5.3 : (continued).

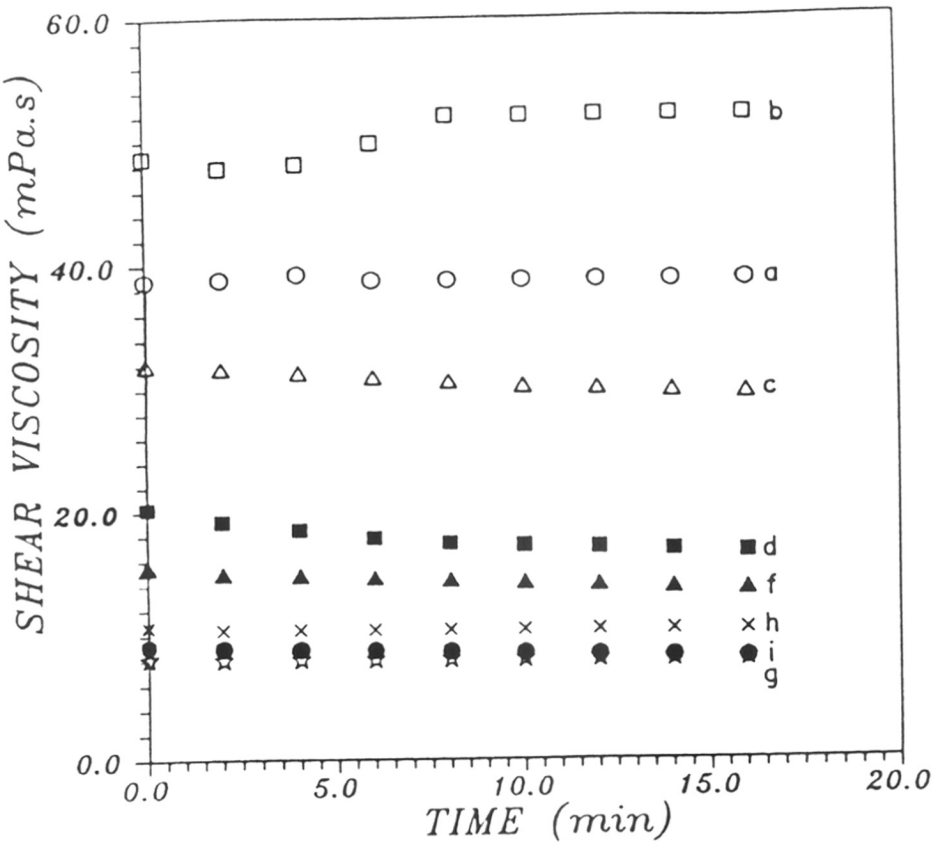

(e)

Figure 5.3 : (continued).

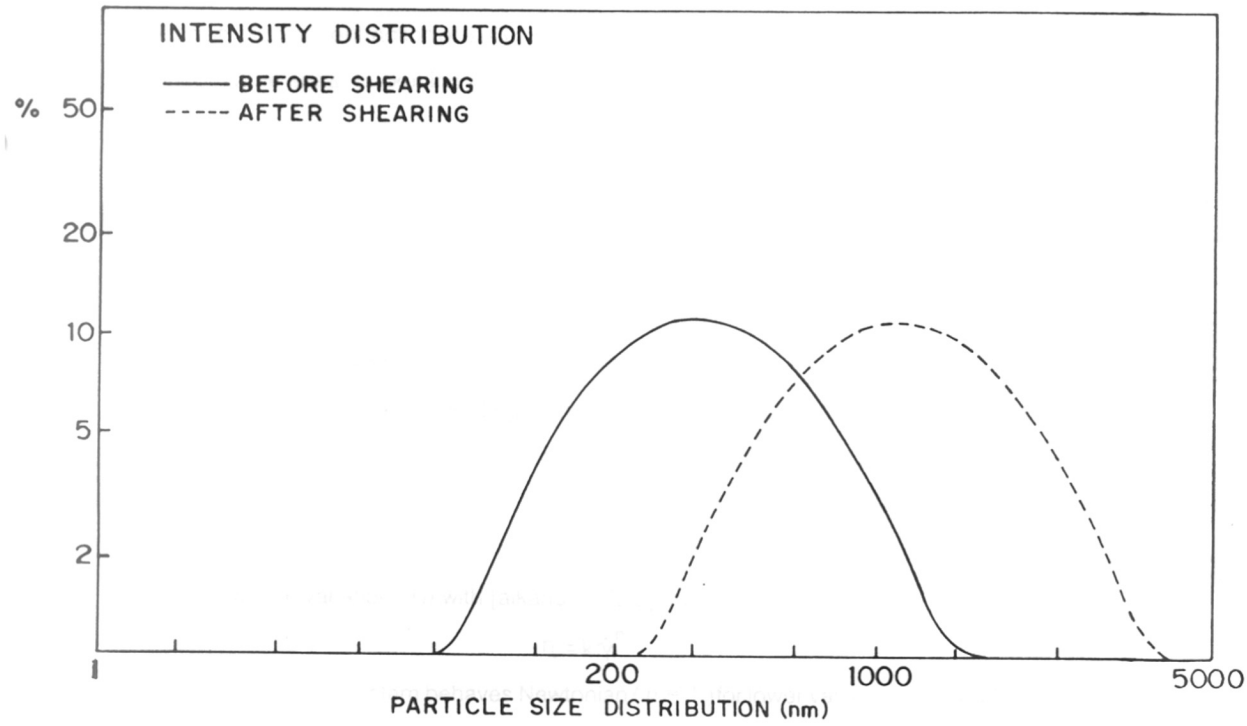

Figure 5.4 : The percentage intensity distribution plotted against particle size.

temperature. The flow behavior of sample I was measured as a function of shear rate for three different temperatures. The respective flow curves are shown in Figure 5.5. As can be observed, a decrease in shear viscosity is indicated, regardless of the temperature. Transient flow curves as a function of temperature at a SDS concentration 34.0 % (sample I) and shear rate of $1\,1843.09 s^{-1}$ are illustrated in Figure 5.6. The system is nearly Newtonian at 20 ^{o}C, but sudden change in shear viscosity appears at 25 ^{o}C and 30 ^{o}C. With increasing temperature there is decrease in the solvent viscosity, so that contraction of SDS molecules occurs following the initial stress over-shoot, further retarding the shear thickening process. This effect is due to the transformation of microscopic structures of droplets which transform into macroscopic size and further into networks suggesting a shift toward more intermolecular associations in SDS molecules at high temperature. The system thus exhibits a complicated dependence of shear viscosity on temperature and shows that temperature can significantly affect the formation of shear induced structures.

5.3.5 Effect of [alkanol]/[SDS] molar ratio

Analysis of the data according to the power-law model [35, 36] (Eq (5.1)) shows a good fit. In this equation η represents shear viscosity, $\dot{\gamma}$ the shear rate, and k and n are fluid-consistency and flow-behavior indices. Exponent n calculated from the double logarithmic plot of shear viscosity against shear rate for a few representative points is plotted against [alkanol]/[SDS] in Figure 5.7 and shows the variation in n with [alkanol]/[SDS] molar ratio.

$$\eta = k\dot{\gamma}^{n-1} \qquad (5.1)$$

Interestingly, system behaves Newtonian ($n \approx 1$) for lower values of [alkanol]/[SDS] molar ratio. However n increases with increasing concentration of alkanol. The addition of pentan-1-ol or heptan-1-ol changes the solution characteristics of SDS/water solution and induces the non-Newtonian type behavior. The changes observed are more stronger in pentan-1-ol than in heptan-1-ol since the dynamics of micellar system is strongly influenced and also the formation of small aggregates is favoured by short chain alcohols [20]. Figure 5.7 also depicts that the

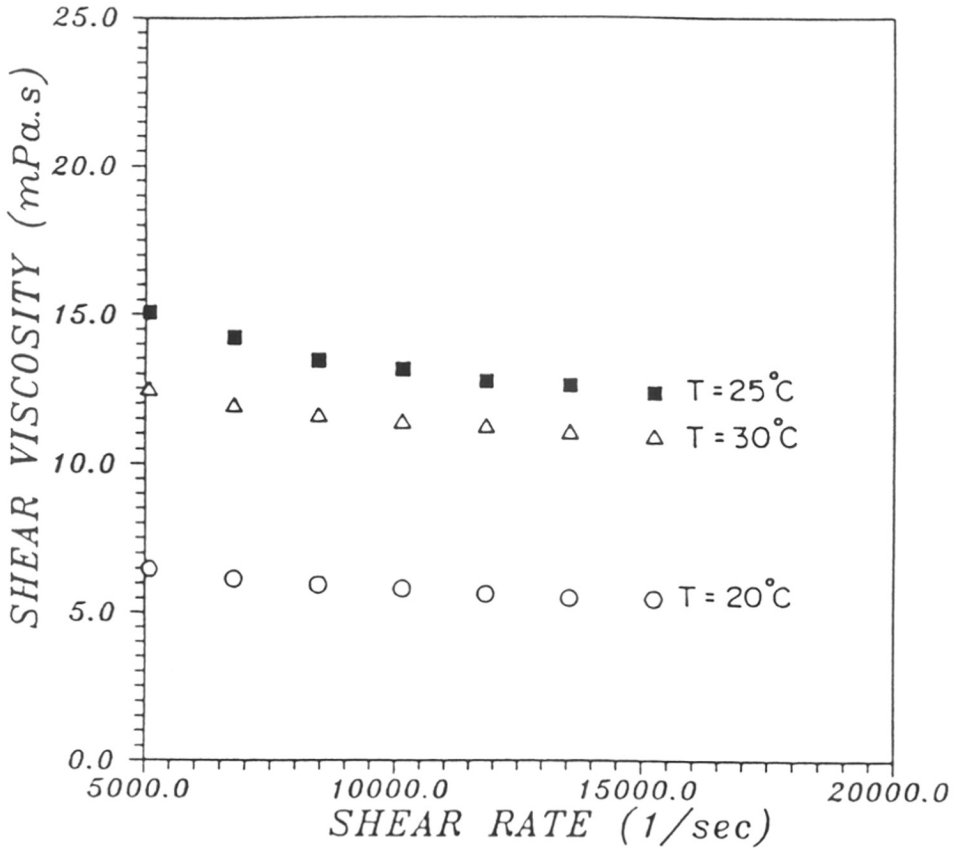

Figure 5.5 : Influence of the temperature on the variation of shear viscosity versus shear rate.

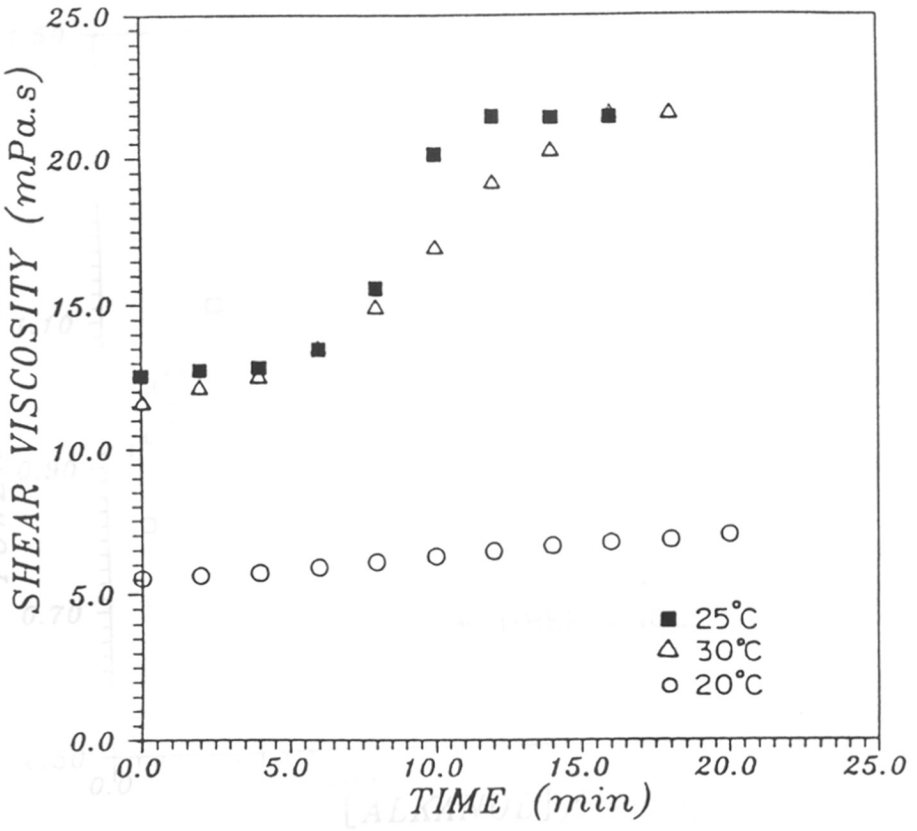

Figure 5.6 : Influence of the temperature on the time dependence of the shear viscosity at $\dot{\gamma} \approx 11843.09 s^{-1}$.

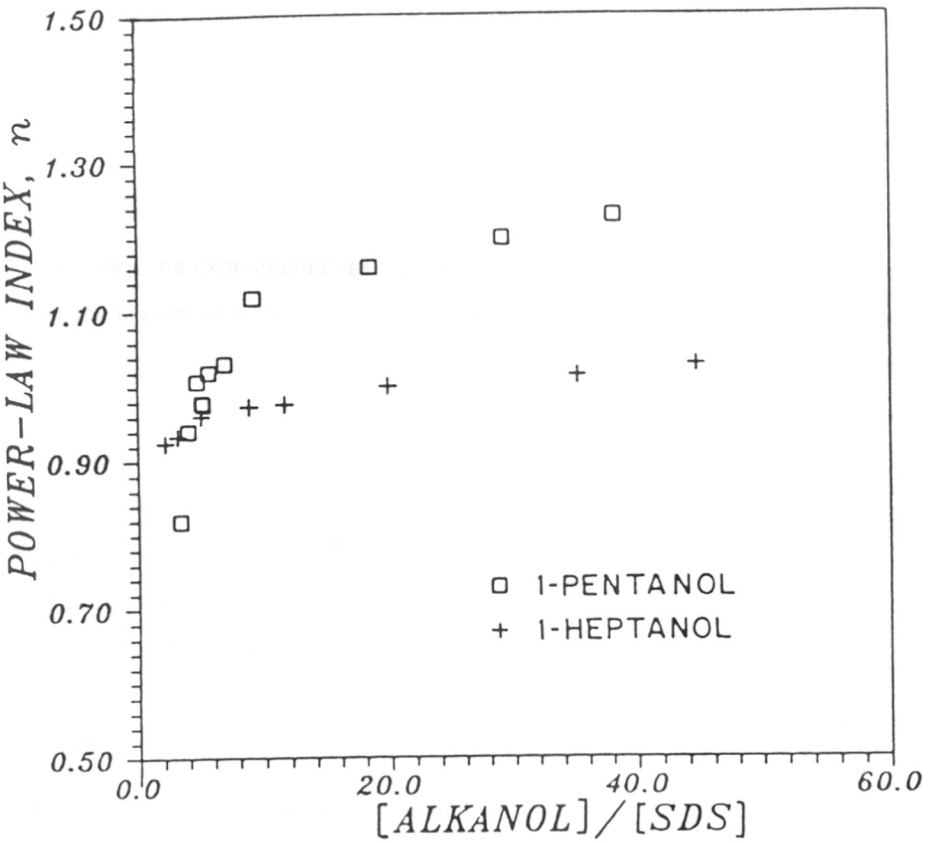

Figure 5.7 : The power-law index n at high shear rate ($\gamma \approx 11843.09 s^{-1}$) as a function of [alkanol]/[SDS] at 25 °C.

threshold concentration for both alcohol is nearly the same and shear thickening is more pronounced once this threshold is crossed. The present observation corroborates the observations of Nguyen and Bertrand [37] that the added alcohol causes a microscopic structural change in micelles.

5.4 CONCLUSIONS

In summary, the experimental results show that the shear viscosity is different depending on whether the system belongs to L_2 or L_2/D region. The flow behavior of samples varies significantly even within the L_2 or L_2/D region and thus formation of the shear induced structures depend on the compositions. The time evolution of micellar structure after applying a shear flow at constant shear rate has provided an evidence for a kinetic coagulation mechanism and also show an irreversible structural build-up. The magnitude of shear thickening increases with increasing [alkanol]/[SDS] molar ratio and is more effective for pentan-1-ol as compared to heptan-1-ol. The temperature dependence of the flow properties are also observed and is relevant for the formation of shear induced structures in surfactant assemblies.

NOTATIONS

L_1	oil-in-water or "direct" solubilization
L_2	water-in-oil or "inverse" solubilization
D	lamellar liquid crystal
t_R	resting time
η	shear viscosity
$\dot{\gamma}$	shear rate
n	flow-behavir or power-law index
k	fluid-consistency index

REFERENCES

[1] H. Hoffmann, *Advanced Materials*, **6** (1994) 117.

[2] S. Radiman, C. Toprakcioglu and T. Mcleish, *Langmuir*, **10** (1994) 61.

[3] S. E. Friberg, S. M. Jones, A. Motyka and G. Broze, *J. Mater. Sci.*, **29** (1994) 1753.

[4] Th. F. Tadros, *Colloids Surfaces* A, **91** (1994) 39.

[5] J. C. Brakman and J. B. F. N. Engberts, *J. Am. Chem. Soc.*, **112** (1990) 872.

[6] Y. Hu, C. V. Rajaram, S. Q. Wang and A. M. Jamieson, *Langmuir*, **10** (1994) 80.

[7] K. Shinoda and B. Lindman, *Langmuir*, **3** (1987) 134.

[8] J. Tabony, *Nature*, **319** (1986) 390.

[9] H. Hoffmann and G. Ebert, *Angew. Chem. Int. Ed. Engl.*, **27** (1988) 902.

[10] B. K. Jha, S. S. Tambe and B. D. Kulkarni, *J. Colloid Interface Sci.*, **170** (1995) 392.

[11] A. Khatory, F. Lequeux, F. Kern and S. J. Candau, *Langmuir*, **9** (1993) 1456.

[12] U. S. Agrawal and D. V. Khakhar, *Nature*, **360** (1992) 53.

[13] S. J. Candau, E. Hirsch and R. Zana, *J. Phys.* (Paris), **45** (1984) 1263.

[14] H. Rehage, I. Wunderlich and H. Hoffmann, *Progr. Colloid Polym. Sci.*, **72** (1986) 51.

[15] C. Y. Young, P. J. Missel, N. A. Mazer, G. B. Benedek and M. C. Carey, *J. Phys. Chem.*, **82** (1978) 1375.

[16] M. Clausse, L. Nicolas-Morgantini, A. Zradba and D. Touraud, Water/Ionic Surfactant/Alkanol/Hydrocarbon Systems: Influence of Certain Constitution and Composition Parameters on the Realms-of-Existence and Transport Properties of Microemulsion Type Media. In *Microemulsion system: Surfactant Science Series*; H. L. Rosano and M. Clausse, Eds.; Dekker: New York, 1987; Vol. **24**, Chapter 2, pp 15-62.

[17] E. Sjoblom and S. Friberg, *J. Colloid Interface Sci.*, **67** (1978) 16.

[18] A. Bellocq and G. Fourche, *J. Colloid Interface Sci.*, **78** (1980) 275.

[19] S. Brunetti, D. Roux, A. M. Bellocq, G. Fourche and P. Bothorel, *J. Phys. Chem.*, **87** (1983) 1028.

[20] P. G. de-Gennes and C. Taupin, *J. Phys. Chem.*, **86** (1982) 2294.

[21] M. Valiente and E. Rodenas, *Colloids Surfaces* A, **85** (1994) 97.

[22] C. Candaue and R. Zana, *J. Colloid Interface Sci.*, **84** (1981) 206.

[23] Y. Hu, S. Q. Wang and A. M. Jamieson, *J. Colloid Interface Sci.*, **156** (1993) 31.

[24] S. Hoffman, A. Rauscher and H. Hoffmann, *Ber. Bunsenges. Phys. Chem.*, **95** (1991) 153.

[25] Y. Hu, C. V. Rajaram, S. Q. Wang and A. M. Jamieson, *J. Phys. Chem.*, **98** (1994) 8555.

[26] G. G. Viola and D. G. Bard, *J. Rheol.* **30** (1986) 601.

[27] S. L. Wunder, S. Ramchandran, S. R. Gochanour and M. Weinberg, *Macromolecules*, **19** (1986) 1696.

[28] T. A. Strivens, *Colloid Polym. Sci.*, **267** (1989) 269.

[29] R. B. Bird, C. F. Curtiss, R. C. Armstrong, O. Hassager, In *Dynamics of Polymeric Liquids*; Wiley: New York, 1980; Vols. **1-2**.

[30] H. A. Barnes, J. F. Hutton and K. Walters, Rheology of Suspension. In *An Introduction to Rheology*: *Rheology Series*; Elsevier: New York, 1989; Chapter 7, pp 115-137.

[31] H. Rehagea and H. Hoffmann, *Rheol. Acta*, **21** (1982) 561.

[32] Y. Hu, S. Q. Wang, A. M. Jamieson, *J. Rheol.*, **37** (1993), 531.

[33] D. Ohlendorf, W. Intrthal, and H. Hoffmann, *Rheol. Acta*, **25** (1986) 468.
[34] D. Blankshtein, G. Thurston and G. B. Benedek, *J. Chem. Phys.*, **85** (1986) 7268.
[35] W. Ostwald, *Kolloid-Z*, **36** (1925) 99.
[36] A. Dewaele, *Oil Color Chem. Assoc.*, **6** (1923) 33.
[37] D. Nguyen, G. L. Bertrand, *J. Phys. Chem.*, **96** (1992) 1994.

CHAPTER 6

ESTIMATING MICELLAR DIFFUSION COEFFICIENTS USING AN ARTIFICIAL NEURAL NETWORK

6.1 INTRODUCTION

Microheterogeneous assemblies such as micelles and microemulsions have been used extensively as a media for carrying out chemical reactions [1-5], to enhance solubilization of insoluble materials [6], to transport molecules through cell membranes [7] and also for waste water treatment [8]. These applications take the advantage of the surfactant property of forming association complexes [9]. The self-assembled surfactant (micelles) are dynamic fluctuating entities constantly forming and dissociating on a time scale ranging between microseconds to milliseconds. Micelles are highly sensitive to electrolyte and surfactant concentrations, and also to temperature [10-11]. The physico-chemical characterization of such systems is mainly carried out by measuring the *self-diffusion coefficient* (hereafter termed as diffusion coefficient) which provides vital information about the micelle size, shape, and associated transport phenomenon.

Several measurements of the diffusion coefficient of micelles have been performed using quasi-elastic light scattering (QELS) [12-14], Taylor dispersion (TD) [15], boundary spreading [16], nuclear magnetic resonance (NMR) [17] and electrochemical techniques [18, 19]. The quasielastic light scattering spectroscopy allows one to measure the diffusion coefficient of macromolecules and micelles rapidly, and also provides a measure of the size of micelles even in relatively concentrated solution [20, 21]. Statistical and thermodynamic approaches have also been used for molecular description of micelles [22-25] and the theoretical predictions of micellar shape and polydispersity, based on the diffusion coefficient and intensity data are available [26, 27]. However, the nonlinear dependence of micellar diffusion coefficient on temperature, and concentrations of surfactant and electrolyte together with the complex nature of interactions between them, make it difficult to describe the diffusion phenomenon by computationally simple and unique phenomenological or empirical models. For example, Weinheimer et al. [15] have developed excellent

correlations for predicting diffusion coefficients of micelles, however these require measurements of several experimentally determined parameters. On the other hand, *Artificial Neural Networks* (ANN) which possess the ability to learn and generalize nonlinear functional relationship(s) can be very effectively employed to arrive at a correlation for estimating diffusion coefficients based on a set of limited and easily measurable experimental conditions.

Among a variety of micellar systems, the one consisting of sodium dodecyl sulfate (SDS) is the most extensively and systematically studied. The experimental properties of SDS micelles such as diffusion coefficient, micellar radii, and aggregation behavior have been well documented at various NaCl concentrations, and over a wide range of temperatures by several techniques [12-19]. It is observed that the diffusion coefficient of SDS micelles is dependent nonlinearly on NaCl and SDS concentrations and temperature. In this study we show how an ANN can be used to model the nonlinear dependence of diffusion coefficient on the mentioned experimental conditions.

6.2 ARTIFICIAL NEURAL NETWORKS

ANNs have been widely used in chemical, biochemical and respective engineering sciences [29-31]. In chemistry, they have been employed for; determining quantitative structure-activity relationship (QSAR) [32, 33], physico-chemical parameters of organic compounds [34, 35], chemical reactivity [36], process monitoring [37], PVT data analysis [38] and fluid property predictions [39]. ANNs were originally developed to simulate the brain's learning process by mathematically modeling its fundamental unit i.e., the nerve cell and the network structure arising out of their interconnections with other cells. In an ANN, the nerve cells are replaced by computational units called neurons and the synaptic strengths of the interconnections are represented by weights.

Among the variety of neural network architectures that have been proposed [see e.g., review by Lippman [40], and books by Wasserman [41] and Hecht-Nielsen [42] the *error-back-propagation* (EBP) model by Rumelhart et al. [43] appears to be the most commonly used network paradigm for approximating the nonlinear functional relationship(s) between input-output variables of complex systems.

The EBP neural network is a hierarchical architecture wherein neurons in the neighboring layers are fully interconnected. The strength of connection between two neurons is known as weight. The schematic diagram of the EBP as used in this study is shown in Figure 6.1. The back-propagation networks learn to approximate nonlinear relationship(s) between a set of input-output data by a procedure called *network training*. During training, an input pattern with corresponding desired (or target) output values is applied to network for computing its output. The network outputs are compared with the desired outputs and the error is propagated backwards for adapting the connection weights. This procedure is repeated till the error between the desired and network outputs for all the input patterns satisfies the prescribed error criterion. At this point the network is said to be trained and possesses a very useful property known as *generalization.* That is, when presented with inputs not belonging to the training set, the network still predicts the correct output. This mode of operation is termed as *prediction mode*. It is to be noted that the prediction ability of an ANN is due to the rigorous learning it has undergone during the training session.

The most basic type of EBP network consists of three layers of neurons; *input, hidden* and *output* layers. The input layer neurons do not perform any processing and serve just as distribution points. Every neuron in the hidden layer first computes the weighted sum of all its inputs and transforms this sum using a nonlinear activation function. The transformed sum represents hidden

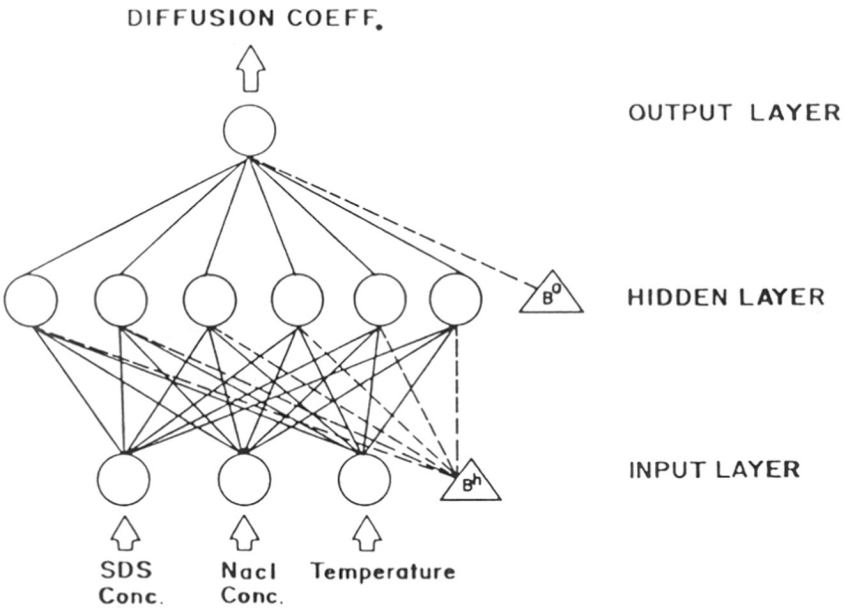

Figure 6.1 : Schematic of the neural network used in the study. B^h and B^O represent the bias neurons.

neuron's output and also forms an input to the output layer neuron(s). The outputs of the output layer neurons (also known as network outputs) are computed analogous to the hidden layer neurons.

The EBP training algorithm consists of two types of passes, namely, *forward* and *reverse* through the network. During the forward pass, the outputs of different network layers are established as described in the previous paragraph. In the reverse pass, the connection weights are adjusted to reduce the error between the network's actual and desired outputs using *generalized delta rule* [41]. The stepwise procedure for implementing forward and reverse passes for a three layer feedforward network is given in Appendix.

6.2.1 Network simulation

The diffusion coefficients (D) of micelles at various SDS, NaCl concentrations, and over a wide range of temperatures (T) were taken from literature (11, 13, 15, 44, 45). A total of 101 patterns were divided into sets of 76 and 25 each. In the simulation, these two sets (Tables 6.1a and 6.1b) form "training" and "test" sets respectively. The training set is used for the network training and the test set is used to evaluate the network's performance during the training cycle when a different set of inputs, not belonging to the training set is applied. If the network correctly estimates the outputs corresponding to the test set also, then the network has satisfactorily captured the relationship between input-output data. Since we have used the Sigmoidal form of the activation function, the three network inputs listed in Tables 6.1a and 6.1b were normalized so as to lie between 0 and 1. SDS and T were normalized by dividing with 0.16 and 100 respectively, and D was normalized by dividing with 50×10^{-7}. Note that NaCl concentrations were not normalised since they are well distributed between 0 and 1.

Table 6.1a : Training data set

No	SDS (M)	NaCl (M)	T (°C)	D^a	No.	SDS(M)	NaCl (M)	T (°C)	D^a
1	0.010	0.00	25	17.6	39	0.069	0.60	23	1.76
2	0.020	0.00	25	24.0	40	0.069	0.60	25	2.03
3	0.030	0.00	25	30.3	41	0.069	0.60	30	2.92
4	0.040	0.00	25	36.5	42	0.069	0.60	35	3.96
5	0.050	0.00	25	40.3	43	0.069	0.60	40	5.92
6	0.060	0.00	25	40.5	44	0.069	0.60	45	8.01
7	0.070	0.00	25	43.8	45	0.069	0.60	50	11.20
8	0.125	0.00	25	45.3	46	0.069	0.60	55	14.30
9	0.017	0.60	16	1.77	47	0.069	0.60	60	17.20
10	0.017	0.60	18	2.03	48	0.069	0.60	65	19.0
11	0.017	0.60	20	2.36	49	0.069	0.60	75	24.0
12	0.017	0.60	25	3.42	50	0.069	0.60	85	29.8
13	0.017	0.60	35	7.13	51	0.069	0.70	20	0.8518
14	0.017	0.60	45	11.7	52	0.069	0.70	25	1.382
15	0.017	0.60	55	15.5	53	0.069	0.70	30	2.1881
16	0.069	0.15	11	5.59	54	0.069	0.70	35	2.8813
17	0.069	0.15	13	6.06	55	0.069	0.70	40	4.4811
18	0.069	0.15	15	6.67	56	0.069	0.70	50	9.7642
19	0.069	0.15	17	7.17	57	0.069	0.80	17	0.4307
20	0.069	0.15	20	8.32	58	0.069	0.80	20	0.5559
21	0.069	0.15	25	9.69	59	0.069	0.80	25	0.8661
22	0.069	0.15	35	13.3	60	0.069	0.80	30	1.298
23	0.069	0.45	10	2.40	61	0.069	0.80	40	3.0726
24	0.069	0.45	17	2.84	62	0.069	0.80	50	6.197
25	0.069	0.45	18	3.12	63	0.0345	1.00	25	0.537
26	0.069	0.45	20	3.65	64	0.0345	1.00	30	0.8711
27	0.069	0.45	25	5.69	65	0.0345	1.00	40	1.9315
28	0.069	0.45	30	8.00	66	0.0345	1.00	50	3.780
29	0.069	0.45	35	9.98	67	0.040	0.05	25	10.10
30	0.069	0.45	40	12.1	68	0.060	0.05	25	12.10
31	0.069	0.45	50	16.1	69	0.080	0.05	25	14.0
32	0.069	0.45	60	21.0	70	0.100	0.05	25	16.0
33	0.069	0.45	70	25.6	71	0.120	0.05	25	18.0
34	0.069	0.60	18	1.13	72	0.160	0.05	25	20.0
35	0.069	0.60	19	1.22	73	0.0046	0.10	25	9.60
36	0.069	0.60	20	1.34	74	0.0362	0.10	25	11.2
37	0.069	0.60	21	1.43	75	0.0693	0.10	25	12.4
38	0.069	0.60	22	1.53	76	0.1064	0.10	25	14.0

[a] The units of D are $10^{-7} cm^2 s^{-1}$.

Table 6.1b : Test data set

No	SDS (M)	NaCl (M)	T (°C)	D^a	No.	SDS(M)	NaCl (M)	T (°C)	D^a
1	0.035	0.60	17	1.40	14	0.069	0.30	30	9.92
2	0.035	0.60	18	1.54	15	0.069	0.30	40	13.30
3	0.035	0.60	20	1.78	16	0.069	0.30	50	16.40
4	0.035	0.60	25	2.63	17	0.069	0.55	17	1.56
5	0.035	0.60	35	5.77	18	0.069	0.55	18	1.67
6	0.035	0.60	45	10.30	19	0.069	0.55	20	1.90
7	0.035	0.60	55	14.90	20	0.069	0.55	25	2.77
8	0.035	0.60	65	19.20	21	0.069	0.55	35	5.75
9	0.069	0.30	15	5.44	22	0.069	0.55	45	10.8
10	0.069	0.30	17	5.92	23	0.069	0.55	55	15.6
11	0.069	0.30	18	6.23	24	0.01085	0.10	25	10.0
12	0.069	0.30	20	6.78	25	0.0169	0.10	25	10.4
13	0.069	0.30	25	8.23					

[a] The units of D are $10^{-7}cm^2s^{-1}$.

For the network training, SDS, NaCl concentrations and *T* form three input variables and *D*, the output variable. Consequently, the network architecture consists of three neurons in the input layer ($N = 3$) and one neuron in the output layer ($M = 1$). In order to arrive at the optimum network configuration, ten network training runs taking respectively 1 to 10 neurons ($L = 1 - 10$) in the hidden layer were performed. The network was trained according to the steps described in Appendix. The network training consisted of 50,000 iterations (sweeps) through the training set. A single iteration involves as many forward and reverse passes as the number of input patterns in the training set. The learning coefficient β was decreased progressively from 0.9 to begin with up to 0.1 wherein the reduction was granted at the end of each sweep. The momentum coefficient α was fixed at 0.6.

After every sweep, the network outputs for the test set also were computed and the overall errors with respect to training (E_{trn}) and test (E_{tst}) sets were evaluated. At the end of 50,000 iterations, the overall errors E_{trn} and E_{tst} were examined to locate their minimum. Figure 6.2 shows the minimum of E_{trn} and E_{tst} as a function of number of hidden layer neurons. It can be seen that for six neurons, the E_{tst} magnitude is smallest. It tells us that the optimal network architecture should have 6 neurons in the hidden layer. The behavior of E_{trn} and E_{tst} as a function of iteration number, for *L* = 6 is shown in Figure 6.3. It is observed that E_{tst} reaches a minimum at *40722* th iteration and increases thereafter. Therefore weights at *40722* th iteration are taken to be optimal and the same are listed in Tables 6.2a and 6.2b. The *average overall error* (i.e., $\frac{Overall\ error,\ E}{Number\ of\ input\ patterns}$) with respect to the training and test set using optimal weights have been found to be 6.4×10^{-5} and 1.02×10^{-4} respectively. It is also observed that the trained network estimates the diffusion coefficients within 10% accuracy. Detailed experimental and estimated results for training and test data sets are presented graphically in Figures 6.4(a-b). The correlation coefficients between the network estimated and actual diffusion coefficients for training

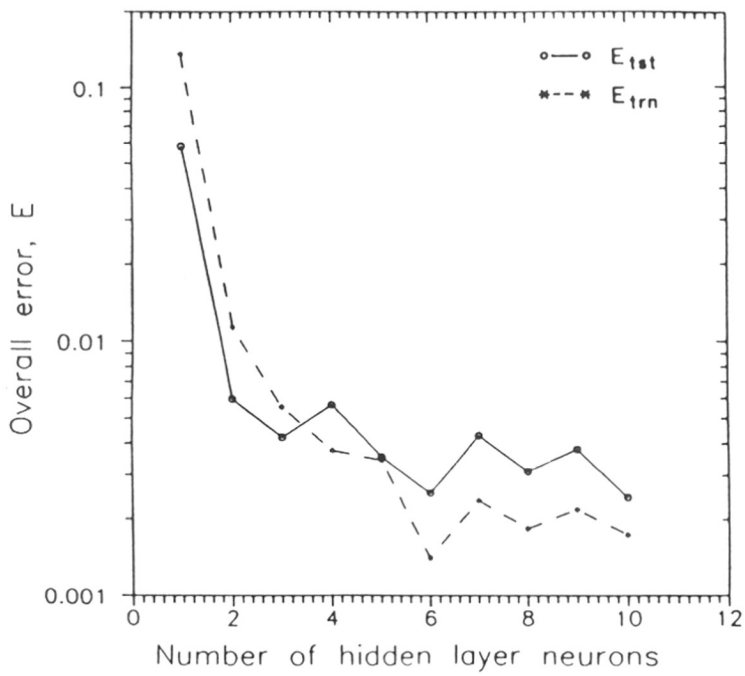

Figure 6.2 : Plot showing overall errors with respect to training and test sets as a function of number of hidden layer neurons.

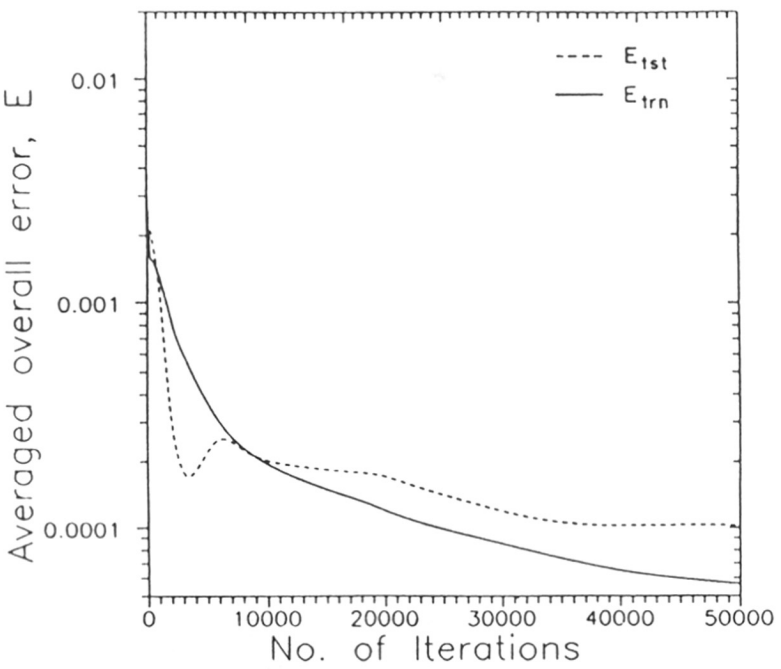

Figure 6.3 : Evolution of averaged overall errors, E_{trn} and E_{tst} as a function of iteration number for six neurons in the hidden layer.

Table 6.2a : Optimal weights connecting the hidden layer neurons

From	To j th hidden layer neuron					
	$j = 1$	$j = 2$	$j = 3$	$j = 4$	$j = 5$	$j = 6$
Input neuron 1	.196424E+01	-.278597E+01	-.346238E+00	-.526830E+01	-.525615E+01	.387599E+00
Input neuron 2	.941704E+01	-.206534E+01	-.456666E+02	-.209767E+02	-.230784E+00	.414819E+01
Input neuron 3	-.753164E+00	-.335487E+01	-.372813E+00	-.105455E+01	.595421E+00	-.920081E+01
Bias neuron, B^h	-.608079E+01	.521641E+01	-.958772E+00	.165539E+00	-.111107E+01	-.149236E+00

Table 6.2b : Optimal weights connecting the output neuron

From	To the output neuron
hidden neuron 1	-.190458E+01
hidden neuron 2	-.421077E+01
hidden neuron 3	.164216E+02
hidden neuron 4	-.107332E+02
hidden neuron 5	.308686E+01
hidden neuron 6	-.286951E+01
Bias neuron, B^o	313240E+01

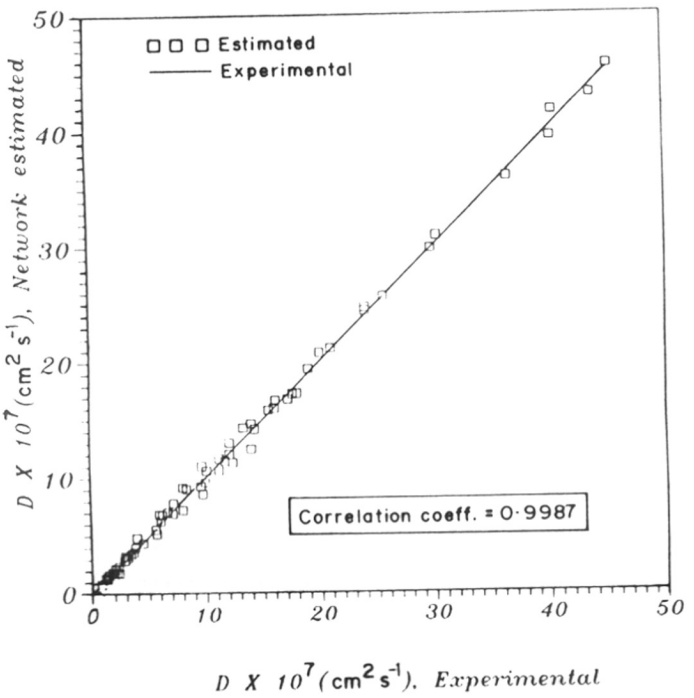

Figure 6.4(a) : Comparison of network estimated diffusion coefficient with experimental values for training set.

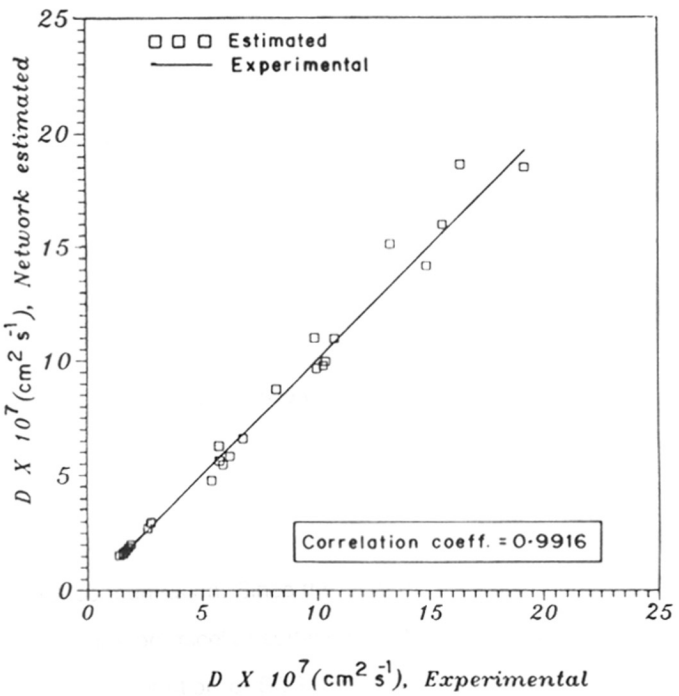

Figure 6.4(b) : Comparison of network estimated diffusion coefficient with experimental values for test set.

and test sets have been evaluated as 0.9987 and 0.9916 respectively. These statistical quantities suggest that the network model provides a very good approximation to the underlying phenomenon. Considering the fact that the data used for modelling is experimental and contains small inaccuracies, the prediction error below 10% is tolerable.

6.3 RESULTS AND DISCUSSION

Having obtained the optimal weights, we tested the generalization capability of the trained network. Several data sets which span a wide range of SDS and NaCl concentrations as well as temperatures were constructed, and the respective diffusion coefficients were evaluated. Such data are termed as *validation test set* (Hecht-Nielsen, 1990). The numerical procedure can be viewed as evaluating *Steps* 2 to 6 of forward pass after the network is initialised with the optimal weights. The motivation behind such an exercise is to rigorously test the network's ability in a real life situation over a wide range of input values.

6.3.1 Influence of NaCl concentration

The influence of low and relatively high NaCl concentrations in 0.06 M SDS on D is plotted as a function of temperature in Figures 6.5(a) and 6.5(b) and show an increase in D values regardless of NaCl concentration. It is also seen that at a fixed temperature, D decreases with increasing NaCl concentration. Since the SDS micelles are charged, the electrostatic repulsion between like charges on micellar surface is high in the absence of NaCl. However, addition of NaCl to the aqueous solution of SDS lowers the electrostatic repulsion. With increasing ionic strength the Coulomb potential is screened more and more effectively and at a particular threshold of NaCl concentration, the attraction and repulsion effects (i.e., hard-core repulsion and

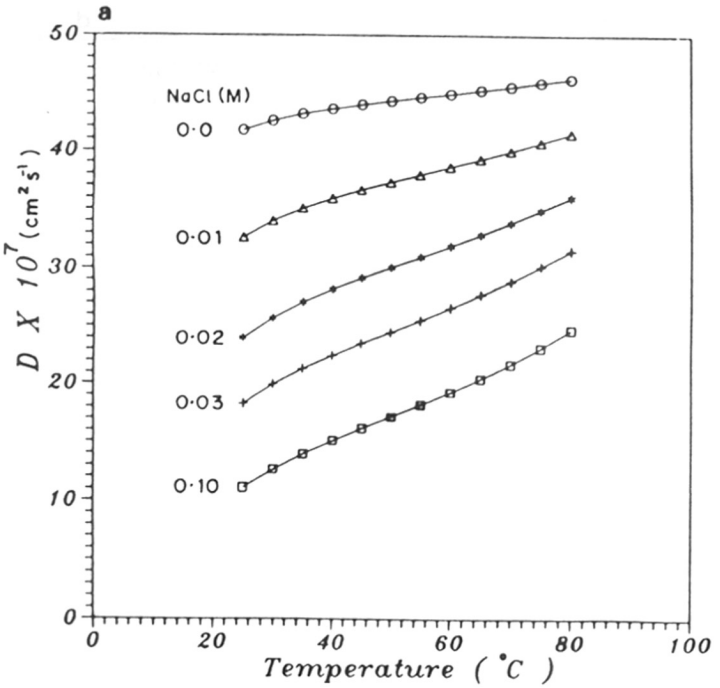

Figure 6.5(a) : Network estimated diffusion coefficients for 0.06 M SDS at different NaCl concentrations (0.0-0.10 M) as a function of temperature.

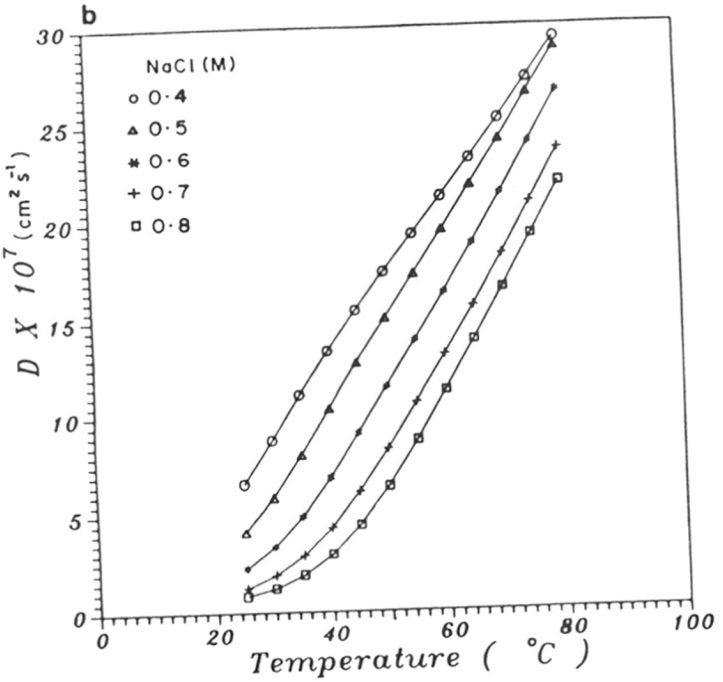

Figure 6.5(b) : Network estimated diffusion coefficients for 0.06 M SDS at different NaCl concentrations (0.4-0.8 M) as a function of temperature.

London-van der waals attraction) are in balance [45, 46]. As a result, beyond this concentration limit the aggregation number (i.e., average number of SDS molecules present in micelles) is expected to increase with salinity. This phenomena causes the micelles to grow in size (decrease in *D*) and become long rod-shaped micelles [10, 47]. The network estimated diffusion coefficients as plotted in Figures 6.5(a) and 6.5(b) exactly follow the described trend and are also in good agreement with the earlier studies [11, 15] .

6.3.2 Influence of SDS concentration

As observed by Mazer et al. [11], and Hayashi et al. [48], the ionic micelles are spherical or globular at low salt concentrations and become rodlike when salt concentrations exceed the threshold value. The network model is used to verify this phenomenon and the results are plotted in Figure 6.6. The four plots correspond to SDS concentrations of 0.07 to 0.10 M. It can be clearly seen that in the beginning (below threshold salt concentration) *D* decreses slowly and thereafter rapidly before eventually flattening out. It has been reported in the literature [49] that the threshold salt concentration for sphere to rodlike transition in SDS micelles is in the range 0.17 M to 0.30 M of NaCl. The network estimated diffusion coefficients indicate the threshold salt concentration to be $\approx$ 0.20 M.

Figure 6.7 shows the influence of varying SDS concentration on *D* as a function of temperature when NaCl concentration is fixed (0.6 M). The chosen NaCl concentration is high enough to suppress the electrostatic effects between the charged SDS micelles. The decrease in *D* with increasing SDS concentration for a specific *T* is due to the micellar growth and formation of large micelles. On the other hand, for all SDS concentrations considered, *D* increases with temperature. The observed trends are in accordance with that found experimentally for ionic surfactants [45,50].

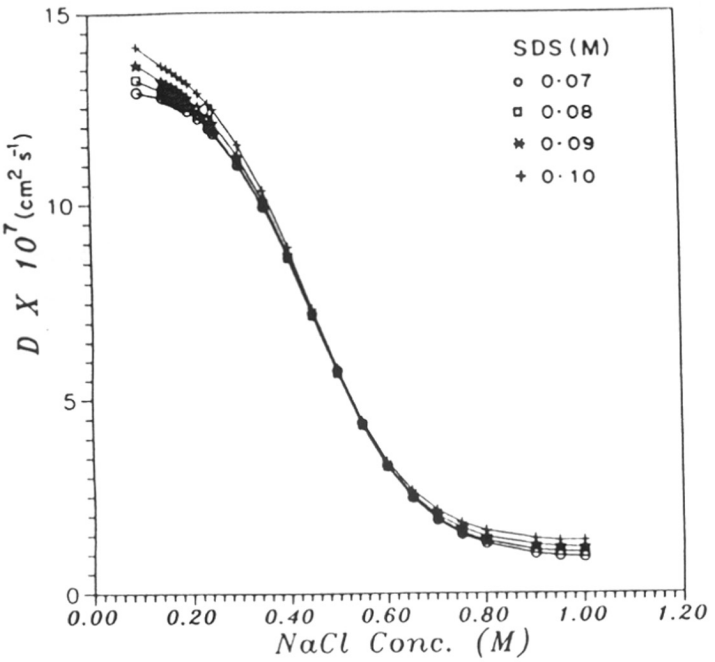

Figure 6.6 : Network estimated diffusion coefficients at fixed temperature (30 °C) for various NaCl concentrations.

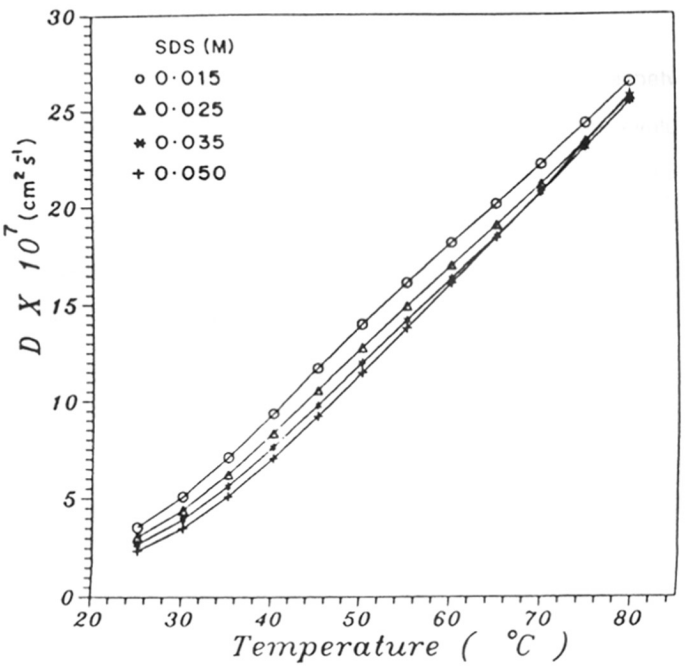

Figure 6.7 : Network estimated diffusion coefficient at 0.6 M NaCl with varying concentration of SDS as a function of temperature.

6.4 CONCLUSIONS

In this study we have provided a correlation in the form of artificial neural network model for evaluating the diffusion coefficient of SDS micellar system. The network evaluated diffusion coefficients are in good qualitative and quantitaive agrrement with the experimental observations. We found that the neural networks make best use of the information in the given data, resulting in an excellent grading compared to other approaches. Moreover, the obtained network weights should prove useful for estimating diffusion coefficients over a wide range of experimental conditions.

NOTATIONS

D	diffusion coefficient
T	temperature
L	number of hidden neurons
M	number of output neurons
N	number of input neurons
B^h	bias neuron for hidden layer
B^o	bias neuron for output layer
β	learning coefficient
α	momentem coefficient
E_{trn}	overall errors with respect to training set
E_{tst}	overall errors with respect to test set

REFERENCES

[1] J. H. Fendler and E. J. Fendler, In *Catalysis in Micellar and Macromolecular Systems*; Academic: New York, 1976.

[2] R. Leung, M. J. Hou and D. O. Shah, Microemulsions: Formation, Structure, Properties and Novel Applications. In *Surfactants in Chemical/Process Engineering: Surfactant Science Series*; D. T. Wasan, M. E. Ginn and D. O. Shah, Eds.; Dekker: New York, 1988; Vol. **28**, pp 315-367.

[3] R. A. Mackay, *Adv. Colloid Interface Sci.*, **15** (1981) 131.

[4] B. K. Jha, A. S. Chhatre and B. D. Kulkarni, *J. Chem. Soc. Perkin Trans.* 2, **6** (1994) 1383.

[5] C. A. Bunton and G. Savelli, *Adv. Phys. Org. Chem.*, **22** (1986) 213.

[6] B. K. Jha, A. S. Chhatre, B. D. Kulkarni, R. A. Joshi, R. R. Joshi and U. R. Kalkote, *J. Colloid Interface Sci.*, **163** (1994) 1.

[7] J. H. Fendler, In *Membrane and Mimetic Chemistry*; Wiley: New York, 1982.

[8] N. N. Li and A. L. Shreier, Liquid Membrane Water Treating. In *Recent Advances in Separation Science*; N. N. Li, Ed.; CRC: Cleveland, 1972; Chapter 9, pp 315-367.

[9] C. Tanford, The Effect of Temperature: Anomalous Entropy and Heat Capacity. In *The Hydrophobic Effect: Formation of Micelles and Biological Membranes*; Wiley: New York, 1980; Chapter 5.

[10] J. N. Israelachivili, D. J. Mitchell and B. W. Ninham, *J. Chem. Soc., Faraday Trans. 2*, **72** (1976) 1525 .

[11] N. A. Mazer, G. B. Benedeck and M. C. Carey, *J. Phys. Chem.*, **80** (1976) 1075.

[12] M. Corti and V. Degiorgio, *J. Phys. Chem.*, **85** (1981) 711 .

[13] P. J. Missel, N. A. Mazer, G. B. Benedek and M. C. Carey, *J. Phys. Chem.*, **87** (1983) 1264.

[14] R. Dorshow, J. Briggs, C. A. Bunton and D. F. Nicoli, *J. Phys. Chem.*, **86** (1982) 1264.

[15] R. M. Weinheimer, D. F. Evans and E. L. Cussler, *J. Colloid Interface Sci.*, **80** (1981) 357.

[16] J. P. Kratohvil and T. M. Aminabhavi, *J. Phys. Chem.*, **86** (1981) 1254.

[17] D. A. Doughty, *J. Phys. Chem.*, **83** (1979) 2621.

[18] R. Zana and R. A. Mackay, *Langmuir*, **2** (1986) 109.

[19] A. B. Mandal and B. U. Nair, *J. Phys. Chem.*, **95** (1991) 9008.

[20] G. D. Phillies, *J. Chem. Phys.*, **60** (1974) 976.

[21] D. E. Koppel, *J. Chem. Phys.* **57** (1972) 4814.

[22] D. J. Mitchell and B. W. Ninham, *J.Chem. Soc., Faraday Trans.* 2, **77** (1981) 601.

[23] R. Nagarajan and E. Ruckenstein, *J. Colloid Interface Sci.*, **60** (1977) 221.

[24] P. G. de Gennes and C. Taupin *J. Phys. Chem.*, **86** (1982) 2294.

[25] S. A. Safran, D. Roux, M. E. Cates and D. Andelman, *Phys. Rev. Lett.*, **57** (1986) 491.

[26] C. Tanford, *J. Phys. Chem.*, **78** (1974) 2469.

[27] C. Tanford, *Proc. Natl. Acad. Sci.* USA, **71** (1974) 1811.

[28] P. Neogi, *Langmuir*, **10** (1994) 1410.
[29] J. Gasteiger and J. Zupan, *Angew. Chem. Int. Ed. Engli.*, **32** (1993) 503.
[30] J. A. Burns and G. M. Whitesides, *Chemical Rev.*, **93** (1993) 2583.
[31] J. Zupan and J. Gasteiger, *Anal. Chim. Acta.*, **248** (1991) 1.
[32] T. Aoyama and H. Ichikawa, *J. Med. Chem.* **33** (1990) 2583.
[33] T. Aoyama and H. Ichikawa, *Chem. Pharm. Bull.*, **39** (1991) 358.
[34] D. Cherqaoui and D. Villemin, *J. Chem. Soc. Faraday Trans.*, **90** (1994) 97.
[35] N. Bodor, A. Harget and M. J. Haung, *J. Am. Chem. Soc.*, **113** (1991) 9480.
[36] H. H. Luce and R. Govind, *Tetrahedron Comp. Methodol.*, 3 (1990) 143
[37] Y. Liu, B. R. Upadhyaya and M. Naghedolfeizi, *Applied Spectroscopy*, **47** (1993) 12.
[38] A. Normandin, B. P. A. Grandjean and J. Thibault, *Ind. Eng. Chem. Res.*, **32** (1993) 970
[39] M. J. Lee and J. T. Chen, *Ind. Eng. Chem. Res.*, **32** (1993) 995.
[40] R. P. Lippman, *IEEE ASSP Mag.*, 1987.
[41] P. D. Wasserman, In *Neural Computing: Theory and Practice*; Van Nostrand Reinhold: New York, 1989.
[42] R. Hecht-Nielsen, In *Neurocomputing*; Addision-Wesley: New York, 1990.
[43] D. E. Rumelhart, G. E. Hinton and R. J. Williams, In *Parallel Distributed Processing*; D. E. Rumelhart and J. L. McClelland, Eds.; MIT: Cambridge, 1988; Vol. 1, pp 318.
[44] A. B. Mandal, *Langmuir*, **9** (1993) 1932.
[45] M. Corti and V. Degiorgio, *Ann. Phys.*, 3 (1978) 303 .
[46] B. Goldstein and B. H. Zimm., *J. Chem. Phys.*, **54** (1971) 4408.
[47] H. Wennerstrom and B. Lindman, *Phys. Rep.*, **52** (1979) 1
[48] S. Hayashi and S. Ikeda, *J. Phys. Chem.*, **84** (1980) 565 .
[49] I. V. Rao and E. Ruckenstein, *J. Colloid Interface Sci.*, **119** (1987) 221.
[50] M. Corti and V. Degiorgio, Investigation of Aggregation Phenomena in Aqueous Sodium Dodecyl Sulfate Solutions at High NaCl Concentration by Quasielastic Light Scattering. In *Solution Chemistry of Surfactants*; K. L. Mittal, Ed., Plenum: New York, 1979; Vol. 1, pp 377-390.

APPENDIX :

ERROR-BACK-PROPAGATION ALGORITHM

The detailed numerical steps to train a three layer feedforward neural network by error-back-propagation algorithm are as follows.

Step 1 : Initialize the connection weights to small random values so as to lie between -1 and 1.

Step 2 : Apply an input pattern from a set containing P patterns to the input layer neurons.

Step 3: Compute the weighted sum of inputs for individual neurons in the hidden layer according to

$$net^h_{pj} = \sum_{i=1}^{N} W^h_{ji} x_{pi} + B^h_j \qquad (6.1)$$

where net^h_{pj} denotes the weighted sum for *j*th hidden layer neuron when *p*th input pattern has been applied; W^h_{ji} denotes the weight between *i*th input layer neuron and *j*th hidden layer neuron; x_{pi} represents the *i*th input of pattern p ; N refers to the number of input layer neurons and B^h_j represents the bias weight for *j*th hidden layer neuron.

Step 4 : Transform the weighted sum using an activation function (e.g. Sigmoid activation function) to get the outputs of the hidden layer neurons according to :

$$P^h_{pj} = \frac{1}{1 + \exp(-net^h_{pj})} \qquad (6.2)$$

where P^h_{pj} refers to the output of *j*th hidden layer neuron.

Step 5 : Compute the weighted sum of inputs for individual neurons in the output layer as

$$net^{O}_{pk} = \sum_{j=1}^{L} W^{O}_{kj} P^{h}_{pj} + B^{O}_{k}, \quad k = 1, M \tag{6.3}$$

where superscript *O* refers to the output layer and *L* denotes the number of hidden layer neurons. W^{O}_{kj} is the connection weight between neuron *k* in the output layer and neuron *j* in the hidden layer, M denotes the number of neurons in the output layer and B^{o}_{k} represents the bias weight for *k*th output layer neuron.

Step 6 : Transform the weighted sum using the same activation function as in *Step 4* to get the outputs of the output layer neurons as follows.

$$P^{O}_{pk} = \frac{1}{1 + \exp(-net^{O}_{pk})} \tag{6.4}$$

where P^{O}_{pk} refers to the output of the *k*th output layer neuron.

Step 7 : Obtain the error δ^{O}_{pk} associated with each neuron in the output layer as

$$\delta^{O}_{pk} = (y_{pk} - P^{O}_{pk})[P^{O}_{pk}(1 - P^{O}_{pk})] \tag{6.5}$$

where y_{pk} = desired output of neuron *k* for pattern p and P^{O}_{pk} = actual output of the k^{th} output layer neuron.

Step 8 : Compute the error δ^{h}_{pj} associated with each neuron in the hidden layer by

$$\delta^{h}_{pj} = \sum_{k=1}^{M} \delta^{O}_{pk} W^{O}_{kj}[P^{h}_{pj}(1 - P^{h}_{pj})], \quad j = 1, L \tag{6.6}$$

Step 9 : Update the weights between output and hidden layer as

$$W^{O}_{kj}(t+1) = W^{O}_{kj}(t) + \eta \delta^{O}_{pk} P^{O}_{pj} + \alpha[W^{O}_{kj}(t) - W^{O}_{kj}(t-1)] \tag{6.7}$$

LIST OF PUBLICATIONS AND PATENTS

Research Papers:

[1] Enhanced decarbamoylation of D(-)-N-carbamoyl phenylglycine by its interfacial solubilization under micellar conditions; B.K. Jha, A.S. Chhatre, B.D. Kulkarni, R.A. Joshi, R.R. Joshi and U.R. Kalkote, *J. Colloid Interface Sci.*, **163** (1994) 1-9.

[2] Cyclization and molecular rearrangement under micellar and microemulsion conditions; B.K. Jha, A.S. Chhatre and B.D. Kulkarni, *J. Chem. Soc. Perk. Trans. 2*, **6** (1994) 1383-1385.

[3] Estimating diffusion coefficient of a micellar system using an artificial neural network; B.K. Jha, S.S. Tambe and B.D. Kulkarni, *J. Colloid Interface Sci.*, **170** (1995) 392-398.

[4] An unusual electron-transfer behavior of ferrocene in aqueous microemulsion systems; B.K. Jha, B.D. Kulkarni, M.P. Vinod and K. Vijayamohanan, *Chem. Phys. Lett.*, **240** (1995) 442-448.

[5] Beckmann rearrangement of cyclohexanone oxime under dilute acidic conditions in micellar media; B.K. Jha and B.D. Kulkarni, *Ind. Eng. Chem. Res.*, (accepted).

[6] Rheological study of the L_2 and L_2/D phases in a ternary system; B.K. Jha, A. Manna, S.N. Shintre and B.D. Kulkarni, (communicated).

[7] Electrochemical investigations of redox species in aqueous surfactant solutions using ultramicroelectrode; B.K. Jha, A.S. Chhatre, B.D. Kulkarni, M.P. Vinod and K. Vijayamohanan, (communicated).

Patents:

[1] An improved process for the preparation of amino acid by decarbamoylation of its N-carbamoyl derivative using macroemulsion and microemulsion systems, B.K. Jha, A.S. Chhatre, B.D. Kulkarni, R.A. Joshi, R.R. Joshi, U.R. Kalkote and T. Ravindranathan, **INDIAN** (197/DEL/93).

[2] An improved process for the preparation of caprolactam from cyclohexanone oxime using micellar solutions, macroemulsions and microemulsion systems, B.K. Jha, A.S. Chhatre, B.D. Kulkarni and S. Sivasanker, **INDIAN** (1238/DEL/93).

[3] Process for the preparation of caprolactam, B.K. Jha, A.S. Chhatre, B.D. Kulkarni and S. Sivasanker, **US Patent No.** 5401843 (1995).

where training iteration number is represented by t and η denotes the learning coefficient ($0 < \eta < 1$). The third term on the right hand side is referred to as *momentum term* where α denotes the momentum coefficient ($0 < \alpha < 1$). The addition of momentum term speeds up the training process and also helps to avoid local minima in the error surface.

Step 10 :Update the weights between the hidden and input layer as given below and go to *Step 2*.

$$W^h_{ji}(t+1) = W^h_{ji}(t) + \eta \delta^h_{pj} x_{pi} + \alpha [W^h_{ji}(t) - W^h_{ji}(t-1)] \qquad (6.8)$$

In this procedure, *Steps* (1-6) and *Steps* (6-10) correspond to the forward and reverse passes respectively. The procedure (barring *Step 1*) is repeated for all the input patterns until the network weights are optimized such that the overall prediction error, $E = 0.5 \sum_{p=1}^{P} \sum_{k=1}^{M} (y_{pk} - P^o_{pk})^2$ reaches a minimum. Note that the bias neuron always possesses an output of "1" and weights B^h_j and B^o_k are adjusted in a similar fashion to the hidden and output layer weights.

LIST OF PUBLICATIONS AND PATENTS

Research Papers:

[1] Enhanced decarbamoylation of D(-)-N-carbamoyl phenylglycine by its interfacial solubilization under micellar conditions; B.K. Jha, A.S. Chhatre, B.D. Kulkarni, R.A. Joshi, R.R. Joshi and U.R. Kalkote, *J. Colloid Interface Sci.*, **163** (1994) 1-9.

[2] Cyclization and molecular rearrangement under micellar and microemulsion conditions; B.K. Jha, A.S. Chhatre and B.D. Kulkarni, *J. Chem. Soc. Perk. Trans. 2*, **6** (1994) 1383-1385.

[3] Estimating diffusion coefficient of a micellar system using an artificial neural network; B.K. Jha, S.S. Tambe and B.D. Kulkarni, *J. Colloid Interface Sci.*, **170** (1995) 392-398.

[4] An unusual electron-transfer behavior of ferrocene in aqueous microemulsion systems; B.K. Jha, B.D. Kulkarni, M.P. Vinod and K. Vijayamohanan, *Chem. Phys. Lett.*, **240** (1995) 442-448.

[5] Beckmann rearrangement of cyclohexanone oxime under dilute acidic conditions in micellar media; B.K. Jha and B.D. Kulkarni, *Ind. Eng. Chem. Res.*, (accepted).

[6] Rheological study of the L_2 and L_2/D phases in a ternary system; B.K. Jha, A. Manna, S.N. Shintre and B.D. Kulkarni, (communicated).

[7] Electrochemical investigations of redox species in aqueous surfactant solutions using ultramicroelectrode; B.K. Jha, A.S. Chhatre, B.D. Kulkarni, M.P. Vinod and K. Vijayamohanan, (communicated).

Patents:

[1] An improved process for the preparation of amino acid by decarbamoylation of its N-carbamoyl derivative using macroemulsion and microemulsion systems, B.K. Jha, A.S. Chhatre, B.D. Kulkarni, R.A. Joshi, R.R. Joshi, U.R. Kalkote and T. Ravindranathan, **INDIAN** (197/DEL/93).

[2] An improved process for the preparation of caprolactam from cyclohexanone oxime using micellar solutions, macroemulsions and microemulsion systems, B.K. Jha, A.S. Chhatre, B.D. Kulkarni and S. Sivasanker, **INDIAN** (1238/DEL/93).

[3] Process for the preparation of caprolactam, B.K. Jha, A.S. Chhatre, B.D. Kulkarni and S. Sivasanker, **US Patent No.** 5401843 (1995).